ATTACHMENT 2

SCIE-NRC-224-94
Revision 1

TECHNICAL EVALUATION REPORT
(Non-Proprietary Version)

- RELAP5/MOD2-B&W -

An Advanced Computer Program for Light Water Reactor LOCA and Non-LOCA Transient Analysis
BAW-10164P, Revisions 2 and 3

W. C. Arcieri
D. A. Prelewicz

Prepared for

U. S. Nuclear Regulatory Commission
Washington, D. C. 20555

March 1995

SCIENTECH, Inc.
11140 Rockville Pike, Suite 500
Rockville, Maryland 20852

TECHNICAL EVALUATION REPORT
(Non-Proprietary Version)
- RELAP5/MOD2-B&W -
An Advanced Computer Program for Light Water
Reactor LOCA and Non-LOCA Transient Analysis
BAW-10164P, Revisions 2 and 3

1.0 INTRODUCTION

By letter dated September 18, 1992, the B&W Nuclear Technologies Company submitted the topical report BAW-10164P, Revisions 2 and 3 for NRC review. The report describes a pressurized water reactor (PWR) thermal-hydraulics transient analysis code for LOCA and non-LOCA transients analysis based on the RELAP5/MOD2 code.

RELAP5/MOD2-B&W is a B&W Nuclear Technologies (BWNT) adaptation of the Idaho National Engineering Laboratory (INEL) RELAP5/MOD2[1] code used for PWR licensing and best estimate thermal hydraulics transient analysis. RELAP5/MOD2 was developed by INEL as a best-estimate computer code for light water reactor transient analysis. B&W Nuclear Technologies has added features to permit use of the RELAP5/MOD2-B&W code for ECCS evaluation model (EM) calculations. The previous revision of the RELAP5-B&W code, Revision 1[2], was approved for use in the analysis of small break and large break LOCAs[3] (SBLOCA and LBLOCA) for recirculating steam generator plants.

Revision 2 of BAW-10164P[5] describes updates for use in performing small break LOCA analysis. These updates include an additional critical heat flux (CHF) correlation referred to as BWUMV, addition of the Wilson model for determining interphase drag, addition of a counter-current flow limiting (CCFL) model and correction of minor code errors. Benchmarks are included in Revision 2 to specifically address the Wilson interphase drag model and the small break LOCA EM model. The

SBLOCA benchmark is against experimental data from the ROSA-IV large scale test facility.

In addition to the correction of minor errors, Revision 3 of BAW-10164P[6] includes enhancements to the EM fuel pin model, EM heat transfer model, and models to support use of the code for analysis of once through steam generator (OTSG) plants. These models include the Becker CHF correlation, further modifications to the slug-drag model, the high auxiliary feedwater model and the Chen nucleate boiling heat transfer coefficient void ramp. Benchmarks against model 19-tube OTSG data and against SBLOCA test data from the MIST facility, which has simulated OTSGs, are included. The modifications to the approved licensing model proposed in References 4 and 5 are the subject of the review and evaluation documented in this report.

2. SUMMARY OF THE TOPICAL REPORT

BAW-10164P Revisions 2 and 3 present best estimate and licensing type calculation for PWRs. Simulation methods are presented for large and small break LOCAs as well as operational transients such as anticipated transients without scram, loss of off-site power, loss of feedwater, and loss of flow. The solution is based on a two energy equation scheme, a two step numerical option, a gap conductance model, constitutive models and control system models. Control system and secondary system components have been added to permit modeling of plant controls, turbines, condensers, and secondary feedwater conditioning systems. Benchmark comparison of code predictions to integral system test results are also presented.

Revision 2 deals mainly with the small break LOCA. Revision 3 includes enhancements to the evaluation model for fuel pin heat transfer modelling to extent the code applicability to the once through steam generators.

3.0 EVALUATION

Review and evaluation of the RELAP5/MOD2-B&W code includes Revision 2 and Revision 3 of BAW-10164P. Revision 2 provides additional models specifically intended for SBLOCA applications. Revision 3 includes enhancements to the EM fuel pin and heat transfer model, additions and benchmarks which extend application of the code to the once through steam generator plants. An initial review of Revisions 2 and 3 led to generation of Requests for Additional Information[8,9]. Supplemental information was also submitted by BWNT during the review process[10]. Each of the model additions or modifications is discussed and evaluated in the following sections.

3.1 BAW-10164P, Revision 2

3.1.1 Model Changes for the Slug Flow Regime

BWNT added an option for determining the Taylor bubble interphase drag during slug flow based on the Wilson drag model. The Wilson drag model is based on the Wilson bubble rise velocity in a vertical pipe. BWNT applied the Wilson drag model for reflood applications using the BEACH program and is now applying the model for non-reflood applications in RELAP5/MOD2-B&W. These changes are discussed on pages 2.1-51 to 2.1-54 of BAW-10164P. Benchmarks are provided in Appendix H.

In implementing the Wilson drag model for RELAP5/MOD2, BWNT derived an expression for the interphasic friction for Taylor bubbles. Flow was assumed to be in a quasi-steady state. The derivation of this expression was checked. The formulation was determined to be correct. BWNT also incorporated improvements to match the bubble rise data at higher void fractions. An apparent difference between the interphase friction model for slug flow used in RELAP5/MOD2 B&W compared to that used in the BEACH[7] program was questioned. BEACH uses the same Wilson

drag model with a different multiplier, on the Taylor bubble term. BWNT responded that the different multipliers were selected based on comparisons to reflood benchmarks in the case of BEACH and small break LOCA benchmarks in the case of RELAP5/MOD2-B&W.

An option to remove smoothing in selected junctions, (not used in BEACH), was added to RELAP5/MOD2-B&W. This option allows smoothing to be bypassed. Since discontinuous void distributions may occur during a small break LOCA, use of this option for small break calculations may be appropriate.

Benchmarks were performed by BWNT using the Wilson drag model against results obtained from the NRC-approved computer code FOAM2[11] and with small break LOCA experiments performed at the Thermal Hydraulic Test Facility (THTF) at the Oak Ridge National Laboratory. These benchmarks are presented in Appendix H to BAW-10164P.

The FOAM2 program, developed by BWNT and previously approved by the NRC, is used to determine whether the water content of a reactor core is sufficient to cover the core with a combination of liquid and two phase mixture based on a given core void distribution. If it is determined that the core is uncovered, FOAM2 calculates the two-phase swell level and steaming rate. The FOAM2 program utilizes the Wilson bubble rise correlation to directly calculate the core void distribution. The Wilson bubble velocity correlation used in FOAM2 is somewhat different from that used in RELAP5/MOD2-B&W since it does not include the changes made by BWNT to better match the bubble rise data at higher void fractions. BWNT stated that the core void distribution results calculated by RELAP5/MOD2 B&W and FOAM2 should be similar except potentially at higher void fractions because of differences in the formulation of the Wilson model. The benchmarks show that RELAP5/MOD2-B&W predicts void distributions which are comparable to FOAM2 predictions.

Calculations using FOAM2 were performed for reactor powers of 1.5, 2.5, and 5.0 percent of full power. System pressures ranging from 100 to 1600 psia were included in the analysis. BWNT presented plots of core void fraction vs. core elevation comparing the RELAP5/MOD2-B&W results and the FOAM2 results. These plots show acceptable agreement between RELAP5/MOD2-B&W and FOAM2, with RELAP5/MOD2-B&W showing very slightly different results at high void fractions.

The RELAP5/MOD2-B&W code predictions were compared to THTF test results for a range of pressures (520 to 1170 psia), power densities (0.08 to 0.68 kw/ft), and mass flux (3395 to 21943 lbm/hr-ft^2). BWNT presented plots of the results of core void fraction vs. core elevation as well as rod surface and vapor temperature vs. core elevation comparing the RELAP5/MOD2-B&W results and the THTF test results. In general, the void fractions predicted by RELAP5/MOD2-B&W are somewhat higher than the THTF results. Additionally, RELAP5/MOD2-B&W generally overpredicts the vapor and surface temperature relative to the THTF tests. There is a dip in surface temperature in the THTF tests at the core elevation of 11 feet. BWNT attributes the dip to grid effects on the heat transfer rate which are not accounted for in the RELAP5/MOD2-B&W model. The dip in surface temperature caused by the grid effect, was questioned. The surface temperature would be underpredicted for THTF tests 3.09.10 i, j, l, and m. Underprediction of the surface temperature could indicate that the heat transfer coefficient to the vapor is high and non-conservative. It was requested that BWNT discuss the comparisons between RELAP5/MOD2-B&W and the THTF tests and show that the comparisons do not rely on systematic underprediction of the vapor temperature. In their response, BWNT indicated that the heat transfer coefficient for single phase vapor is computed using the McEligot-plus radiation correlation set. BWNT pointed out that use of the correlation is widely accepted and was reviewed and accepted in previous submittals of RELAP5 and FRAP-T6 topical reports. BWNT also noted that the measurement of vapor temperature is low because the thermocouples were mounted on the unheated rods used to simulate guide tubes. Actual temperatures measured at THTF would be higher and more in agreement with

RELAP5/MOD2-B&W. The BWNT response was deemed satisfactory. This benchmark shows that use of the Wilson model for interphase drag produces reasonably accurate predictions of SBLOCA experimental data.

3.1.2 Model Changes for the Annular Mist Flow Regime

BWNT has added an option to RELAP5/MOD2-B&W to include calculation of the overall drag computed for control volumes in an annular mist flow regime. This change is used in the OTSG and MIST benchmarks discussed in Sections 3.2.7 and 3.2.8 of this evaluation.

3.1.3 Counter-Current Flow Limiting Model

BWNT added optional counter-current flow limiting (CCFL) models which are intended for use in predicting flows at the steam generator U-tube inlets and steam generator plenum inlets during the reflux condensation period of a SBLOCA. Addition of the CCFL model is described on pages 2.1-133 to 2.1-133.3 of BAW-10164P.

The CCFL model modifications, consisting of a correlation for flooding in vertical tubes, are included in the form of a general relationship between the dimensionless vapor flux, j_g^* and the dimensionless liquid flux, j_f^*. The relationship is implemented in the code in a manner similar to the implementation in RELAP5/MOD3. Different values of the correlation parameters are used at the U-tube inlets and at the steam generator plenum inlet. This model was benchmarked against ROSA-IV small break LOCA data in Appendix J of the Topical Report. Flow predictions were in reasonable agreement with the test data. Therefore, the use of the CCFL model at the steam generator plenum and tube inlet, with the parameters used in the benchmark, is acceptable for the analysis of SBLOCAs in recirculating steam generators. As demonstrated by the fact that different correlation parameters are required at the inlet

plenum and the tubes, CCFL is very geometry specific. Other uses of the CCFL model will require that the model be validated for that application.

3.1.4 Condensation Heat Transfer Correlation Modifications

Modifications were made to the condensation heat transfer correlation for vertical or horizontal surfaces. These changes are discussed on pages 2.2-31 and 2.2-32 of BAW-10164P.

The Nusselt laminar film correlations for a horizontal surface and for a vertical surface are used in RELAP5/MOD2-B&W. For condensation on a horizontal surface, laminar film condensation in a horizontal tube is assumed. Comparing the formulation given in Collier[12] against that given by BWNT for condensation within a horizontal tube shows that BWNT did not include the equation developed by Rohsenow for the modified latent heat of vaporization. Omission of this equation will have a small effect for the heat transfer coefficient result. The expression for a vertical surface was found to be in agreement with Collier.

3.1.5 Changes to the Metal-Water Reaction (Swelled Radius) Model

When a fuel rod swells the radius and hence the surface area of the rod will increase in the swelled region. The rate of heat generation and the molar production rate of hydrogen are proportional to the exposed surface area of the clad. These models have been modified by BWNT as described in Section 2.3.2.4 of BAW-10164P to increase the surface area in proportion to the ratio of the swelled clad radius to the cold clad radius. This increase in area is applied to both the clad inside and outside surfaces. Consideration of the increase in clad radius in the swelled region is appropriate and conservative. Both the energy generation rate and the rate of hydrogen production will increase when this model is used compared to the constant

surface area model. This model satisfies the requirements of Appendix K and is acceptable for ECCS EM calculations.

3.1.6 Core Heat Transfer Selection Model Modifications

BWNT installed a separate heat transfer option for use in SBLOCA analysis. The changes are discussed on pages 2.3-60 to 2.3-61.2, 2.3-64, 2.3-67, 2.3-83, and 2.3-84 of BAW-10164P. The changes to the switching logic for SBLOCA include the removal of Appendix K restrictions regarding no return to nucleate boiling and the lock into film boiling after the wall superheat exceeds 300^0 F. The switching logic is unchanged for LBLOCA. BWNT stated that the no return to nucleate boiling and the lock into film boiling restrictions of Appendix K are not applicable to SBLOCA. This assertion is acceptable. While the acceptance criteria of 10 CFR 50.46 apply to LBLOCA, the possible core heatup scenarios following a SBLOCA are varied and more complex than those for the LBLOCA. The use of a reflood heat transfer model lockout of return to nucleate boiling and prediction of quenching is inappropriate for the small break.

An option to allow use of the BWUMV critical heat flux correlation can be selected by the user depending on the fuel design being evaluated. This correlation is used only at pressures greater than 1300 psia at mass fluxes greater than 500,000 lbm/hr-ft^2 in the core heat transfer selection logic in RELAP5/MOD2-B&W. The BWUMV correlation is reviewed in the next section.

3.1.7 BWUMV Critical Heat Flux Correlation

The BWUMV (B&W Universal Mixing Vane) critical heat flux correlation was developed for the analysis of SBLOCA. The development of the BWUMV correlation is presented in Appendix I to BAW-10164P. BWNT developed this correlation from the database for the previously approved BWCMV correlation[13] with additional mid-flow regime data from three Westinghouse tests.

BWUMV utilizes a third order polynomial fit using three independent variables based on pressure (P), mass flux (G), and quality (X_{eth}). Typographical errors in the CHF equation, units conversion errors, and the FLS equation, were questioned. The responses with the corrected equations and units are provided in Reference 8.

The number of data points and their distribution in the mass flux range below 0.95×10^6 lb/hr-ft^2 was questioned. BWNT indicated in their response that the total number of data points with mass fluxes below 1.25×10^6 lb/hr-ft^2 is 77. In addition to the 22 points from Table I.3 of Appendix I, 20 points are from the data presented in Appendix B of BAW-10159 and 35 test points are from the data presented in Appendix F of BAW-10159. Of these 77 points, a total of 32 points were measured at a local mass flux of between 0.4×10^6 and 1.0×10^6 lb/hr-ft^2. This total is comparable to the number of points at the lower end of the flow range of the BWCMV correlation.

In evaluating the distribution of points about the measured/predicted ratio for pressure and mass flux, it is noted that the data clustered about 750 psia and 1000 psia on Figure I.5 are not uniformly distributed about the mean value of 1.0. It appears that 10 of the 11 points measured at 750 psia are below the mean and 10 of the 12 points measured at 1000 psia are above the mean. Because of this bias and because of the small number of points, we believe that the BWUMV results are biased at pressures of 750 and 1000 psia. It is recognized that this bias does not affect BWUMV predictions above 1300 psia. However, BWNT did conclude in Appendix I to BAW-10164P that the BWUMV correlation is applicable to CHF calculations for pressures and flow rates above 750 psia. Given the apparent bias in the data points at 750 and 1000 psia, the BWUMV correlation should not be used for CHF calculations at pressures below 1300 psia.

Numerical checks of the BWUMV correlation were performed. These calculations were done to determine how well the BWUMV correlation reproduces predicted results, to determine the behavior of the BWUMV correlation over a range of pressure

flow rate and quality, and to compare the BWUMV to the BWCMV correlation since they were developed from the same database for the most part.

In general, the numerical checks show that the BWUMV and the BWCMV correlations are in agreement within the statistical uncertainty band. Some differences in the results are noted in cases where the flow is varied over the BWCMV range of validity. These differences are more significant when the pressure is at 1500 and 1800 psia. Evaluations performed where the pressure is varied over the BWCMV range of validity also show some difference between the two correlations.

The statement is made in Appendix I that the Tong factor is set equal to one in the RELAP5/MOD2 B&W implementation of BWUMV. In discussions with BWNT they stated that the Tong factor is included in the development of the BWUMV correlation. It is during the SBLOCA transient analysis that the Tong factor is set equal to 1. BWNT also indicated that their standard practice is to set the Tong factor equal to 1 for LOCA analysis and indicated several references where this practice has been previously approved.

Based on this review, it is concluded that the BWUMV correlation is acceptable for used in RELAP5/MOD2 B&W subject to the restriction that the correlation should not be used below pressures of 1300 psia.

3.1.8 SBLOCA EM Benchmark

BWNT performed a benchmark using RELAP5/MOD2 B&W against a SBLOCA experiment performed at the ROSA-IV facility in 1988. The ROSA-IV facility simulates a recirculating steam generator plant. The results of this benchmark are presented in Appendix J to BAW-10164P. It is important to note that this is not the only benchmark of RELAP5/MOD2-B&W for a SBLOCA. As noted in appendix J, the peak clad temperatures during the experiment are not significant relative to the acceptance

criteria. Benchmarks against LOFT and Semiscale SBLOCA data, presented in Section 5 of BAW-10164, provide additional coverage of SBLOCA phenomenology, including clad temperature prediction. This benchmark serves to show that the additional models for SBLOCA, such as CCFL and Wilson drag, are performing correctly and will adequately predict test data.

The RELAP5/MOD2-B&W model for ROSA-IV, and other benchmarks and applications models, use equilibrium thermodynamics nodes in the core region and non-equilibrium nodes in the remainder of the system. Since the RELAP5/MOD2 Code Manual specifically states that equilibrium nodes cannot be connected to non-equilibrium nodes, BWNT was questioned on node connectivity. In their response BWNT stated that RELAP5/MOD2 has always been fully capable of connecting equilibrium and non-equilibrium nodes, and that this is consistent with the approved EM core modeling. This was confirmed by INEL (the RELAP5 code development organization), that the equilibrium option is obtained using the same basic equations with the interphase heat transfer coefficient set to a very high value. This assures that sufficient heat transfer will occur to keep both phases at saturation conditions. Contrary to the statements in the code manual, it is possible to connect equilibrium and non-equilibrium nodes without adversely affecting the calculational algorithms. BWNT uses equilibrium nodes in the core region to obtain saturation fluid temperature as the boundary condition for the core heat transfer correlations, which were developed on this basis.

When modeling complex systems, it is sometimes necessary to slightly modify the representation to compensate for code model limitations. BWNT used two such modifications in their representation of the ROSA-IV facility. First, the friction factor for the accumulator injection line was increased by a factor of 100 above the nominal value, to eliminate unrealistic injection flow oscillations. Also, the angle of the inlet pipe to the steam generator plenum was decreased to less than 15 degrees to permit use of the horizontal pipe stratification model. BWNT provided justification for these

model modifications. In both cases, the BWNT responses adequately explained the need for modifications to overcome code limitations.

BWNT performed a time step sensitivity study which demonstrated that the 0.05 second time step used for the calculations was adequate.

Results of the calculations showed that the basic thermal-hydraulic phenomena which occurred during the SBLOCA were predicted with reasonable accuracy. Key events were predicted to occur in essentially the correct sequence. Differential pressures in the core and recirculation loops, key determinants of the flows, were adequately predicted. This benchmark further demonstrates that the RELAP5/MOD2-B&W computer program is capable of predicting the important thermal-hydraulic phenomena which occur during a SBLOCA in a recirculating steam generator plant.

3.2 BAW-10164P, Revision 3

3.2.1 Revision to the Slug Flow Drag Model

BWNT incorporated a third option for evaluating the Taylor bubble interphase drag in slug flow. The three models now available are the base INEL model, the Wilson drag model submitted with Revision 2 of BAW-10164P, and the B&W modified slug-drag model, as described on pages 2.1-52.4 and 2.1-52.5 of Revision 3 of BAW-10164P. (The Wilson drag model was reviewed in Section 3.1.1 above).

In the B&W modified slug-drag model, adjustments are made to the interphase friction terms through the use of empirically derived coefficients. BWNT states that these adjustments were based on numerous benchmarks. BWNT listed the benchmarks used which included those documented in Appendices K and L to BAW-10164P. These benchmarks are discussed in Sections 3.2.7 and 3.2.8 of this evaluation.

3.2.2 Modifications to the Chen Heat Transfer Coefficient

The saturated nucleate boiling heat transfer coefficients used in RELAP5/MOD2-B&W are calculated using the Chen heat transfer correlation to model the boiling component of the heat transfer coefficient. The Chen heat transfer correlation employs a nucleate boiling suppression factor S. S was modified by including a multiplicative weighing factor to force S, and the boiling heat transfer coefficient to zero as the steam void fraction approaches one. B&W notes that this ramp is needed for once-through steam generator applications to preclude sharp increases in S that result in disproportionally high overall heat transfer as the void fraction approaches one.

3.2.3 Incorporation of the Becker CHF Model

The Becker CHF correlation for rod bundles is incorporated into RELAP5/MOD2-B&W as described in Section 2.2.2.2 of Revision 3 of BAW-10164P. BWNT states that this correlation was used to obtain better predictions of secondary side heat transfer relative to the Biasi-Zuber correlation used in RELAP5/MOD2 at power levels below 80 percent of full power. The Becker CHF correlation is used up to a pressure of 90 bar (1306 psia). Linear interpolation between the Becker and Biasi-Zuber correlations is performed between 80 and 90 psia to obtain a smooth transition between the two correlations.

Benchmarks comparing results of RELAP5/MOD2-B&W to OTSG test data are presented in Appendix K of BAW-10164P and are discussed in Section 3.2.7 of this SER. These benchmarks show good agreement between RELAP5/MOD2-B&W results using the Becker CHF correlation and the OTSG test data as discussed in Section 3.2.7.

3.2.4 EM Pin Model Modifications

BWNT enhanced the fuel pin model in RELAP5/MOD2-B&W by adding features which had previously been approved for use in the FRAP-T6-B&W[14] and TACO3[15] computer programs. These changes are discussed in Section 2.3.2 of Revision 3 of BAW-10164P. There are three basic areas in which the fuel pin model provides calculations: dynamic fuel/clad gap conductance, fuel rod swelling, and rupture based on the NUREG-0630[16] approach and clad metal-water reaction. Enhancements in Revision 3 include addition of a closed gap contribution to gap conductance to allow modeling of high burnup cases, fuel pin axial expansion, automated clad rupture calculation, implicit metal-water reaction option and automated steady-state gap multiplier option.

The RELAP5/MOD2-B&W enhanced fuel pin model has some differences compared to the previously approved models in FRAP-T6-B&W and TACO3. These are due to the less detailed nature of the model used in RELAP5/MOD2-B&W compared to the fuel performance codes.

The previously approved gap conductance model allowed for modeling of a non concentric fuel stack within the clad, but did not include a contact conductance term in the calculation of total gap conductance. The option to include a contact resistance contribution has been added based upon the model presently used in the TACO3 computer program. Since Appendix K does not prohibit the use of contact resistance, this model is acceptable for cases of high burnup fuel with a closed gap.

The gap gas pressure is used to determine the amount of clad swelling and rupture. One of the variables which determines the gap gas pressure is the amount of volume available for the gas to occupy. A portion of this volume is located in the gas plenum at the top of each fuel rod. When the clad and fuel expand axially at different rates the volume of the plenum will change. The axial expansion model accounts for this

change in plenum volume due to differential thermal expansion of the fuel and clad from the cold condition. Thermal strain correlations from MATPRO[17], or user input fits, are used to determine the amount of fuel and clad axial expansion. Including the effects of axial fuel rod expansion on plenum volume is appropriate for a best-estimate calculation, and is acceptable for Appendix K to 10 CFR 50 LOCA analysis, which does not prohibit including this model. Only minimal differences exist between the enhanced fuel pin model and the FRAP-T6-B&W model. The enhanced model is acceptable for use in ECCS evaluation model calculations.

Addition of an automated clad rupture model introduces heat transfer enhancement downstream of a rupture location. The model used for this option has been previously approved for use in the BEACH computer program. This option automates the calculation of rupture location for use in BEACH. Use of this model in RELAP5/MOD2-B&W is consistent with the Appendix K to 10 CFR 50 approved model and is, therefore, acceptable.

An implicit formulation of the Baker-Just metal water reaction model has been implemented in RELAP5/MOD2-B&W. The model is the same as that which is used in the FRAP-T6-B&W computer code. Appendix K to 10 CFR 50 requires use of the Baker-Just model but does not specify the numerical solution technique to be used. The implicit solution will improve accuracy for calculations which use a larger time step. Use of this option is acceptable for compliance with Appendix K to 10 CFR 50.

Initialization of the RELAP5/MOD2-B&W model must comply with Appendix K to 10 CFR 50 in the sense that initial stored energy in the fuel must be conservatively specified. This is done by adjusting the fuel clad gap conductance to obtain the desired value of volume average fuel temperature. In earlier versions of the program a user specified multiplier on the gas conductance term of the gap conductance was provided to permit adjustment and matching of volume average fuel temperature. This required that an iterative process be performed by the user. An option has been

added to automate this iteration process. The user can specify the desired volume average fuel temperature, rather than the multiplier on the gas conductance term, and the code will iterate to determine the gas conductance multiplier. This is a user convenience feature which is acceptable for ECCS evaluation model calculations.

3.2.5 EM Heat Transfer Model Modifications

BWNT incorporated a filtered flow option to be used with the core heat transfer model. This option was added to facilitate addressing the Appendix K to 10 CFR 50 requirement to eliminate any calculated rapid flow oscillations with a period of less than 0.1 seconds during the LBLOCA blowdown phase. This requirement is mandated because rapid flow oscillations can cause overprediction of the amount of energy removed from the core which would cause peak clad temperature to be underpredicted. The method, described in Section 2.3.3 of BAW-10164P, is consistent with the requirements of Appendix K to 10 CFR 50.

3.2.6 Post-CHF Model Modifications

User defined correction factors were added to the equation used to determine the total wall-to-fluid heat flux due to transition boiling as shown on page 2.3-86 of Revision 3 to BAW-10164P. These constants are defined as $C1_{TR}$ and $C1_{TR1}$ which have a default value of 1.0. BWNT did not identify any benchmarks that used values other than 1.0 for these correction factors.

A user option was added to allow adjustment of the surface heat transfer coefficient following cladding rupture of a fuel pin on page 2.3-89 of Revision 3 to BAW-10164P. If this option is invoked, the heat flux in a ruptured segment single heat structure is multiplied by the ratio of the ruptured to cold outside cladding radius. The heat flux is then computed using the increased surface area resulting from clad swelling and

rupture. This change is physically realistic and does not violate Appendix K requirements. It is, therefore, acceptable.

3.2.7 OTSG Benchmarks

BWNT performed two benchmarks of the RELAP5/MOD2-B&W code to demonstrate the adequacy of the OTSG modelling. These benchmarks are discussed in Appendix K to BAW-10164P. The first set of benchmarks are comparisons to steady-state tests performed in 1969 to demonstrate the ability of the code to predict the shell side nucleate boiling length at various power levels. The second benchmark is a comparison to a loss of feedwater flow test performed in 1977 to demonstrate the ability of the code to predict boil-down and refill of a OTSG.

The tests were performed at the Alliance Research Center (ARC) Nuclear Steam Generator Test Facility. This facility provided the capability of testing steam generators at full system pressure and temperature conditions. The primary side of the test loop consisted of a gas-fired furnace to simulate reactor heat input into the primary fluid, a pressurizer, flow control valves, flow measuring elements, and a water conditioning system. The secondary system was a closed circuit test loop consisting of steam flow control valves, steam flow measuring equipment, feedwater heaters, back pressure control valves, a flash tank, circulating pumps, feedwater control valves, feedwater flow measuring equipment, feedwater flow bypass valves, and a water conditioning system.

The model steam generator used for these benchmarks, referred to as the 19-tube OTSG, is a single pass, counterflow, tube and shell heat exchanger. The tube bundle consisted of 19 full length tubes, each 5/8 inch diameter, spaced on a triangular pitch on 7/8 inch centers. Primary inlet flow entered at the top of the steam generator, flowed downward through the tube bundle and exited at the bottom. Secondary feedwater flow entered the tube bundle at the bottom, was boiled as it passed by the

outside of the tube bundle, and exited at the top. The feedwater was raised to saturation conditions by mixing the water with steam from the tube region via a steam bleed pipe connected from the secondary side of the generator to the steam/feedwater mixer. A question on where the feedwater temperature is measured was raised. BWNT stated that the feedwater temperature is measured with a thermocouple located approximately three feet upstream of the steam/feedwater mixer.

In the steady state tests, boiling length (dryout location) was determined from primary tube and secondary side thermocouples for a range from 0 to 100 percent of the full scaled power consistent with a 2700 MWth plant. The loss of feedwater flow test initialized to full scaled power consistent with a 2772 MWth plant. The test was initiated by the simultaneous trip of the feedwater pump and closure of the feedwater isolation valve. The steam generator was allowed to boil dry and then the feedwater was restarted. Secondary steam flow and temperature and primary outlet temperature were measured during the test.

The RELAP5/MOD2-B&W model utilized 11 axial control volumes in the primary tube region and in the secondary shell region. Primary to secondary heat transfer was modelled using eleven heat structures between the primary and secondary sides. The external downcomer was modeled with five axial control volumes that represented the piping from the steam/feedwater mixing region to the tube bundle inlet. Feedwater aspiration was provided by a single junction component that connected the tube bundle region to the external downcomer. A junction connection between the shell side of the heat exchanger and the control volume representing the steam/water mixer is included in the model. Time dependent volume and time dependent junction components were used to set inlet flowrate and temperature of the primary and secondary side coolant.

A question on the modeling of the steam/feedwater mixing or aspiration process, addressed the relative pressures between the control volume representing the mixer

and the volume representing the source of aspiration steam from the secondary to the mixer. Assuming a normal flow junction connecting these volumes, the pressure in the secondary must be higher than the mixer in order to provide steam flow to the mixer. BWNT responded that the bundle collapsed liquid level remains below the downcomer level (presumably below the level of the steam/feedwater mixer) during the tests. As a result the pressure gradient that sustains the steam flow from the secondary is maintained by manometric effects. BWNT also noted that this process is self-governing due to changes in the pressure gradient as the downcomer fluid approaches saturation.

BWNT employed some of the features incorporated into RELAP5/MOD2-B&W for the 19-tube OTSG benchmark. These features are summarized below:

- The Becker critical heat flux correlation, discussed in Section 3.2.3, are used on the shell side of the tube heat structure,
- The multipliers defined by the B&W modified slug-drag model and the annular mist model are used, and
- A linear ramp was applied to the Chen boiling suppression factor. This adjustment to the suppression factor was discussed in Section 3.2.2.

The first set of results for the steady state benchmark compared the boiling lengths predicted by RELAP5/MOD2-B&W to those measured during the 19-tube OTSG tests. BWNT presented tabulated results and a plot comparing the boiling length above the lower tube sheet predicted by RELAP5/MOD2-B&W to the 19-tube OTSG tests at power levels ranging from 20 to 100 percent of the scaled power levels relative to a 2700 MWth plant. The results show that the boiling lengths predicted by RELAP5/MOD2-B&W are in good agreement with the test data. In contrast, results from RELAP5/MOD2 Cycle 36.05 also shown on these plots, differ significantly from the test data below 80 percent scaled power. BWNT attributes this agreement in the

boiling length results between RELAP5/MOD2-B&W and the 19-tube OTSG test to the use of the Becker critical heat flux correlation.

For the LOFW benchmark, BWNT presented comparison plots between RELAP5/MOD2-B&W and 19-tube OTSG data for steam flow rate and the primary outlet temperature after the initiation of the LOFW transient. Plots of the primary and secondary system fluid temperatures prior to the initiation of the LOFW test are also presented to show initial conditions. The plots of steam flow rate and primary outlet temperature show that the magnitude and trend of the results are in good agreement between RELAP5/MOD2-B&W and the 19-tube OTSG test.

BWNT was requested to provide comparison plots between RELAP5/MOD2-B&W and 19-tube OTSG data comparing steam generator secondary level or mass. In their response, BWNT noted that determination of collapsed liquid level is difficult to obtain under two phase high flow conditions. BWNT did provide comparisons of the steady state and transient differential pressure in the boiler. The response of BWNT to this question was reviewed and found adequate.

3.2.8 MIST Benchmarks

As part of their evaluation of the Revision 3 modifications to the RELAP5/MOD2-B&W code, BWNT included an integral system benchmark of a SBLOCA for a simulated reactor system using OTSGs. BWNT included this benchmark as a further check of the modifications made to reduce interphase drag in the slug flow regime (Wilson bubble rise model) and in the annular flow regimes.

The integral system benchmark was performed using data from the Multi-Loop Integral System Test (MIST) facility which is a scale model of a B&W lowered-loop 177 fuel assembly pressurized water reactor. The MIST facility is designed to operate at pressures and temperatures typical of an operating B&W plant. The MIST facility

consists of two 19-tube once-through steam generators, a reactor vessel with a heated core and external downcomer, pressurizer with a power operated relief valve, two hot legs and four cold legs. Further information on facility scaling and instrumentation is found in Appendix L to BAW-10164P.

BWNT notes in Appendix L to BAW-10164P, that a number of pre- and post-test predictions have been made for MIST tests using the RELAP5/MOD2 code as a part of the MIST program. These predictions were made with earlier versions of the code, which did not include the recent modifications. The benchmark presented in Appendix L includes a comparison of experimental data with RELAP5/MOD2 results obtained with both the current and earlier versions of the code. This allows an evaluation of the effects of the recent model changes, in particular upon the prediction of collapsed liquid level in the reactor vessel and steam generator secondary. The results show that the code modifications clearly improve the collapsed liquid level predictions.

The RELAP5/MOD2-B&W model simulates the MIST reactor vessel, downcomer, hot and cold legs, OTSGs, reactor coolant pumps, and other major components. A double flow path connection to the external reactor vessel downcomer is used in this model so that countercurrent two-phase flow can be predicted. The steam generator modelling employs two radial regions to account for tubes directly wetted by auxiliary feedwater (AFW) injection on the shell side of the steam generator. The other region represents the 16 tubes in contact with secondary steam. BWNT notes in their response that the BWNT modified slug-drag model was employed in the core and primary tube region. For the secondary side of the steam generator tube region, the BWNT slug-drag model is used on the annular mist drag.

In the RELAP5/MOD2-B&W model, the core region was modified so that twenty control volumes represent the full height core. BWNT states that this noding is necessary for consistency with the revised models. BWNT was requested to discuss the implications of increasing the number of core volumes focusing on the degree of

improvement resulting from the use of the new interphase drag model as compared to just increasing the number of core nodes.

BWNT performed a noding sensitivity study based on ORNL THTF Test 3.09.10j discussed in Appendix H to BAW-10164P. In this study, BWNT ran cases using 4 and 24 nodes in the core region using both the INEL drag model and the BWNT slug-drag model. Plots presented by BWNT show good agreement between the RELAP5/MOD2-B&W results using the BWNT slug-drag model for both the 4 and 24 node core models and the THTF data. The results from the INEL model show poor agreement with the THTF data. BWNT notes in their response that the INEL model is known to overpredict the interphase drag in heated regions with small hydraulic diameters. In this context, the BWNT response regarding the nodalization of the steam generator secondary was reviewed and is acceptable.

MIST test 320201, used for the RELAP5/MOD2-B&W benchmark, simulated a scaled 50 cm^2 pump discharge break. This is reported by BWNT to be the most limiting small break size for B&W designed plants. The MIST facility was initialized in natural circulation mode with the core power scaled to 3.5 percent for this test. BWNT noted that since the MIST facility was capable of only ten percent full-scaled power operation, the facility was initialized to conditions corresponding to 145 seconds after trip. Other initial conditions include primary system pressure corresponding to 22° F core exit subcooling, pressurizer level of 5 feet above the bottom of the pressurizer, steam generator pressure of 1010 psia, and a steam generator secondary level controlled to five feet above the lower tube sheet by throttling high elevation AFW injection.

The MIST test was initiated by turning off the pressurizer heaters and opening the leak. When the pressurizer level reached one foot, full high pressure injection flow was started and steam generator secondary refill using full capacity AFW was initiated.

BWNT presented comparison plots between RELAP5/MOD2-B&W and MIST for primary pressure, secondary pressure, reactor vessel liquid level and secondary liquid level. A tabulation of the timing of key events is presented in Table L.2 of BAW-10164P. Additional information was provided on the elevation of the steam generators and reactor vessel at the MIST facility. The results for BWNT Versions 5 and 14 of RELAP5/MOD2-B&W are presented. The main difference in these code versions is that Version 14 utilizes the revised interphase drag models.

In general, there is good agreement between the RELAP5/MOD2-B&W Version 14 results and the MIST data. BWNT noted that the improved prediction of reactor vessel and secondary liquid levels is due to the revised slug drag model. The large difference in timing of the hot leg voiding between Revisions 5 and 14 of RELAP5/MOD2-B&W was questioned. BWNT attributed this to differences in the initial temperature conditions in the pressurizer and surge line used in the Revision 5 and Revision 14 calculations. BWNT also revised Table L.2 which corrects the reported time of operator actions.

In reviewing the MIST benchmark, it is noted that no fuel rod temperature excursion occurred during this test. This issue was discussed with BWNT. BWNT responded that the mixture level in the vessel remained above the core during the test, resulting in removal of the stored energy in the fuel by nucleate boiling. In view of this lack of core uncovery, BWNT noted that MIST is not the best benchmark for the core mixture level calculation. The stand-alone FOAM2 and ORNL benchmarks presented in Appendix H to BAW-10164P were provided to better address the code's predictive capability.

MIST benchmarks address the capability to predict system pressure, liquid inventory and liquid distribution. In this respect, the MIST test 320201 benchmark demonstrates that the modifications made to the code improve its predictive capability in these areas. When considered along with the other benchmarks, including additional MIST

benchmarks, BWNT has demonstrated that RELAP5/MOD2 B&W is capable of adequately predicting the system response for an OTSG plant.

In discussing cladding temperature during an SBLOCA, BWNT argues that the cladding temperature excursion during SBLOCA is governed by the same physical processes for all current PWR designs. During core boildown, the vapor temperature and fuel cladding heat transfer are dependent upon local mechanisms and not upon integral system parameters. Therefore, heatup during core boiloff depends upon the core geometry, but not the integral system geometry. Benchmarks against ROSA-IV, ORNL and Semiscale test data are hence acceptable for demonstrating that RELAP5/MOD2-B&W is capable of adequately predicting fuel clad temperatures during this heatup phase.

3.3 High Auxiliary Feedwater Model

BWNT developed the high auxiliary feedwater model to calculate the B&W OTSG heat transfer correctly during auxiliary feedwater injection from high elevation locations. This model was included in the Revision 1 submittal but was not reviewed because B&W did not intend to use RELAP5/MOD2-B&W for OTSG analysis at that time as noted in Section 5 of the Revision 1 safety evaluation report. BWNT requested a review of this model and has provided additional information to support this request.

The high auxiliary feedwater model was reviewed as part of the CRAFT2 code Topical Report transmittal in 1985. This report included several benchmarks against plant and experimental data. BWNT has made some modifications to the heat transfer models since that time. Therefore, an additional RELAP5/MOD2-B&W benchmark of the revised heat transfer models against test data from the MIST facility was provided by BWNT. Included is a plot comparing RELAP5/MOD2 predicted primary side temperature as a function of elevation above the tube sheet against steady-state MIST measurements. This plot shows good agreement between the RELAP5/MOD2 B&W

predictions and the MIST measurements along the length of the steam generator tubes. The steady-state nature of this test allowed the calculated heat transfer coefficients used in the model to be justified. The high AFW model was also used for the additional MIST benchmarks performed by BWNT. These serve to demonstrate the adequacy of the model for transient applications.

Based upon the discussions and benchmarks provided by BWNT, it is concluded that the revisions to the high auxiliary feedwater model have not changed significantly from the model previously accepted. Therefore, we find it acceptable for use in SBLOCA analysis.

3.4 Parameters Used in RELAP5/MOD2-B&W Benchmarks

BWNT has incorporated a number of user specified input parameters in RELAP5/MOD2-B&W. The value of these parameters used in the RELAP5/MOD2 B&W benchmarks are listed in Table 1 of this evaluation. The values of these parameters were selected to improve the agreement between RELAP5/MOD2-B&W and the FOAM2, THTF, OTSG, and MIST benchmark data. The values of the user specified parameters listed in Table 1 are the only acceptable values for LOCA licensing calculations.

One of the motivations driving the initial development of the RELAP5 code was the need to eliminate user choice of modeling options and input dials. When an analysis is performed with RELAP5, one can be certain of what models and fitting parameters are used. The addition of numerous options and dials by BWNT is contrary to this characteristic of RELAP5. The last condition listed above is intended to eliminate the use of user specified dials in keeping with the intent of the RELAP5 approach.

Table 1
Summary of User Specified Parameters Used in the
RELAP5/MOD 2-B&W Benchmarks

Parameter	Description	Page Where Parameter Is Described	Affected Benchmark
C_{WB}	Multiplier on bubble velocity in the Wilson Bubble Rise Model	2.1-52.3 (Revision 2)	FOAM2 code, ORNL THTF tests (Appendix H)
C_{WSL}	Multiplier on the interphase drag predicted for slug flow	2.1-52.3 (Revision 2)	FOAM2 code, ORNL THTF tests (Appendix H)
xms	Multiplier on the interphase drag computed for annular mist flow	2.1-53 (Revision 2)	OTSG benchmarks (Appendix K), MIST benchmarks (Appendix L)
xsg	High void fraction slug coefficient	2.1-52.5 (Revision 3)	OTSG benchmarks (Appendix K), MIST benchmarks (Appendix L)

Table 1
Summary of User Specified Parameters Used in the
RELAP5/MOD 2-B&W Benchmarks

Parameter	Description	Page Where Parameter Is Described	Affected Benchmark
α_s	Low end of void fraction for adjustment	2.1-52.5 (Revision 3)	OTSG benchmarks (Appendix K), MIST benchmarks (Appendix L)
α_{sh}	High end of void fraction for adjustment	2.1-52.5 (Revision 3)	OTSG benchmarks (Appendix K), MIST benchmarks (Appendix L)
xslg	Slope of drag pressure term	2.1-52.5 (Revision 3)	OTSG benchmarks (Appendix K), MIST benchmarks (Appendix L)
cxslg	x-intercept for pressure term	2.1-52.5 (Revision 3)	OTSG benchmarks (Appendix K), MIST benchmarks (Appendix L)

Table 1
Summary of User Specified Parameters Used in the
RELAP5/MOD 2-B&W Benchmarks

Parameter	Description	Page Where Parameter Is Described	Affected Benchmark
α_{gr}	Void fraction at which to begin the S ramp	2.2-22 (Revision 3)	OTSG benchmarks (Appendix K)
$C1_{TR}$, $C1_{TR1}$	User multiplicative constants used in the equation to determine wall-to-fluid heat flux during transition boiling.	2.3-86 (Revision 3)	

5-394

4.0 COMPLIANCE WITH NRC REQUIREMENTS

Appendix K to 10-CFR-50 specifies required and acceptable features of ECCS evaluation models. Previous revisions of the RELAP5/MOD2-B&W program, through Rev. 1, have been reviewed and found to satisfy the requirements of Appendix K when used with the approved B&W ECCS methodology, subject to any restrictions cited in the SER.

The modifications documented in Revisions 2 and 3 of BAW-10164P do not affect compliance with any of the required features of Appendix K. Modifications of the fuel pin model are such that the requirements of Appendix K continue to be satisfied. Inclusion of a contact conductance term in the calculation of fuel clad gap conductance does not affect compliance with Appendix K which states that "thermal conductance of the gap between the UO_2 and the cladding shall be evaluated as a function of the burnup, taking into consideration fuel densification and expansion, the composition and pressure of the gases within the fuel rod, the initial cold gap dimension with its tolerances, and cladding creep." Section B of Appendix K also specifies that "The gap conductance shall be varied in accordance with changes in gap dimensions and any other applicable variables."

Inclusion of axial thermal expansion of the cladding and fuel in the gas plenum volume calculation also does not affect compliance with Appendix K. The plenum volume is used in the calculation of internal rod pressure which is a key determinant of the amount of swelling and rupture. Appendix K requires that "the swelling and rupture calculations shall be based on applicable data in such a way that the degree of swelling and incidence of rupture are not underestimated." Calculation of gas gap pressure using plenum volume which accounts for axial thermal expansion of the fuel and cladding improves accuracy and should not result in underestimating the pressure or the incidence of swelling and rupture.

Appendix K specifies that the Baker-Just model be used to calculate the metal-water reaction rate, but does not specify the solution method. Therefore, the implicit solution technique is acceptable, given that it yields a mathematically correct solution of the required equation. Appendix K also requires that "The degree of swelling and rupture shall be taken into account in calculations of gap conductance, cladding oxidation and embrittlement, and hydrogen generation." The "swelled radius" modification to the metal-water reaction model accounts for the increase in clad radius, and hence surface area, due to swelling. This model change affects the hydrogen generation and cladding oxidation, and is in compliance with the Appendix K requirements listed above. The iterative technique for determining a multiplier on gap conductance which yields a desired initial stored energy is a user convenience feature which does not affect the previously approved model.

Section C.4.e of Appendix K to 10 CFR 50 states: "After CHF is first predicted at an axial fuel rod location during blowdown, the calculation shall not use nucleate boiling heat transfer correlations at that location subsequently during the blowdown even if the calculated local fluid and surface conditions would apparently justify the reestablishment of nucleate boiling. Heat transfer assumptions characteristic of return to nucleate boiling (rewetting) shall be permitted when justified by the calculated local fluid conditions during the reflood portion of a LOCA." The core heat transfer selection model modifications assure that no return to nucleate boiling will occur before the end of blowdown for the large break LOCA. Since the definitions of blowdown and reflood are inappropriate for SBLOCA, it is acceptable to bypass this "no return to nucleate boiling" requirement in that case. The modification is therefore in compliance for LBLOCA analysis, and acceptable for the SBLOCA analysis where the requirement is inappropriate.

CHF correlations acceptable for use in LOCA analysis are listed in Sections C.4.b and d. Section C.4.a states that "Correlations developed from appropriate steady-state and transient-state experimental data are acceptable for use in predicting the critical

heat flux (CHF) during LOCA transients. The computer programs in which these correlations are used shall contain suitable checks to assure that the physical parameters are within the range of parameters specified for use of the correlation by their respective authors". As discussed in Section 2.1.7 of this report, the BWUMV CHF correlation has been developed using appropriate experimental data for fuel with mixing vanes. The correlation is therefore acceptable for use within the ranges of parameters specified. It is noted that BWNT requested that the correlation be approved for pressures down to 750 psia. Based upon the data comparison provided by BWNT, the staff concludes that the correlation is acceptable down to pressures of 1300 psia and mass fluxes of 500,000 lb/hr-ft^2. Checks which restrict use of the correlation to this range must be included in RELAP5/MOD2-B&W for the code to be acceptable.

Benchmarks against calculations of the approved computer program FOAM2 and THTF experimental test data have shown that addition of the Wilson drag model improves predictions of void distribution in the core region. Appendix K does not list specific requirements in this area. The modification, which improves modeling accuracy, is therefore acceptable. A number of the other code enhancements fall into this same category. They cover areas where Appendix K does not specify required features. These include the annular mist flow regime overall drag multiplier, condensation heat transfer correlation modifications, Wilson slug flow drag model, and the CCFL model. Appropriate justification has been provided to show that these enhancements improve modeling accuracy.

5.0 CONCLUSIONS AND LIMITATIONS

Modifications made to RELAP5/MOD2-B&W as described in Revisions 2 and 3 of BAW-10164P have been reviewed and evaluated. Based on the benchmarks presented, the staff finds that the models described in version 19 of RELAP5/MOD2-B&W to be acceptable for LOCA and non-LOCA analysis for PWRs with recirculating and OTSGs subject to the following limitations:

- Use of the Wallis and UPTF parameters at the tube bundle and steam generator plenum inlet are acceptable. The parameters used in the CCFL model for any other application must be validated, and the validation reviewed and approved by the staff for that application (see section 3.1.3 of this evaluation).
- The BWUMV correlation is limited to pressures above 1300 psia.
- For large break LOCA ECCS evaluation model calculations, form losses due to ruptured cladding should not be excluded using the user option described in Section 3.2.4 of this evaluation.
- The value of the user specified parameters listed in Table 1 of this evaluation (i.e. those used for the benchmark calculations) are the only acceptable values for LOCA licensing calculations.

Table 2 lists typographical errors that were found during the course of this review. Correction of these errors should be incorporated into the approved version of BAW-10164P. The automated blockage droplet breakup calculation, the implicit formulation of the Baker-Just metal water reaction model and the fuel rod Evaluation Model improvements referred to in Section 5 of the BEACH safety evaluation report[16] were reviewed in this evaluation and found acceptable. Contingency 4 given in Section 5 of the BEACH safety evaluation report is no longer applicable. That contingency states: "Use of the automated blockage droplet breakup calculation, implicit formulation of the Baker-Just metal water reaction model and the fuel rod Evaluation Model (EM)

improvements should be made contingent upon their approval in Revision 3 of BAW-10164P, which describes these updates."

Table 2
Summary of Changes That Should Be Made To The
Approved Version of BAW-10164, Revision 2 and 3

Affected Report Revision and Section	Change Summary
Revision 2, Appendix H, Figure H.1	Correction to Figure H.1 in response to Question 2 of the Revision 2 RAI
Revision 2, Appendix H, Table H.2	Correction to Table H.2 in response to Question 4 of the Revision 2 RAI
Revision 2, Section 2.3.3 and Appendix I	Correction to Equation I-1, I-2 and pressure and mass flux units in response to Questions 5, 6, and 7 of the Revision 2 RAI
Revision 2, Appendix I, Table I.3	Duplication in point numbers in Test 160 (point 789) and Test 164 (points 2060 and 2065) should be corrected or clarified.
Revision 2, Appendix J, Page J-8	Reference to Table 2 should be Table J.2 per Question 11 of the Revision 2 TER
Revision 3, Section 2.3.2	Correction of ε_{TC} value on Table 2.3.2-2 in response to Question 4 to the Revision 3 RAI.
Revision 3, Page 2.3-46	Correction to β^2 definition in text in response to Question 5 of the Revision 3 RAI. Other correction noted by BWNT on Page 2.3-36 should also be included.
Revision 3, Appendix L, Table L.1	Revision to Table L.1 in response to Question 10 of the Revision 3 RAI.
Revision 3, Appendix L, Table L.2	Revision to Table L.2 in response to Question 11 of the Revision 3 RAI.

5.0 REFERENCES

1. Ransom, V. H., et. al., RELAP5/MOD2 Code Manual -- Volume 1: Code Structures, System Models and Solution Methods and Volume 2: Users Guide and Input Requirements, NUREG/CR-4312 - Volume 1, August, 1985 and NUREG/CR-4312 - Volume 2, December 1985.

2. B&W Nuclear Technologies, RELAP5/MOD2-B&W -- An Advanced Computer Program for Light Water Reactor LOCA and non-LOCA Transient Analysis, BAW-10164P, Revision 1, October 1988.

3. Letter from A. C. Thadani (USNRC) to J. H. Taylor (B&W Nuclear Technologies), Acceptance for Referencing of Topical Report BAW-10164P, Revision 1, RELAP5/MOD2-B&W, An Advanced Computer Program for Light Water Reactor LOCA and Non-LOCA Transient Analysis, April 18, 1990.

4. Code of Federal Regulations, ECCS Evaluation Models, Chapter 10, Part 50, Appendix K

5. B&W Nuclear Technologies, RELAP5/MOD2-B&W -- An Advanced Computer Program for Light Water Reactor LOCA and Non-LOCA Transient Analysis, BAW-10164P, Revision 2, August 1992.

6. B&W Nuclear Technologies, RELAP5/MOD2-B&W -- An Advanced Computer Program for Light Water Reactor LOCA and non-LOCA Transient Analysis, BAW-10164P, Revision 3, October 1992.

7. Letter from J. H. Taylor (B&W Nuclear Technologies) to R. C. Jones (USNRC), BEACH Topical Report BAW-10166P, JHT/93-214, August 31, 1993.

8. Letter from J.H. Taylor (B&W Nuclear Technologies), Response to NRC's Request for Additional Information on BAW-10164, Revision 2, August, 1992; RELAP5/MOD2-B&W, An Advanced Computer Program for Light Water Reactor LOCA and NON-LOCA Transient Analysis, JHT/93-279, November 16, 1993

9. Letter from J.H. Taylor (B&W Nuclear Technologies), Response to NRC's Request for Additional Information on BAW-10164, Revision 3, October, 1992; RELAP5/MOD2-B&W, An Advanced Computer Program for Light Water Reactor LOCA and NON-LOCA Transient Analysis, JHT/94-7, January 21, 1994

10. Letter from J.H. Taylor (B&W Nuclear Technologies), Response to NRC's Supplemental Request for Additional Information on BAW-10164, Revision 2, August, 1992; RELAP5/MOD2-B&W, An Advanced Computer Program for Light Water Reactor LOCA and Non- LOCA Transient Analysis, JHT/94-146, September 20, 1994.

11. B&W Nuclear Technologies, FOAM2 – Computer Program to Calculate Core Swell Level and Mass Flow Rate During Small Break LOCA, BAW-10155A, October 1990.

12. Collier, John G., Convective Boiling and Condensation, Mc-Graw-Hill International Book Company, 2nd. edition, 1972

13. B&W Fuel Company, Correlation of Critical Heat Flux in Mixing Vane Grid Fuel Assemblies, BAW-10159P-A, July 1990

14. B&W Nuclear Technologies, FRAP-T6-B&W - A Computer Code for the Transient Analysis of Light Water Reactor Fuel Rods, BAW-10165P, October 1988.

15. B&W Nuclear Technologies, TACO3 - Fuel Pin Thermal Analysis Computer Code, BAW-10162P-A, October 1989.

16. D.A. Powers and R.O. Meyers, Cladding Swelling and Rupture Models for LOCA Analysis, NUREG-0630, April, 1980

17. D.L. Hagrman, et. al., MATPRO - Version 11 (Revision 2), NUREG/CR-4079, August 1981

18. D.A. Prelewicz, Technical Evaluation Report - BEACH - Best Estimate Analysis Core Heat Transfer, A Computer Program for Reflood Heat Transfer During LOCA, BAW-10166P, Revision 4, SCIENTECH, Inc., SCIE-NRC-219-93, November, 1993

5.0 LICENSING DOCUMENTS

This section contains documents generated as a result of U.S. Nuclear Regulatory Commission (NRC) review of previous versions of this topical report. Sections 5.1 and 5.2 contain responses to rounds one and two questions, respectively, for revision 1 of this report. These documents were previously issued in the approved proprietary and non-proprietary versions as appendices H and I. Section 5.3 contains the Safety Evaluation Report (SER) issued for revision 1.

Section 5.4 and 5.5 contain responses to NRC questions on revisions 2 and 3, respectively, of this report. Section 5.6 contain supplemental information to revisions 2 and 3. Section 5.7 contains the SER issued for revisions 2 and 3. Section 5.8 contains responses to NRC questions on revision 4. Section 5.9 contains the SER issued for revision 4. Finally, Section 5.10 contains the pages removed or replaced from revision 3 to create revision 4 and Section 5.11 contains pages that were replaced due to SER direction and typographical errors.

FRAMATOME COGEMA FUELS

September 24, 1999
GR99-194.doc

U. S. Nuclear Regulatory Commission
ATTN: Document Control Desk
Washington, D. C. 20555

References:

1. J. L. Birmingham, NRC, to C. F. McPhatter, Framatome Cogema Fuels, Request for Additional Information for Topical report BAW-10227P, "Evaluation of Advanced Cladding and Structural Material (M5) in PWR Reactor Fuel," October 26, 1998.

2. J. L. Birmingham, NRC, to C. F. McPhatter, Framatome Cogema Fuels, Request for Additional Information for Topical report BAW-10227P, "Evaluation of Advanced Cladding and Structural Material (M5) in PWR Reactor Fuel," January 29, 1999.

3. T. A. Coleman to U.S. NRC Document Control Desk, GR99-031.doc, February 5, 1999.

4. T. A. Coleman to U.S. NRC Document Control Desk, GR99-089.doc, April 23, 1999.

5. T. A. Coleman to U.S. NRC Document Control Desk, GR99-156.doc, July 29, 1999.

Gentlemen:

References 1 and 2 contain NRC requests for additional information (RAIs) on topical report BAW-10227P. FCF has provided responses to the RAIs in references 3, 4 and 5. In addition to references 1 and 2, the contract reviewer for BAW-10227P has verbally provided requests for information in numerous telecons that have taken place since mid-July. FCF has informally provided all the requested information via Fax, Email, and FedEx. The purpose of this letter is to provide a formal record of those transmittals.

In accordance with 10 CFR 2.790, FCF requests that these responses be considered proprietary and withheld from public disclosure. Attachment 1 is the FCF proprietary version of the responses. Attachment 2 is the affidavit identifying the criteria for the proprietary request. Attachment 3 is the non-proprietary version of the responses.

FRAMATOME TECHNOLOGIES

Framatome Cogema Fuels
3315 Old Forest Road, P.O. Box 10935, Lynchburg, VA 24506-0935
Telephone: 804-832-3000 Fax: 804-832-3653

These responses will be incorporated into the NRC-approved version of BAW-10227P as Appendix K. K.1 is the response to verbal RAIs on the original response to question 2. K.2 is the response to verbal RAIs on the original response to question 5. K.3 is the response to the verbal RAIs on the original response to question 12. K.4 is the response to the verbal RAIs on the original response to question 14. K.5 is the response to the verbal RAIs on the original response on question 19. K.6 is a supplemental addition to Enclosure 1 of the April 23 responses (reference 4). K.7 provides FCF's plans for post irradiation examinations (PIEs) of fuel with M5 cladding.

All the enclosed information has already been provided to the NRC contract reviewer. It has been reviewed and the NRC has concluded that there no outstanding technical issues on BAW-10227P. Since additional review is not required, the NRC is requested to issue the SER for BAW-10227P by October 15, 1999.

Very truly yours,

T A Coleman

T. A. Coleman, Vice President
Government Relations

cc: J. S. Wermiel, NRC
S. L. Wu, NRC
M. A. Schoppman
R. N. Edwards
C. E. Beyer, PNL
20A13 File/Records Management

Attachment 1

The FCF proprietary version of responses to NRC requests for additional information (RAI) has not been included in this report. Please see BAW-10227P-A, "Evaluation of Advanced Cladding and Structural Material (M5) in PWR Reactor Fuels", pages k-1 - k-39.

K.8 Additional Change Pages for BAW-10164

The April 23, 1999 response to request for additional information included documentation of several changes to RELAP5 that were required to allow the input of M5 data. These changes replaced Zircaloy appropriate correlations that had been incorporated directly in the coding with input tables to alloy the use of M5 correlations and data. At that time, Framatome had not proposed any change to the Chapman cladding stress versus rupture temperature correlation. Section K.5 of this submittal alters the coefficients of the Chapman correlation to better represent the M5 alloy. This requires the incorporation of input values for the cladding stress versus rupture temperature correlation coefficients. The change page documentation for BAW-10164 in Enclosure 1 accomplishes those changes. In addition Framatome Technologies Incorporated (FTI) would like to have only one revision level to BAW-10164 for M5 application. Therefore, all of the BAW-10164 change pages submitted in April have been re-dated to September and are included in Enclosure 1. Enclosure 1 is thus a complete record of the required changes and Framatome requests the approval for these changes to BAW-10164.

Beginning of Enclosure 1

LISTING OF CHANGES IMPLEMENTED IN REVISION 4 OF RELAP5/MOD2-B&W TOPICAL REPORT

Page	Type/Change	Item	Reason
--	Revision	Title page	Revision & Date
i-ii	Revision	Abstract	Revision & Date
v	Addition	Revision Record	New topical version
xii	Revision	Table/Contents, etc.	New revisions
1-1	Addition	Introduction	Zirconium-based alloy clad
2.1-126 to 2.1-126.2	Addition	Void-Dependent Cross-flow	New code option
2.3-25 to 2.3-28	Addition	EM Pin Model Changes	Zirconium-based alloy clad
2.3-33	Addition	EM Pin Model Changes	Zirconium-based alloy clad
2.3-35 to 2.3-37	Addition	EM Pin Model Changes	Zirconium-based alloy clad
2.3-39 to 2.3-41	Addition	EM Pin Model Changes	Zirconium-based alloy clad
2.3-45 to 2.3-46.2.2	Addition	EM Pin Model Changes	Zirconium-based alloy clad
2.3-52	Correction	EM Pin Model	Zirconium-based alloy clad
2.3-55	Addition	Steady-State EM Pin Model	Fuel temperature convergence
5-364.1 to 5-364.2	Correction	Missing SER Page	Include missing page

(NOTE: Pages 2.1-126.1, 2.1-126.2, 2.3-27.1, 2.3-27.2, 2.3-46.2.1, 2.3-46.2.2, 5-364.1, and 5-364.2 were added in Revision 4)

BAW-10164P
Topical Report
Revision 4
September 1999

- RELAP5/MOD2-B&W -

An Advanced Computer Program for Light Water Reactor LOCA and Non-LOCA Transient Analysis

Framatome Technologies Inc.
P. O. Box 10935
Lynchburg, Virginia 24506

Framatome Technologies Inc.
Lynchburg, Virginia

Topical Report BAW-10164P
Revision 4
September 1999

RELAP5/MOD2-B&W

An Advanced Computer Program for Light Water Reactor LOCA and Non-LOCA Transient Analysis

Key Words: RELAP5/MOD2, LOCA, Transient, Water Reactors

Abstract

This document describes the physical solution technique used by the RELAP5/MOD2-B&W computer code. RELAP5/MOD2-B&W is a Framatome Technologies Incorporated (previously known as and refered to in the text as B&W or B&W Nuclear Technologies) adaption of the Idaho National Engineering Laboratory RELAP5/MOD2. The code developed for best estimate transient simulation of pressurized water reactors has been modified to include models required for licensing analysis of zircaloy or zirconium-based alloy fuel assemblies. Modeling capabilities are simulation of large and small break loss-of-coolant accidents, as well as operational transients such as anticipated transient without SCRAM, loss-of-offsite power, loss of feedwater, and loss of flow. The solution technique contains two energy equations, a two-step numerics option, a gap conductance model, constitutive models, and component and control system models. Control system and secondary system components have been added to permit modeling of plant controls, turbines, condensers, and secondary feedwater conditioning systems. Some discussion of the numerical techniques is presented. Benchmark comparison of code

predictions to integral system test results are presented in an appendix.

Topical Revision Record

Documentation Revision	Description	Program Change?	Program Version
0	Original issue	____	8.0
1	Typographical corrections Replace CSO correlation with Condie-Bengston IV	yes	10.0
2	SBLOCA modifications Miscellaneous corrections	yes	18.0
3	EM Pin Enhancements Filtered Flows for Hot Channel Heat Transfer Rupture Area Enhancement for Surface Heat Transfer OTSG Improvements and Benchmarks using the Becker CHF, Slug Drag, and Chen Void Ramp	yes	19.0
4	Zirconium-based alloy pin model changes Option for multiple pin channels in a single core fluid channel Void-dependent core cross flow option Zirconium-based alloy rupture temperature	yes	24.0

This page is intentionally left blank.

LIST OF FIGURES (Cont'd)

LIST OF FIGURES (Cont'd)

1. INTRODUCTION

RELAP5/MOD2 is an advanced system analysis computer code designed to analyze a variety of thermal-hydraulic transients in light water reactor systems. It is the latest of the RELAP series of codes, developed by the Idaho National Engineering Laboratory (INEL) under the NRC Advanced Code Program. RELAP5/MOD2 is advanced over its predecessors by its six-equation, full nonequilibrium two-fluid model for the vapor-liquid flow field and partially implicit numerical integration scheme for more rapid execution. As a system code, it provides simulation capabilities for the reactor primary coolant system, secondary system, feedwater trains, control systems, and core neutronics. Special component models include pumps, valves, heat structures, electric heaters, turbines, separators, and accumulators. Code applications include the full range of safety evaluation transients, loss-of-coolant accidents (LOCAs), and operating events.

RELAP5/MOD2 has been adopted and modified by B&W for licensing and best estimate analyses of PWR transients in both the LOCA and non-LOCA categories. RELAP5/MOD2-B&W retains virtually all of the features of the original RELAP5/MOD2. Certain modifications have been made either to add to the predictive capabilities of the constitutive models or to improve code execution. More significant, however, are the B&W additions to RELAP5/MOD2 of models and features to meet the 10CFR50 Appendix K requirements for ECCS evaluation models. The Appendix K modifications are concentrated in the following areas: (1) critical flow and break discharge, (2) fuel pin heat transfer correlations and switching, and (3) fuel clad swelling and rupture for both zircaloy and zirconium-based alloy cladding types.

This report describes the physical models, formulation, and structure of the B&W version of RELAP5/MOD2 as it will be applied to ECCS and system safety analyses. It has been prepared as a stand-alone document; therefore substantial portions of the text that describe the formulation and numerics have been taken directly from original public domain reports, particularly NUREG/CR-4312[1]. Chapter 2 presents the method of solution in a series of subsections, beginning with the basic hydrodynamic solution including the field equations, state equations, and constitutive models in section 2.1. Certain special process models, which require some modification of the basic hydrodynamic approach, and component models are also described. The general solution for heat structures is discussed in section 2.2. Because of the importance of the reactor core and the thermal and hydraulic interaction between the core region and the rest of the system, a separate section is dedicated to core modeling. Contained in section 2.3 are the reactor kinetics solution, the core heat structure model, and the modeling for fuel rod rupture and its consequences. Auxiliary equipment and other boundary conditions are discussed in section 2.4 and reactor control and trip function techniques in section 2.5. Chapter 3 provides an overview of the code structure, numerical solution technique, method and order of advancement, and initialization. Time step limitation and error control are presented in section 3.3.

The INEL versions of RELAP5/MOD2 contain certain solution techniques, correlations, and physical models that have not been selected for use by B&W. These options have been left intact in the coding of the B&W version, but descriptions have not been included in the main body of this report. Appendix A contains a list of those options that remain in the RELAP5/MOD2 programming but are not used by B&W and not submitted for review. A brief description of each along with a reference to an appropriate full discussion is provided in the appendix. Appendix B defines the nomenclature used throughout this report. Appendix G documents

$v_{J,3}$ not be included in the volume average (axial) velocity calculation for cell L.

The second area of numerical modification relates to the reduced form of the momentum equations to be used at a crossflow junction. In crossflow junctions, the cross product momentum flux terms are neglected, that is, there is no x-direction transport of momentum due to the y velocity.

For the case of a small crossflow junction between two axial-flow streams (J_2 in Figure 2.1.4-7) all the geometric input (AVOL, DX, DZ) for both of the volumes relates to the axial flow direction as does the wall drag and code calculated form losses. Since the crossflow has a different flow geometry and resistance (for example, crossflow resistance in a rod bundle) the friction and form losses must be user input and must be appropriate for the crossflow direction geometry. For crossflow junctions the user input form losses should include all crossflow resistance (form losses and wall drag). The normal terms representing wall drag and abrupt area change losses are not included in the formulation of the momentum equation at a crossflow junction as these refer to the axial properties of the K and L volumes.

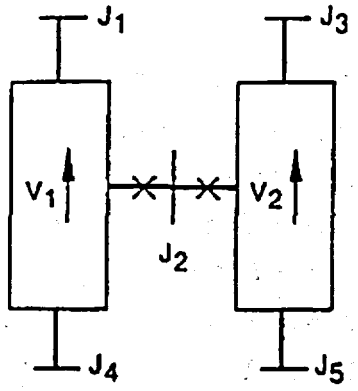

Figure 2.1.4-7. Modeling of Crossflows or Leak.

Since the connecting K and L volumes are assumed to be predominately axial-flow volumes, the crossflow junction momentum flux (related to the axial volume velocity in K and L) is neglected along with the associated numerical viscous term. In addition, the horizontal stratified pressure gradient is neglected.

All lengths and elevation changes in the one-dimensional representation are based upon the axial geometry of the K and L volumes and the crossflow junction is assumed to be perpendicular to the axial direction and of zero elevation change, thus, no gravity force term is included.

The resulting vapor momentum finite difference equation for a crossflow junction is

$$\left(\alpha_g \rho_g\right)_j^n \left(v_g^{n+1} - v_g^n\right)_j \Delta x_j = - \alpha_{g,j}^n \left(P_L - P_K\right)^{n+1} \Delta t$$

$$- \left(\alpha_g \rho_g\right)_j^n \mathrm{HLOSSG}_j^n \, v_{g,j}^{n+1} \Delta t$$

$$- \left(\alpha_g \rho_g\right)_j^n \mathrm{FIG}_j^n \left(v_{g,j}^{n+1} - v_{f,j}^{n+1}\right) \Delta x_j \Delta t$$

$$+ \text{ADDED MASS + MASS TRANSFER MOMENTUM.} \qquad 2.1.4\text{-}72$$

A similar equation can be written for the liquid phase. In Equation 2.1.4-72, HLOSSG_j^n contains only the user-input crossflow resistance. The Δx_j term that is used to estimate the inertial length associated with crossflow is defined using the diameters of volumes K and L,

$$\Delta x_j = \frac{1}{2} [D(K) + D(L)] \ .$$ 2.1.4-73

A special void-dependent form loss option of the full crossflow model has been added for certain multi-core channel applications. This option allows the user to alter the input constant form loss coefficient based on the void fraction in the upstream volume. The specific applications are possibly multi-channel core analyses such as SBLOCA scenarios with significant core uncovering or future multi-channel BEACH reflooding calculations. This model allows the regions of the core covered by a two-phase mixture or pool to have a resistance that is different from that in the uncovered or steam region. The crossflow resistance changes can alter the volume-average axial velocities that are used to determine the core surface heat transfer. Any cross flow is excluded from the volume average velocity used for heat transfer.

The model uses the input form loss coefficients whenever the upstream steam void fraction is less than a user-supplied minimum void fraction value given as $\alpha_{min\text{-}Kcross}$. The model allows user input of a forward, $M_{K\text{-}forward}$, and reverse, $M_{K\text{-}reverse}$, crossflow resistance multiplier when the upstream steam void fraction is greater than the maximum user-input void fraction, $\alpha_{max\text{-}Kcross}$. Linear interpolation is used to determine the multiplicative factor when the void fraction is between minimum and maximum input void fractions as indicated in the following equations. For the forward flow direction (from Volume K to Volume L),

If $\alpha_g(K) < \alpha_{min\text{-}Kcross}$	$K_{jun} = K_{jun\ forward}$
If $\alpha_{max\text{-}Kcross} \leq \alpha_g(K)$	$K_{jun} = K_{jun\ forward} * M_{K\text{-}forward}$
If $\alpha_{min\text{-}Kcross} \leq \alpha_g(K) < \alpha_{max\text{-}Kcross}$	$K_{jun} = K_{jun\ forward} * M_{Kf\ interp}$

2.1.4-73.1

ere

$$M_{kf\ interp} = 1 - (1 - M_{K\text{-}forward}) * [\ \alpha_{min\text{-}Kcross} - \alpha_g(K)] / (\alpha_{min\text{-}Kcross} - \alpha_{max\text{-}Kcross})$$

and $K_{jun\ forward}$ is the user-supplied forward loss coefficient specified in this junction input.

The equation for the reverse flow direction (from Volume L to Volume K) is similar.

If	$\alpha_g(L) < \alpha_{min\text{-}Kcross}$	$K_{jun} = K_{jun\ reverse}$
If	$\alpha_{max\text{-}Kcross} \le \alpha_g(L)$	$K_{jun} = K_{jun\ reverse} * M_{K\text{-}reverse}$
If	$\alpha_{min\text{-}Kcross} \le \alpha_g(L) < \alpha_{max\text{-}Kcross}$	$K_{jun} = K_{jun\ reverse} * M_{Kr\ interp}$

2.1.4-73.2

where

$$_{interp} = 1 - (1 - M_{K\text{-}reverse}) * [\ \alpha_{min\text{-}Kcross} - \alpha_g(L)] / (\alpha_{min\text{-}Kcross} - \alpha_{max\text{-}Kcross})$$

and $K_{jun\ reverse}$ is the user-supplied reverse loss coefficient specified in this junction input.

The code performs several input checks to ensure that the user input will not cause code failures. These checks include tests to see if the input form loss multipliers are greater than zero. The minimum void fraction must be greater than zero and less than the maximum void fraction input. The maximum void fraction must be less than or equal to one.

The crossflow option can be used with the crossflow junction perpendicular to the axial flow in Volume L (or K) but parallel

2.3.2. Core Heat Structure Model

The ordinary RELAP5 heat structures are general in nature and can be used for modeling core fuel pins; however, licensing calculations require special treatment of the fuel pin heat transfer. To accommodate these requirements, two additional models, commonly referred to as the EM (Evaluation Model) pin and core surface heat transfer models, were added to the code. The EM pin model calculates dynamic fuel-clad gap conductance, fuel rod swell and rupture using either NUREG-0630[117] or user input options (for modeling M5 cladding or other zirconium-based alloy cladding material types), and cladding metal-water reaction. The core fuel pin surface heat transfer is calculated with a flow regime-dependent set of correlations that include restrictions on which correlations can be selected per NRC licensing requirements. These new models are independent and mutually exclusive of the original system heat transfer model (described in section 2.2.2) and the existing simple gap conductance model[118] (referenced in Appendix A). The new models are explicitly coupled to the solution scheme through the modification of the gap conductance term, addition of fluid hydraulic resistance upon rupture, deposition of metal-water reaction energy in the clad, and determination of fuel pin surface heat transfer. The new EM pin model calculations are described in this section, while the EM heat transfer description is contained in section 2.3.3.

The EM pin model consists of three basic parts:

1. Dynamic fuel-clad gap conductance,
2. Fuel rod swell and rupture using NUREG-0630 or user specified swell and rupture options, and
3. Clad metal-water reaction,

hich couple explicitly to the heat structure solution scheme or dd fluid hydraulic resistance upon rupture. The model may be executed either in a steady-state initialization or transient mode determined by user input.

The pin calculations are performed on single fuel rod which represent the average behavior of a large number of rods. Each rod (also termed channel) can be broken into up to ninety heat structures, each having an associated pin segment. The gap conductance, deformation mode, and metal-water reaction are determined for each individual segment based on the channel specific pin pressure.

The changes to the EM pin model included in Version 21 and later code versions are:

1. User options to model zircaloy and/or M5 cladding (or other zirconium-based alloy material types) in the same problem,

2. User options to specify the pin channel as a primary or supplemental channel for additive form loss and BEACH droplet breakup calculations upon pin rupture, and

3. Integration of the NRC SER limitation (BEACH code-BAW-10166, Rev. 2 dated 8/13/90) for use of a maximum flow blockage of 60 percent in the ruptured cladding droplet breakup calculations.

The option to allow zirconium-based alloy cladding types requires user input to identify which pin channels are zircaloy and which are not. The zirconium-based alloy cladding also requires additional user input to specify the material properties necessary to calculate the transient cladding swell and rupture behavior.

The supplemental pin capability was added to improve the calculational methods that require modeling of multiple EM pin channels within a single hydrodynamic fluid channel (i.e., an assembly or a group of assemblies) for LOCA applications. The relationship between the supplemental pin and the remainder of the pins in a common fluid channel is one in which the supplemental pin swell and rupture will not define the rupture flow blockage for the entire channel. Rather it will define a local effect that should not be used in determination of the channel droplet breakup parameters and the additive form loss due to rupture. These parameters should be controlled by the larger group of pins (i.e. primary channel) and not the smaller grouping (i.e. supplemental channel). The supplemental rod modeling is particularly useful for gadolinia or lead test pin (M5) analyses. It may also be used in future EM revisions for hot pin applications, in which the hot pin has a higher radial peak or a different initial fuel temperature.

2.3.2.1. Transient Dynamic Fuel-Clad Gap Conductance

The RELAP5 heat structure conduction scheme uses cold, unstressed geometrical dimensions for its solution technique. The dynamic gap conductance, h_{gap}, is calculated from hot stressed conditions from which an effective gap thermal conductivity, $\bar{K}_{gap}$, based on cold gap size, $\tau_{g_{cold}}$, is determined for each pin segment.

$$\bar{K}_{gap} = h_{gap} \cdot \tau_{g_{cold}} . \qquad 2.3.2\text{-}1$$

The gap conductance is determined by calculating the gap gas conductivity, temperature jump gap distance, radiation component, and dynamic fuel-clad gap from the deformation models. An

dditive fuel-clad contact conductance term has also been included as an option to simulate the closed gap contribution for high fuel rod burn-up applications. Two options are provided to calculate the conductance. The first option assumes that the fuel pellet is concentric within the clad, while the second option assumes the fuel pellet is non-concentric within the clad as illustrated in Figure 2.3.2-1.

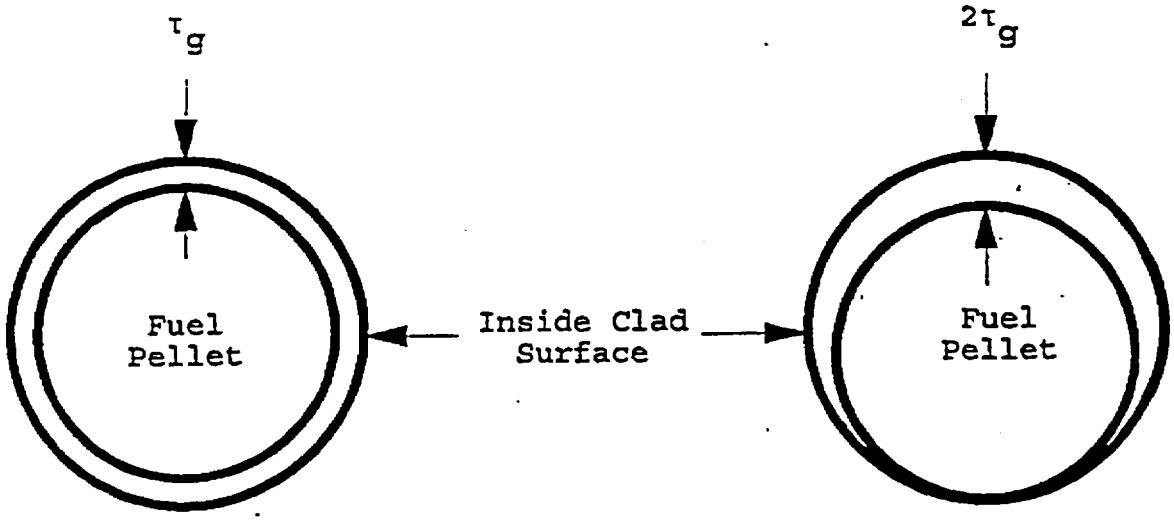

Figure 2.3.2-1. Gap Conductance Options.

Eight half-symmetrical azimuthal sections are used for determining the overall conductance for the second option without calculating an azimuthal temperature gradient. The total gap conductance is determined by

$$h_{gap} = M_g \, h_{\substack{gap \\ gas}} + h_{rad} + h_{fcc} \qquad 2.3.2\text{-}2$$

with

h_{gap} = conductance through gap gas (w/m^2-K),

M_g = user input multiplier used to acquire correct initial temperature within fuel,

$h_{\substack{gap \\ gas}}$ = gap gas conductance contribution (w/m^2-K),

h_{rad} = conductance due to radiation contribution from fuel to clad (w/m^2-K), and

h_{fcc} = gap contact conductance contribution due to fuel-cladding mechanical interaction (w/m^2-K).

The radiation gap conductance contribution is calculated by

$$h_{rad} = \frac{\sigma}{\frac{1}{e_f} + \frac{r_f}{r_{ic}}\left(\frac{1}{e_c} - 1\right)} \left[\frac{T_{fs}^4 - T_{ics}^4}{T_{fs} - T_{ics}}\right]$$

$$= \frac{\sigma(T_{fs}^2 + T_{ics}^2)(T_{fs} + T_{ics})}{\frac{1}{e_f} + \frac{r_f}{r_{ic}}\left(\frac{1}{e_c} - 1\right)}, \qquad 2.3.2\text{-}2.1$$

where

σ = Stefan-Boltzmann constant,

= 5.6697×10^{-8} $(w/m^2\text{-}K^4)$,

e_f = emissivity of fuel surface,

e_c = emissivity of clad-inside surface,

T_{fs} = fuel outside surface temperature (K), and

T_{ics} = clad-inside surface temperature (K).

$C_1 = 1.0 \cdot 10^{-5}\ (K^{-1})$,
$C_2 = -3.0 \cdot 10^{-3}$,
$C_3 = 4.0 \cdot 10^{-2}$, and
$C_4 = -5.0 \cdot 10^{3}\ (K)$.

The fuel is defined by the first material type specified in the heat structure input, with the next material type being the gap and the third the clad as shown in Figure 2.3.2-2. Any deviation from the geometry will result in an error or misinterpretation of the information by the pin model. The gap can only be one mesh interval wide, while fuel or clad must be greater than or equal to one mesh interval. Currently no provisions are made for annular fuel pellets.

The calculation of the inside clad radius is not as straightforward as the fuel outside radius. Seven different calculational modes are required to cover the possible clad conditions. They are defined as:

1. Elastic and thermal expansion within an unruptured channel,
2. Elastic and thermal expansion within 166.7K (300°F) of the clad rupture temperature within an unruptured channel,
3. Plastic deformation within an unruptured channel,
4. Elastic thermal expansion within a ruptured channel,
5. Plastic deformation in a ruptured channel,
6. Ruptured segment, and
7. Fuel-cladding mechanical iteration (closed gap).

Each mode is related to the NUREG-0630 calculated rupture temperature for zircaloy cladding by the equation:

$$T_{rupt} = 4233 - \frac{20.4\sigma_h}{1 + H} - \frac{(8.51 \cdot 10^{6})\sigma_h}{100(1 + H) + 2790\sigma_h}, \qquad 2.3.2\text{-}17$$

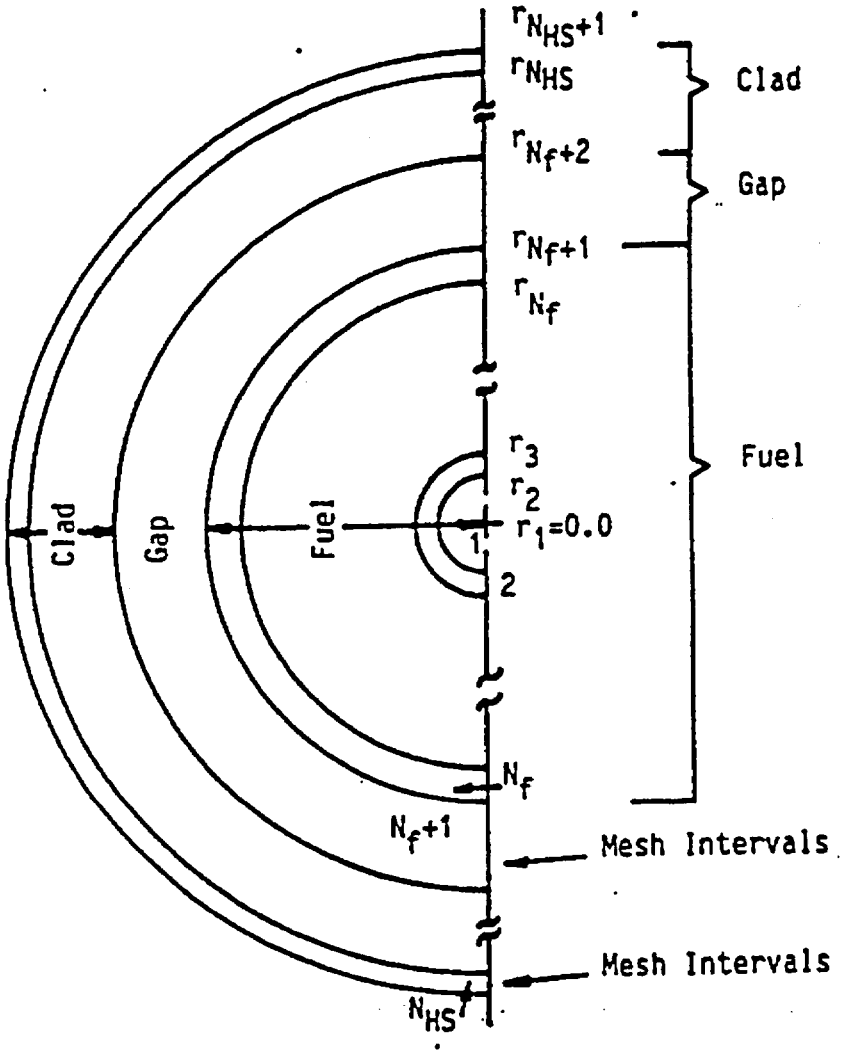

Figure 2.3.2-2. Fuel Pin Representation.

where

T_{rupt} = cladding rupture temperature (K),

σ_h = clad hoop stress (kpsi), and

H = dimensionless clad heating ramp rate, $0 \leq H \leq 1$.

The rupture temperature for other zirconium-based alloys is calculated by the following equation:

$$T_{rupt} = a1 - \frac{a2(\sigma_h - a7)}{a4 + H} - \frac{a3(\sigma_h - a7)}{a5(a4 + H) + a6(\sigma_h - a7)}, \quad 2.3.2\text{-}17a$$

where a1 through a7 are user-specified input constants. The clad hoop stress for any pin segment in either equation is given by

$$\sigma_h = C_p (P_g r_{ic_{cold}} - P_f r_{oc_{cold}})/(r_{oc_{cold}} - r_{ic_{cold}}), \quad 2.3.2\text{-}18$$

with

$r_{ic_{cold}}$ = cold unstressed inside clad radius (m),

$r_{oc_{cold}}$ = cold unstressed outside clad radius (m),

P_g = internal fuel rod pin pressure for that channel (Pa), and

P_f = external fluid pressure of the right-hand side heat structure associated volume (Pa).

$C_p = 1 / 6.894757 \times 10^6$

The heating rate can be either a user input constant or one of three additional transient-dependent algorithms discussed in detail later in this section.

At the beginning of each new time step following a successful RELAP5 time step advancement, the hoop stress and normalized heating ramp rate are computed for each pin segment. The clad average temperature is also known at this time. If the clad

verage temperature is greater than the rupture temperature, then upture occurs. Should the segment still be elastic and the rupture minus the clad temperature is less than 166.7K (300 F), then the segment stays elastic. Between these two temperatures the clad can be either elastic or plastic depending upon this temperature difference and the burst strain as described in the following paragraphs for ruptured or unruptured channels.

Mode 1: Unruptured Elastic and Thermal Deformation

Within an unruptured channel, the clad is considered purely elastic if it has never gone plastic, ruptured, or the temperature difference between rupture and clad average temperatures is less than 166.7 K (300 F). The inside clad radius for this pure elastic mode is determined by

$$r_{ic} = r_{ic_{cold}} + u_{TC} + u_{CC} + u_e \ , \qquad 2.3.2\text{-}19$$

where

u_{TC} = clad radial displacement due to thermal expansion (m), (m),

u_{CC} = clad radius over-specification factor (m), determined during pin transient initiation, and

u_e = clad radial displacement due to elastic deformation (m).

The clad thermal expansion is determined similarly to that for the fuel.

$$u_{TC} = (r_{N_{HS}+1} - r_{N_f+2}) \, \epsilon_{TC} / 2 \ , \qquad 2.3.2\text{-}20$$

with N_{HS} = total number of mesh intervals in the heat structure,

r_n = heat structure radius at the inside of mesh interval n or outside of n-1 (m), and

ϵ_{TC} = radial strain function defining fuel thermal expansion as a function of clad average temperature.

The radial strain function is defined by either a user input table as a function of cladding temperature for zirconium-based material types other than zircaloy or a built in code correlation set for zircaloy cladding[119] consisting of

$$\epsilon_{TC} = -2.0731 \cdot 10^{-3} + 6.721 \cdot 10^{-6} T_C \qquad 2.3.2\text{-}22$$

for $T_C \leq 1073.15$ K (α phase), and

$$\epsilon_{TC} = -9.4495 \cdot 10^{-3} + 9.7 \cdot 10^{-6} T_C \qquad 2.3.2\text{-}23$$

for $T_C \geq 1273.15$ K (β phase), where T_C is the average cladding temperature (K). In the α phase to β phase transition zone, $1073.15 \text{ K} < T_C < 1273.15$ K, a table lookup is used. Some selected values are listed in Table 2.3.2-2.

Table 2.3.2-2. Thermal Strain of Zircaloy for $1073.15 \text{ K} < T < 1273.15$ K.

T(K)	Radial Strain ϵ_{TC}	Axial Strain ϵ_{ATC}
1073.15	$5.14 \cdot 10^{-3}$	$3.53 \cdot 10^{-3}$
1093.15	$5.25 \cdot 10^{-3}$	$3.50 \cdot 10^{-3}$
1103.15	$5.28 \cdot 10^{-3}$	$3.46 \cdot 10^{-3}$
1123.15	$5.24 \cdot 10^{-3}$	$3.33 \cdot 10^{-3}$
1143.15	$5.15 \cdot 10^{-3}$	$3.07 \cdot 10^{-3}$
1183.15	$4.45 \cdot 10^{-3}$	$1.50 \cdot 10^{-3}$
1223.15	$2.97 \cdot 10^{-3}$	$1.10 \cdot 10^{-3}$
1273.15	$2.90 \cdot 10^{-3}$	$1.40 \cdot 10^{-3}$

The average clad temperature is calculated via a volume weighted average.

$$T_C = \sum_{n=N_f+2}^{N_{HS}} \frac{(r_{n+1}^2 - r_n^2)}{(r_{N_{HS}+1}^2 - r_{N_f+2}^2)} \left[\frac{(T_{n+1} + T_n)}{2}\right]. \qquad 2.3.2\text{-}24$$

The maximum clad average temperature is calculated for each EM pin channel and written at each major edit and at the end of each case. The segment number and time of the peak cladding temperature is also specified. The fuel volume weighted average temperature, $\bar{T}_f$, is calculated similarly to the cladding.

$$\bar{T}_f = \sum_{n=1}^{N_f} \frac{(r_{n+1}^2 - r_n^2)}{(r_{N_f+1}^2 - r_1^2)} \left[\frac{(T_{n+1} + T_n)}{2}\right] . \qquad 2.3.2\text{-}25$$

The elastic deformation, u_e, is calculated by

$$u_e = \left[\frac{r_{N_{HS}+1} + r_{N_f+2}}{2}\right] \left[\frac{\sigma_h - \upsilon\sigma_z}{E}\right] , \qquad 2.3.2\text{-}26$$

where

E = Young's modulus for clad (Pa),

σ_h = segment clad hoop stress (Pa),

σ_z = channel clad axial stress (Pa), and

υ = Poisson's ratio for clad (dimensionless).

The channel axial stress is the same for all segments in the channel and is determined by

$$\sigma_z = \frac{P_g\, r_{ic_{cold}}^2 - P_f\, r_{oc_{cold}}^2}{r_{oc_{cold}}^2 - r_{ic_{cold}}^2} \qquad 2.3.2\text{-}27$$

Young's modulus is given either by the code for zircaloy cladding as

$$E = \begin{cases} 1.088 \cdot 10^{11} - 5.475 \cdot 10^{7}\ T_c; & \text{for } 1090K \geq T_c \\ 1.017 \cdot 10^{11} - 4.827 \cdot 10^{7}\ T_c; & \text{for } 1240K \geq T_c > 1090K \\ 9.21 \cdot 10^{10} - 4.05 \cdot 10^{7}\ T_c; & \text{for } 2027K \geq T_c > 1240K \\ 1.0 \cdot 10^{10}; & \text{for } T_c > 2027K, \end{cases}$$

2.3.2-28

or by a user-specified cubic equation that can be used for zirconium-based alloy cladding

$$E = C_1 T_c^{3} + C_2 T_c^{2} + C_3 T_c + C_4 . \qquad 2.3.2\text{-}29$$

Poisson's ratio is a constant which is defined as 0.30 for zircaloy by the code, however, the user can over-ride this value for zirconium-based alloy cladding types.

The normalized heating ramp rate for the elastic mode is determined by one of two methods. The code calculates an instantaneous heating rate for one method, while the other method sets the rate to a normalized user-input value between 0 and 1. The calculated heating rate is normalized via a constant value, H_{Rnorm}, of 28 K/s for zircaloy cladding or a user input for other zirconium-based alloy cladding materials.

$$H = \left\{\frac{dT_c}{dt}\right\} / H_{Rnorm}$$

$$= \left\{\frac{T_c^{n} - T_c^{n-1}}{t^{n} - t^{n-1}}\right\} / H_{Rnorm} . \qquad 2.3.2\text{-}30$$

The normalized heating rate is always limited to values between 0 and 1 or $(0 \text{ K/s} / H_{Rnorm}) \leq H \leq (28 \text{ K/s} / H_{Rnorm} = 1)$ for zircaloy cladding and between $(H_{slow\ input} / H_{Rnorm}) \leq H \leq (H_{fast\ input} / H_{Rnorm})$ for

her zirconium-based alloy cladding types. This limit is applied o H prior to using it in any subsequent checking or calculations. The superscripts reflect the current time, n, and old time, n-1, values. The zirconium-based alloy slow or fast ramp rate divided by the normalized rate is still limited between 0 and 1, but they do not have to be equal to 0 or 1. Values greater than 0 or less than 1 activate the slow or fast ramp curves at different normalized heating rates.

Mode 2: Unruptured Elastic and Thermal Deformation Within 166.7K (300 F) of the Rupture Temperature

When the clad average temperature is within 166.7K (300 F) of the rupture temperature, the elastic inside clad radius is calculated as shown in Mode 1. This radius is compared against the plastic inside clad radius calculated in Mode 3. If the elastic radius is greater than the plastic radius, then Mode 2 is retained and the inside clad radius is set to the elastic radius. If not, the clad comes plastic (Mode 3) and the plastic clad calculations are used. An informative message is printed when a segment first becomes plastic. No return to elastic Modes (1 or 2) is permitted once the clad becomes plastic.

$$r_{ic} = MAX(r_{ic_{elastic}}, r_{ic_{plastic}}) . \qquad 2.3.2\text{-}31$$

If $r_{ic_{elastic}} \geq r_{ic_{plastic}}$, Mode = 2 .

If $r_{ic_{elastic}} < r_{ic_{plastic}}$, Mode = 3 .

Mode 3: Unruptured Plastic Deformation

The unruptured plastic deformation is determined by the plastic strain, ϵ_p.

$$r_{ic} = r_{ic_{cold}}(1 + \epsilon_p), \qquad 2.3.2\text{-}32$$

with

$$\varepsilon_p = \varepsilon_{cps} \exp[-0.02754 (T_{rupt} - T_c)], \qquad 2.3.2\text{-}33$$

where ε_{cps} is 0.2 * ε_B (ε_B is the burst strain) based on NUREG-0630 for maximum cladding plastic strain and on user input tables for zirconium-based alloy cladding. The plastic strain or burst strain is determined by a double interpolation relative to H and T_{rupt} in the user input or default NUREG-0630 burst strain Tables 2.3.2-3 and 2.3.2-4. The plastic strain behaves as a ratchet. Once a given plastic strain is reached, no decrease in its value is allowed. In other words, for plastic mode calculations

$$r_{ic} = MAX(r_{ic}^{n}, r_{ic}^{n-1}), \qquad 2.3.2\text{-}34$$

where the superscripts refer to the current and old time values.

If the plastic mode is selected, the normalized heating ramp rate is calculated from any of three user options: user input constant, average ramp rate, or plastic weighted ramp rate. The normalized average ramp rate is calculated from

$$H = \left\{ \frac{T_c^n - T_c^p}{t^n - t^p} \right\} \Big/ \; H_{Rnorm} \;, \qquad 2.3.2\text{-}35$$

where

t = time (s),

n = superscript defining the current time, and

p = superscript defining the time in which the clad first went plastic.

The normalized plastic weighted ramp is calculated by

$$H = \left[\frac{\int_{t^p}^{t^n} W(T) \left\{ \frac{dT_c}{dt} \right\} dt}{\int_{t^p}^{t^n} W(T)\, dt} \right] \Big/ \; H_{Rnorm} \qquad 2.3.2\text{-}36$$

Table 2.3.2-3. NUREG-0630 Slow-Ramp Correlations for Burst Strain and Flow Blockage.

Rupture temperature, C	≤10 C/S burst strain, %	≤10 C/S flow blockage, %
600	10	6.5
625	11	7.0
650	13	8.4
675	20	13.8
700	45	33.5
725	67	52.5
750	82	65.8
775	89	71.0
800	90	71.5
825	89	71.0
850	82	65.8
875	67	52.5
900	48	35.7
925	28	20.0
950	25	18.0
975	28	20.0
1000	33	24.1
1025	35	25.7
1050	33	24.1
1075	25	18.0
1100	14	9.2
1125	11	7.0
1150	10	6.5
1175	10	6.5
1200	10	6.5

noding options) chosen by the user. The fine mesh noding option computes the inside radius as

$$r_{ic} = r_{ic_{cold}}(1 + \epsilon_B) \quad . \qquad 2.3.2\text{-}39$$

With this option, the gap conductance is calculated as though there is steam in the gap. The steam thermal conductivity is evaluated at the gap temperature and used with the hot gap size to compute the conductance. This option also calculates inside metal-water reaction for the ruptured segment.

The coarse mesh noding option computes the inside clad radius as

$$r_{ic} = r_{ic_{cold}}(1 + \epsilon_{cps}) \quad . \qquad 2.3.2\text{-}40$$

This option uses the regular gap gas conductance and does not consider inside metal-water reaction. It is intended for use nominally when the expected rupture length is small when compared to the total segment length. The microscopic effects at the rupture site considered with the fine mesh option are expected to be negligible when compared to the longer segment behavior. With the coarse mesh option, the overall behavior will be more closely controlled by the entire segment rather than just the rupture site conditions.

Within the ruptured channel various calculations are modified at the time of rupture. Each segment within that channel undergoes a mode change. The pin pressure becomes that of the hydrodynamic volume associated with the ruptured segment. An additive form loss coefficient is calculated at rupture based on the clad flow blockage by a simple expression for an abrupt contraction-expansion.

$$K_{add} = \frac{0.5(1 - \beta^2) + (1 - \beta^2)^2}{(\beta^2)^2}, \qquad 2.3.2\text{-}41$$

where

β^2 = fraction of the channel flow area blocked,

= $(1.0 - A_{blocked}/A_{channel})$.

The flow blockage is obtained via a double table interpolation relative to the normalized heating ramp rate and rupture temperature similarly to the clad burst strain. The table is either user supplied or default NUREG-0630 values listed in Tables 2.3.2-3 and 2.3.2-4. The additive value of the loss coefficient is edited at the time of rupture. The flow blockage loss coefficient is added automatically to the problem for a primary pin channel unless the user overrides via a new optional input. If added, the form loss is applied to the forward flow direction for the inlet (bottom) junction and the reverse flow direction for the exit (top) junction attached to the volume in which the clad ruptured. The user option to exclude this form loss addition from the junctions has been included for supplemental pin channels or for certain non-licensing sensitivity studies with multiple cross-connected channels.

Another option has been added to the EM Pin model to help minimize user burden when running EM reflooding heat transfer analyses with BEACH (BAW-10166 Section 2.1.3.8.4). This user-controlled option automatically includes code-calculated pin rupture, droplet break-up (up to 60 percent blockage) for primary pin channels and convective enhancement adjustments for primary or supplemental pin channels. The input grid parameters are modified with the ruptured values and will be retained for use in the reflooding heat transfer calculations. This model is optional and requires input to activate the calculations. If no input is specified the default is that no rupture enhancements will be calculated and no droplet

breakup calculations will be performed for any supplemental pin channels.

When this option is activated, Equations 2.3.2-41.1 through 2.3.2-41.4 will be calculated following cladding rupture for primary pin channels, only. The first calculation performed determines the midpoint elevation of ruptured segment, referenced from the bottom of the pin channel (which coincides with the bottom of the heat structure geometry or reflood stack). This midpoint elevation, Z_{grid}, is the location where the new "grid" is inserted. This elevation is used to determine the droplet break-up effects for the ruptured segment.

$$Z_{grid} = 0.5 \cdot \Delta Z_{rupt_{seg}} + \sum_{j=1}^{rupt\ seg-1} \Delta Z_{seg_j}, \qquad 2.3.2\text{-}41.1$$

where

ΔZ_{seg} = elevation change of pin segment.

The second set of calculations is to calculate rupture droplet breakup efficiency. These calculations are identical to those described in Sections 2.1.3.7. and 2.1.3.8. of Reference 123. The rupture atomization factor, η_{etamax}, is calculated as

$$\eta_{etamax} = \frac{1}{[\ 1 + \{(n^{1/3} - 1) \cdot \min(0.60\ , \epsilon_{fb})\}]}, \qquad 2.3.2\text{-}41.2$$

where

n = number of equal size droplets resulting from the split-up of the larger droplets,

= 2.7, from a droplet distribution flux, and

ϵ_{fb} = flow blockage fraction (limited to a maximum of 0.60).

The increase in the droplet surface area from that used for interface heat transfer is defined in Equation 2.1.3-105[123] as

$$\Delta a_{gf} = C_{maxDB} \theta \ a_{gf} .$$

The proportionality constant, C_{maxDB}, is determined from the constant, C_1, the rupture flow blockage fraction (limited to a maximum of 0.60), and the length of the ruptured segment.

$$C_{maxDB} = \frac{C_1 * \min(0.6 , e_{fb})}{\Delta Z_{rupt_{seg}}} . \qquad 2.3.2\text{-}41.3$$

The recommended value of C_1 is 1.22 meters (4.0 feet).

The velocity of the fluid at the ruptured location increases because of the flow area reduction. The physical area in the code calculations is not modified, but a velocity multiplier, used for determining the droplet Weber number, is calculated from

$$VELMULT = \frac{1}{1 - \min(0.6 , e_{fb})} . \qquad 2.3.2\text{-}41.4$$

The cladding rupture results in an increase in the pin outside heat transfer surface area. The increase in area is not directly included in the conduction solution in the code calculations. It is accounted for by using the rupture convective enhancement factor and applying it to the grid wall heat transfer enhancement factor, F_{gq}, for primary or supplemental channels. The rupture enhancement, M_{RAR}, is an multiplicative contribution determined by

$$M_{RAR} = \text{Rupture Area Ratio}$$

$$= \frac{2\pi \ r_{rupt_{oc}} \ L}{2\pi \ r_{oc_{cold}} \ L} = \frac{r_{rupt_{oc}}}{r_{oc_{cold}}} , \qquad 2.3.2\text{-}41.5$$

ere

$r_{rupt_{oc}}$ = outside clad radius of the ruptured node given by

$$= r_{ic} + \left[r_{oc_{cold}} - r_{ic_{cold}} \right] \left[r_{ic_{cold}} / r_{ic} \right] . \quad 2.3.2\text{-}41.6$$

The total wall heat transfer convective factor then becomes

$$F_{gq_{tot}} = F_{gq_{grid}} \cdot M_{RAR} . \quad 2.3.2\text{-}41.7$$

These droplet break-up and convective enhancement terms are optionally calculated and edited at rupture by the EM pin model.

This page intentionally blank.

r_{ic_u} = inside clad radius of the top pin segment (m), and

ΔL_p = change in gas plenum length (m).

The change in gas plenum length is calculated from the net change in the fuel and clad stack lengths due to axial thermal expansions as follows. Let

ΔL_{cf} = change in gas plenum length from cold condition (m),

$$= \Delta L_c - \Delta L_f \ , \qquad 2.3.2\text{-}51.4$$

where

ΔL_c = total axial thermal expansion of clad from cold condition (m),

$$= \sum_{j=1}^{\#\ seg} (L_j\ \epsilon_{ATC_j}) \ , \text{ and} \qquad 2.3.2\text{-}51.5$$

ΔL_f = total axial thermal expansion of fuel from cold condition (m),

$$= \sum_{j=1}^{\#\ seg} (L_j\ \epsilon_{ATF_j}) \ . \qquad 2.3.2\text{-}51.6$$

Then

ΔL_p = change in gas plenum length from hot initial condition (m),

$$= \Delta L_{cf} - \Delta L_{cf}^{o} \ , \qquad 2.3.2\text{-}51.7$$

where

ΔL_{cf}^{o} = initial over-specification in gas plenum length (m), determined during pin transient initiation,

L_j = axial length of the jth segment (m),

ϵ_{ATF} = fuel strain function of Equation 2.3.2-15, evaluated at fuel volume weighted average temperature $\bar{T}_f$ of Equation 2.3.2-25, (dimensionless), and

ϵ_{ATC} = axial strain function defining clad axial thermal expansion as a function of clad volume average temperature, (dimensionless).

The axial strain for the cladding is defined by either a user-input table versus cladding temperature for zirconium-based alloy cladding (Note: This table replaces the cubic fit from Rev. 3 Eqn 2.3.2-51.8.) or a built in code correlation set for zircaloy cladding[119]

$$\epsilon_{ATC} = -2.506 \times 10^{-5} + (T_C - 273.15)\ 4.441 \times 10^{-6}$$
$$= -1.2381 \times 10^{-3} + 4.441 \times 10^{-6}\ T_C \qquad 2.3.2\text{-}51.9$$

for $T_C \leq$ 1073.15 K (α phase), or

$$\epsilon_{ATC} = -8.3 \times 10^{-3} + (T_C - 273.15)\ 9.7 \times 10^{-6}$$
$$= -1.0950 \times 10^{-2} + 9.7 \times 10^{-6}\ T_C \qquad 2.3.2\text{-}51.10$$

for $T_C \geq$ 1273.15 K (β phase), where T_C is the volume average cladding temperature (K) of Equation 2.3.2-24. In the α phase to β phase transition zone, 1073.15 K < T_C < 1273.15 K, a table lookup is used. Some selected values are listed in Table 2.3.2-2.

Using the assumption that both the slope of the fuel mesh point temperatures and the overall gap conductance will not change significantly, the last gap multiplier (1.0 for the first iteration) can be adjusted via a ratio to give a new multiplier,

$$M_g^{n+1} = \frac{\Delta T_{gap}}{(\Delta T_{gap} + \Delta \bar{T}_f)} M_g^n \quad . \qquad 2.3.2\text{-}52.3$$

After calculation of the new gap multiplier, another conduction solution iteration step is taken. The fuel volume average temperature differential is recalculated via Equation 2.3.2-52.1. If the absolute value is greater than 2 K, then another iteration step is taken after recalculating a new multiplier via Equations 2.3.2-52.2 and 2.3.2-52.3. If the absolute value is less than 2 K, then the iteration has converged and the last multiplier calculated is edited and used during the steady-state and transient EM pin calculations. Up to twenty-one iterations are allowed. If convergence is not obtained in twenty-one iterations, then the code will stop at the end of the initialization process and appropriate failure messages will be edited. Failure of the iteration to converge is generally related to poor estimates given for the initial mesh point temperature distribution. An improved estimate will normally allow the iteration to converge properly. If convergence is still a problem, user specification of the multiplier is also available.

At the completion of the EM pin steady-state calculations (i.e., after EM pin steady-state trip becomes true or during the first time step if there is no trip) several calculations are required to initiate the pin transient calculations. The user-supplied cold unstressed pin geometry input via the heat structure cards is elastically expanded using the final code calculated temperature and mechanical stresses.

$$r_{f_o} = r_{f_{cold}} + u_{TF} \qquad 2.3.2\text{-}53$$

and

$$r_{ic_o} = r_{ic_{cold}} + u_{TC} + u_e + u_{fcc}, \qquad 2.3.2\text{-}54$$

with

r_{f_o} = thermally expanded outside fuel radius (m),

r_{ic_o} = thermally and mechanically expanded inside clad radius (m),

u_e = elastic deformation due to mechanical stresses (m), and

u_{fcc} = elastic deformation from gap mechanical contact (m). This term is calculated from the user supplied input contact pressure and cladding radii during the initialization.

$$u_{fcc} = \frac{P_{fcc} \cdot r_{ic}}{E_c} \left\{ \left[\frac{r_{oc}^2 + r_{ic}^2}{r_{oc}^2 - r_{ic}^2} \right] + \nu_c + \frac{E_c}{E_f} (1 - \nu_f) \right\} \qquad 2.3.2\text{-}54.1$$

The calculated radii are compared against the input values by

$$u_{FC} = r_{f_{input}} - r_{f_o} \qquad 2.3.2\text{-}55$$

$$u_{CC} = r_{ic_{input}} - r_{ic_o}, \qquad 2.3.2\text{-}56$$

and

$$u_{cg} = \begin{cases} 0.0, & \text{for } P_{fcc_{input}} = 0.0 \\ r_{ic_{input}} - r_{f_{input}}, & \text{for } P_{fcc_{input}} > 0.0 \end{cases} \qquad 2.3.2\text{-}56.1$$

5.0 REFERENCES

1. Ransom, V. H., et. al., RELAP5/MOD2 Code Manual -- Volume 1: Code Structures, System Models and Solution Methods and Volume 2: Users Guide and Input Requirements, NUREG/CR-4312 - Volume 1, August, 1985 and NUREG/CR-4312 - Volume 2, December 1985.

2. B&W Nuclear Technologies, RELAP5/MOD2-B&W -- An Advanced Computer Program for Light Water Reactor LOCA and non-LOCA Transient Analysis, BAW-10164P, Revision 1, October 1988.

3. Letter from A. C. Thadani (USNRC) to J. H. Taylor (B&W Nuclear Technologies), Acceptance for Referencing of Topical Report BAW-10164P, Revision 1, RELAP5/MOD2-B&W, An Advanced Computer Program for Light Water Reactor LOCA and Non-LOCA Transient Analysis, April 18, 1990.

4. Code of Federal Regulations, ECCS Evaluation Models, Chapter 10, Part 50, Appendix K

5. B&W Nuclear Technologies, RELAP5/MOD2-B&W -- An Advanced Computer Program for Light Water Reactor LOCA and Non-LOCA Transient Analysis, BAW-10164P, Revision 2, August 1992.

6. B&W Nuclear Technologies, RELAP5/MOD2-B&W -- An Advanced Computer Program for Light Water Reactor LOCA and non-LOCA Transient Analysis, BAW-10164P, Revision 3, October 1992.

7. Letter from J. H. Taylor (B&W Nuclear Technologies) to R. C. Jones (USNRC) BEACH Topical Report BAW-10166P, JHT/93-214, August 31, 1993.

8. Letter from J.H. Taylor (B&W Nuclear Technologies), Response to NRC's Request for Additional Information on BAW-10164, Revision 2, August, 1992; RELAP5/MOD2-B&W, An Advanced Computer Program for Light Water Reactor LOCA and NON-LOCA Transient Analysis, JHT/93-279, November 16, 1993

9. Letter from J.H. Taylor (B&W Nuclear Technologies), Response to NRC's Request for Additional Information on BAW-10164, Revision 3, October, 1992; RELAP5/MOD2-B&W, An Advanced Computer Program for Light Water Reactor LOCA and NON-LOCA Transient Analysis, JHT/94-7, January 21, 1994

10. Letter from J.H. Taylor (B&W Nuclear Technologies), Response to NRC's Supplemental Request for Additional Information on BAW-10164, Revision 2, August, 1992; RELAP5/MOD2-B&W, An Advanced Computer Program for Light Water Reactor LOCA and NON-LOCA Transient Analysis, JHT/94-146, September 20, 1994.

This page intentionally left blank.

Attachment 2

AFFIDAVIT OF THOMAS A. COLEMAN

A. My name is Thomas A. Coleman. I am Vice President of Government Relations for Framatome Cogema Fuels (FCF). Therefore, I am authorized to execute this Affidavit.

B. I am familiar with the criteria applied by FCF to determine whether certain information of FCF is proprietary and I am familiar with the procedures established within FCF to ensure the proper application of these criteria.

C. In determining whether an FCF document is to be classified as proprietary information, an initial determination is made by the Unit Manager, who is responsible for originating the document, as to whether it falls within the criteria set forth in Paragraph D hereof. If the information falls within any one of these criteria, it is classified as proprietary by the originating Unit Manager. This initial determination is reviewed by the cognizant Section Manager. If the document is designated as proprietary, it is reviewed again by personnel and other management within FCF as designated by the Vice President of Government Relations to assure that the regulatory requirements of 10 CFR Section 2.790 are met.

D. The following information is provided to demonstrate that the provisions of 10 CFR Section 2.790 of the Commission's regulations have been considered:

(i) The information has been held in confidence by FCF. Copies of the document are clearly identified as proprietary. In addition, whenever FCF transmits the information to a customer, customer's agent, potential customer or regulatory agency, the transmittal requests the recipient to hold the information as proprietary. Also, in order to strictly limit any potential or actual customer's use of proprietary information, the substance of the following provision is included in all agreements entered into by FCF, and an equivalent version of the proprietary provision is included in all of FCF's proposals:

"Any proprietary information concerning Company's or its Supplier's products or manufacturing processes which is so designated by Company or its Suppliers and disclosed to Purchaser incident to the performance of such contract shall remain the property of Company or its Suppliers and is disclosed in confidence, and Purchaser shall not publish or otherwise disclose it to others without the written approval of Company, and no rights, implied or otherwise, are granted to produce or have produced any products or to practice or cause to be practiced any manufacturing processes covered thereby.

Notwithstanding the above, Purchaser may provide the NRC or any other regulatory agency with any such proprietary information as the NRC or such other agency may require; provided, however, that Purchaser shall first give Company written notice of such proposed disclosure and Company shall have the right to amend such proprietary information so as to make it non-proprietary. In the event that Company cannot amend such proprietary information, Purchaser shall, prior to disclosing such information, use its best efforts to obtain a commitment from NRC or such other agency to have such information withheld from public inspection.

Company shall be given the right to participate in pursuit of such confidential treatment."

(ii) The following criteria are customarily applied by FCF in a rational decision process to determine whether the information should be classified as proprietary. Information may be classified as proprietary if one or more of the following criteria are met:

a. Information reveals cost or price information, commercial strategies, production capabilities, or budget levels of FCF, its customers or suppliers.

b. The information reveals data or material concerning FCF research or development plans or programs of present or potential competitive advantage to FCF.

c. The use of the information by a competitor would decrease his expenditures, in time or resources, in designing, producing or marketing a similar product.

d. The information consists of test data or other similar data concerning a process, method or component, the application of which results in a competitive advantage to FCF.

e. The information reveals special aspects of a process, method, component or the like, the exclusive use of which results in a competitive advantage to FCF.

f. The information contains ideas for which patent protection may be sought.

The document(s) listed on Exhibit "A", which is attached hereto and made a part hereof, has been evaluated in accordance with normal FCF procedures with respect to classification and has been found to contain information which falls within one or more of the criteria enumerated above. Exhibit "B", which is attached hereto and made a part hereof, specifically identifies the criteria applicable to the document(s) listed in Exhibit "A".

(iii) The document(s) listed in Exhibit "A", which has been made available to the United States Nuclear Regulatory Commission was made available in confidence with a request that the document(s) and the information contained therein be withheld from public disclosure.

(iv) The information is not available in the open literature and to the best of our knowledge is not known by Combustion Engineering, Siemens, General Electric, Westinghouse or other current or potential domestic or foreign competitors of Framatome Cogema Fuels.

(v) Specific information with regard to whether public disclosure of the information is likely to cause harm to the competitive position of FCF, taking into account the value of the information to FCF; the amount of effort or money expended by FCF developing the information; and the ease or difficulty with which the information could be properly duplicated by others is given in Exhibit "B".

I have personally reviewed the document(s) listed on Exhibit "A" and have found that it is considered proprietary by FCF because it contains information which falls within one or more of the criteria enumerated in Paragraph D, and it is information which is customarily held in confidence and protected as proprietary information by FCF. This report comprises information utilized by FCF in its business which afford FCF an

opportunity to obtain a competitive advantage over those who may wish to know or use the information contained in the document(s).

T A Coleman

THOMAS A. COLEMAN

State of Virginia)
) SS. Lynchburg
City of Lynchburg)

Thomas A. Coleman, being duly sworn, on his oath deposes and says that he is the person who subscribed his name to the foregoing statement, and that the matters and facts set forth in the statement are true.

T A Coleman

THOMAS A. COLEMAN

Subscribed and sworn before me
this 21st day of Sept. 1999.

Brenda C. Cardoza
Notary Public in and for the City
of Lynchburg, State of Virginia.

My Commission Expires July 31, 2003

EXHIBITS A & B

EXHIBIT A

Responses to NRC Requests for Additional Information on Topical Report BAW-10227P, "Evaluation of Advanced Cladding and Structural Material (M5) in PWR Reactor Fuel," dated October 26, 1998 and January 29, 1999.

EXHIBIT B

The above listed document contains information that is considered Proprietary in accordance with Criteria b, c, d, and e of the attached affidavit.

Attachment 3

The FCF non-proprietary version of responses to NRC requests for additional information (RAI) has not been included in this report. Please see BAW-10227-A, "Evaluation of Advanced Cladding and Structural Material (M5) in PWR Reactor Fuels", pages k-1 - k-39 and enclosure 1 to that section. There is no proprietary information in the submitted change pages to BAW-10164. Therefore, the pages are identical to those shown in attachment 1.

FRAMATOME TECHNOLOGIES

February 29, 2000
FTI-00-551

Document Control Desk
U. S. Nuclear Regulatory Commission
Washington, DC 20555-0001

Subject: Modeling Refinements to Framatome Technologies' RELAP5-Based, Large Break LOCA Evaluation Models—BAW-10168 for Non-B&W-Designed, Recirculating Steam Generator Plants and BAW-10192 for B&W-Designed, Once-Through Steam Generator Plants.

Gentlemen:

Framatome Technologies Incorporated (FTI) maintains two NRC-approved large break loss-of-coolant accident (LBLOCA) evaluation models (EMs) to demonstrate compliance with the requirements of 10CFR50.46. The EM described in BAW-10168P-A, Revision 3, December 1996 applies to plant designs incorporating recirculating steam generators (RSGs) and the EM described in BAW-10192P-A, Revision 0, June 1998 is applied to the B&W NSS design. FTI is refining the modeling of the hot rod/hot assembly in its LBLOCA EMs to improve the simulation of the LOCA cooling process. The refinements apply equally to LBLOCA licensing calculations performed with the RSG and the B&W EMs.

FTI's existing LBLOCA evaluations do not resolve the difference between the hot rod within the hot fuel assembly and the hot fuel assembly. Without such differentiation, it becomes necessary to apply all fuel temperature uncertainties and margins considered appropriate to the hot rod to the entire hot assembly. This places an undue burden on the calculation of the coolant properties within the hot assembly. To reduce this effect and remove over-conservatism from the evaluations, the heat structure simulating the hot rod/hot assembly is being split, one structure for the hot assembly and one for the hot rod. The refinement allows for the application of more realistic, steady state, volume-averaged, fuel temperature, uncertainty factors.

Future LBLOCA analyses will be performed in the following manner:

> The average core heat structure will be initialized with no uncertainty. The hot assembly heat structure will be initialized at a statistical-based, uncertainty providing 95 percent confidence in 95 percent of all instances that the average fuel temperature in the assembly is bounded. The maximum 95/95, fuel temperature uncertainty will be imposed only on the hot rod heat structure. [Note that a correction to TACO3 predictions at high burnup will still be applied.]

3315 Old Forest Road, P.O. Box 10935, Lynchburg, VA 24506-0935
Telephone: 804-832-3000 Fax: 804-832-3663
Internet: http://www.framatech.com

This approach to the simulation of the thermal evolution of the peak cladding temperature is consistent with generally accepted industry practice and does not, in Framatome Technologies' opinion, comprise a change or revision to the existing approved LBLOCA EMs. Rather, the change in simulation can be accomplished under the dictates of the existing EMs because it lies within the modeling prerogatives retained by FTI.

The heat structure refinements affect the RELAP5 and BEACH (a set of subroutines within the RELAP5 computer code) simulations because they involve the prediction of hot rod cladding temperatures. REFLOD3B is unaffected because only the average core is included in the calculation scheme. Computer code updates were incorporated, as a user convenience, into RELAP5/MOD2-B&W Version 24.0HP, including its BEACH subroutines. They were submitted to the NRC as Revision 4 of the RELAP5/MOD2-B&W topical in April 1998 and replaced in toto in September 1998. The submittal was part of the RELAP5/MOD2-B&W M5 advanced clad implementation package.

Currently, these refinements are not being considered for application to FTI's small break LOCA methods. Framatome Technologies will continue to apply the TACO3-based, hot rod, volume-averaged, fuel temperature, uncertainty factor to all fuel assemblies in its small break LOCA evaluation models.

The attached material is presented to continue close communications with the NRC regarding the status of Framatome Technologies' LOCA licensing applications and modeling techniques. If the NRC disagrees with or is concerned over Framatome Technologies' large break LOCA refinements, an expeditious response to this letter is requested.

Framatome Technologies intends to apply these refined modeling techniques in future large break LOCA analyses. The first application is scheduled for the TVA Sequoyah plants starting in August 2000. Framatome, also requests the approval of the RELAP5/MOD2-B&W changes included in the proposed Revision 4 to BAW010164 by August 2000. Framatome requests that the NRC inform us, by May 2000, of any disagreement with our position on the implementation of these heat structure refinements.

The attachment is considered non-proprietary to Framatome Technologies. If you require additional information, please contact John Biller at 804/832-2600 or John Klingenfus at 804/832-3294.

Sincerely,

J. J. Kelly, Manager
B&W Owners Group Services

/bcc

w/ Attachment

cc: Stewart N. Bailey/NRC
L. Lois/NRC
F. R. Orr/NRC
D. M. Lafever/TVA-SQN
J. R. Biller/FTI/OF53
B. M. Dunn/FTI/OF53
J. A. Klingenfus/FTI/OF53
R. J. Schomaker/FTI-BWOG/OF59
M. A. Schoppman/FTG/MD82

w/o Attachment

J. B. Andrews/FCF/OF19
A. B. Copsey/FCF/OF19
J. J. Cudlin/FTI/OF53
G. E. Hanson/FCF/OF19
G. A. Meyer/FCF/OF13

bc: R. J. Lowe, OF53
M. L. Miller, OF53
C. K. Nithianandan, OF53
D. R. Page, OF53
J. R. Paljug, OF49
M. V. Parece, OF49
J. C. Seals, OF53
N. H. Shah, OF53
D. A. Wesley, OF19
G. J. Wissinger, OF53

Attachment

I. Introduction

Framatome Technologies Incorporated (FTI) maintains two NRC approved large break loss-of-coolant accident (LBLOCA) evaluation models (EMs) to demonstrate compliance with the requirements of 10CFR50.46. The EM described in BAW-10168P-A, Revision 3, December 1996 [1] applies to plant designs incorporating recirculating steam generators (RSGs) and the EM described in BAW-10192P-A, Revision 0, June 1998 [2] is applied to the B&W NSS design. FTI is refining the modeling of the hot rod/hot assembly in our LBLOCA EMs to improve the simulation of the LOCA cooling process. The refinements apply equally to LBLOCA licensing calculations performed with the RSG and the B&W EMs.

FTI's existing LBLOCA evaluations do not resolve the difference between the hot rod within the hot fuel assembly and the hot fuel assembly. Without such differentiation, it becomes necessary to apply all uncertainties and margins considered appropriate to the hot rod to the entire hot assembly. This places an undue burden on the calculation of the coolant properties within the hot assembly. To reduce this effect and remove over-conservatism in the evaluations, the heat structure simulating the hot rod/hot assembly is being split, one structure for the hot assembly and one for the hot rod. This approach does not, in Framatome Technologies' opinion, comprise a change or revision to the existing approved LBLOCA EMs. Rather, the change in simulation can be accomplished under the dictates of the existing EMs because it lies within the modeling prerogatives retained by FTI.

Both the RSG and the B&W LBLOCA evaluation models are composed of three (3), NRC-approved computer codes:

- RELAP5/MOD2-B&W [3], which is used to compute the system thermal-hydraulic response during blowdown including hot rod/hot assembly temperatures.
- REFLOD3B [4], which predicts the refill/reflood system thermal-hydraulic response.
- BEACH [5], which comprises a set of subroutines within the RELAP5 code used to calculate hot rod/hot assembly refill and reflood thermal behavior.

Figure 1 shows the basic interface between these three (3) codes. The heat structure refinements affect the RELAP5 and BEACH simulations because they involve the prediction of hot rod cladding temperatures. Because only the average core is included in the calculation scheme, REFLOD3B is unaffected. Figures 2a and 2b show representative blowdown (RELAP5)/refill-reflood (BEACH) core noding schemes. [Note that for simplicity the blowdown crossflow junctions are not shown in Figures 2a and 2b. During blowdown, each elevation-pair of hot and average core nodes is cross-connected. At the start of refill—the BEACH calculation—the blowdown crossflow junctions are deleted from the problem. The use of and the deletion of crossflow junctions in the LBLOCA simulation is unchanged by the refinements discussed herein.] For the current simulations, the average core and the hot channel each connect to a single heat structure. The heat structure for the hot channel represents one complete fuel assembly (the hot assembly plus the hot rod) with

maximum uncertainties and margins applied to all rods. All rods are driven at the maximum allowable peaking. The heat structure in the average core represents all core fuel assemblies less the one hot channel assembly.

Core heat structures are initialized using steady state, volume-averaged, fuel temperature inputs calculated by the TACO3 fuel code [6]. While not required by the EMs [1,2], the TACO3-specified "hot rod" uncertainty factor (1.115) has usually been applied to both the hot assembly heat structure and the average core heat structure. This provides a conservative overestimation of the initial core stored energy. Some current analyses have removed the hot rod uncertainty factor from the average core heat structure but in all current calculations the full factor is applied to the hot assembly heat structure. This practice substantially overestimates the initial enthalpy of the heat structures. Of particular importance is the overestimation of the enthalpy in the hot assembly and its resultant impact on the coolant properties during blowdown, refill, and reflood. In future LBLOCA analyses, FTI will impose the following conservatism:

> The average core heat structure will be initialized with no uncertainty. The hot assembly heat structure will be initialized at a statistical-based, uncertainty providing 95 percent confidence in 95 percent of all instances that the average fuel temperature in the assembly is bounded. The maximum 95/95, fuel temperature uncertainty will be imposed only on the hot rod heat structure. [Note that a correction to TACO3 predictions at high burnup will still be applied.]

To accomplish this, it is necessary to resolve the heat structure modeling of the hot rod/assembly from one to two heat structures with a shared coolant channel. One structure simulates the hot rod of the hot assembly and the other the hot assembly less the hot rod. Figure 2c illustrates the resulting coolant channel heat structure scheme. The maximum fuel temperature uncertainty is used to initialize the hot rod heat structure and an appropriately conservative fuel temperature uncertainty is used for the hot assembly heat structure. The following sections describe minor RELAP5 code adjustments necessary for multiple heat structure modeling, specific parameter derivations and assignments between the multiple heat structures, and comparative results of the revised modeling for both the B&W and the RSG EMs.

II. RELAP5/MOD-B&W Modifications

For any given core fluid channel, a wide range of reasons exists for use of multiple heat structure capabilities—that is, supplemental rods. Simulation of fuel rod differences within an assembly or a group of fuel assemblies is the essential reason. The capability is particularly useful in modeling gadolinium rods, lead test rods, or in the quantification of peaking or initial enthalpy differences between rods. RELAP5/MOD2-B&W [3], including its BEACH [5] subroutines, has the general ability to model multiple heat structures per coolant channel. However, the code was update to facilitate proper simulation of bundle and individual rod parameters within the confines of a LBLOCA calculation. It becomes important, in a multiple heat structure environment, to distinguish between characteristics created by and important to individual rods and those created by the fuel assembly as a

whole. Updates were incorporated, as a user convenience, into RELAP5/MOD2-B&W Version 24.0HP, including its BEACH subroutines. They were submitted to the NRC as Revision 4 of the RELAP5/MOD2-B&W topical in April 1998. The submittal was part of the RELAP5/MOD2-B&W M5 advanced clad implementation package. (These changes have nothing to do with the M5 cladding but that submittal was convenient and timely.) The changes were replaced in toto in September 1998 because an additional code upgrade required by the M5 cladding had been recognized. The following is a brief discussion of the RELAP5/BEACH upgrades incorporated in Version 24.0HP to support multiple heat structure simulation.

The occurrence of rupture, being dependent on cladding temperature and internal rod pressure, is a heat structure calculation. The effect of rupture, however, may be on individual rods or through an impact on the coolant channel and, hence, on all heat structures within the channel. Therefore, the effects of rupture must be properly sorted and related to the appropriate causative heat structure. The cladding strain and heat transfer area prior to or after rupture, to the extent that they are included in the LOCA calculations, are individual rod- or rod group-related and should be determined from the individual heat structure status. RELAP5/MOD2-B&W has always associated the calculation of these parameters with individual heat structures and that is unchanged. The rupture-induced droplet breakup model, the resultant inter-phase heat transfer parameters, and the rupture flow resistance factor are assembly effects and should be queued to the assembly regardless of the status of individual rods or any other supplemental rods. Accordingly, the hot pin rupture location is hot assembly-based. Within the RELAP5/MOD2-B&W and BEACH rod models, the quench front and incipient boiling locations are determined by the heat structure routines. These parameters are rod- or rod group-related and should be determined from the status of an individual heat structure.

With Version 24.0HP of RELAP5/MOD2-B&W and its BEACH options, a user option specifies each rod or rod group as primary or supplemental. This allows form loss, rupture-induced droplet breakup (BEACH), and quench front and incipient boiling location calculations to be performed based on the appropriate heat structure. Thus, even after an individual rod ruptures, rupture-induced droplet breakup cooling will be based on the specified primary bundle, heat structure prediction of rupture.

The RELAP5/MOD2-B&W and BEACH updates in Version 24.0HP allow each heat structure to have an individual material makeup. One heat structure, for example, could represent Zircaloy-4 fuel rods while a second heat structure in the same fluid channel could represent a set of gadolinium fuel rods or perhaps clad with an advanced material. An "IF" check has also been added to automate compliance with the NRC-imposed limitation on the amount of blockage that can be used in the rupture-induced droplet breakup model. Regardless of the amount of coolant channel blockage calculated, no more than a 60 percent channel blockage will be used in the droplet breakup calculations.

III. Steady State, Volume-Averaged, Fuel Temperature Distribution

The reason for making these refinements in the modeling of the hot rod/hot assembly is to mechanistically incorporate into the solution differences between the two regions in the LOCA predictions. One of these differences occurs in the amount of uncertainty to be used in the initialization of the fuel pellet enthalpy. The large break LOCA evaluation models [1, 2] indirectly specify the value of the fuel temperature uncertainty factor through reference to an approved fuel code, TACO3 [6] (BAW-10162P-A). TACO3 provides essentially a best estimate prediction of the fuel pellet steady state temperature. To assure conservatism in the LOCA initialization, the predicted fuel temperature is increased by the published TACO3 uncertainty providing 95 percent confidence in 95 percent of all instances that the temperature is not underpredicted. The TACO3 topical report specifies an 11.5 percent uncertainty value for the hot spot. The topical report also demonstrates that the average channel uncertainty is zero, and provides data necessary to determine an appropriate hot assembly uncertainty factor. For exposures above 40 GWd/mtU, a bias is added to TACO3 temperature predictions in accordance with the extended burnup topical report [8].

A probabilistic analysis was performed for the immediate vicinity of the hot rod. Based on the TACO3 uncertainty distribution function, a three-percent value was found to assure with a 95/95 percent confidence that the average fuel temperature within this region was bounded. For convenience and ease of application, past evaluations applied the full TACO3 uncertainty to the entire hot assembly and average core. This practice is not specified or required by TACO3 [6] nor is it specified or required by either LBLOCA EM [1, 2]. FTI's prior use of a single, large uncertainty factor (1.115) was a self-imposed conservatism that is now being removed. Discussions of the development of appropriate fuel assembly uncertainties and representative evaluations of the impact for both B&W-designed and RSG plants follow.

1. Fuel Temperature Uncertainty for the Average Core

The recommended uncertainty factor to use for the TACO3 [6], LOCA fuel temperature predictions is one (1) for exposures below 40 GWd/mtU. The value is based on probabilistic analysis (the results of which are documented in Reference 6) performed with TACO3-predicted fuel temperatures. The probabilistic analysis, based on a sample size of over 700, yielded a mean measured-to-predicted fuel temperature quotient of 1.00. (Note that an average channel in either evaluation model easily comprises more than 20,000 fuel rods.) Furthermore, no significant bias was observed with respect to temperature, power, or burnup. Therefore, nearly half of the TACO3 temperature predictions were less than measurements and half were greater than measurements. In essence, TACO3 predictions are best estimate. It follows directly that the mean measured-to-predicted quotient of 1.00 should be applied to core average channel temperature predictions. Again, for exposures above 40 GWd/mtU, a bias is added to TACO3 temperature predictions in accordance with the extended burnup topical report [8].

While not explicitly stated, the recommended fuel temperature, uncertainty factor in the NRC-approved, TACO3 topical report was formulated to apply within hot rods only. Figure I-4 in the topical report illustrates this point. The LOCA rod average linear heat rates in this figure correspond to typical hot rod F_Q's. An average channel fuel temperature uncertainty factor of one (1), therefore, is appropriate and consistent with the intent and approval of the fuel temperature probabilistic predictions and with the LOCA applications uncertainty factor presented in the TACO3 topical report. Average channel modeling remains unchanged. Only an overt and unnecessary input conservatism is being removed.

2. Fuel Temperature Uncertainty for the Hot Assembly

As discussed in Section II, FTI increased the hot channel heat structure detail—a switch from one to multiple heat structures. The large break LOCA hot channel (in both evaluation models) comprises a single fuel assembly, all rods of which are driven at the maximum allowable peaking. In the evaluation of homogeneous fuel assemblies, one heat structure represents the hot rod and a second hot channel heat structure represents the remainder of the hot assembly. Both heat structures are coupled to a single coolant channel representing the hot channel. If the assembly is not homogeneous—a gadolinium or MOX application, for example—an individual heat structure is used to represent each of the hot rods (or rod groups) to be evaluated and another structure represents the remainder of the hot assembly. Again all of these heat structures are coupled to a single coolant channel representing the hot channel.

Using the measured-to-predicted data in the TACO3 [6] topical report, a probabilistic analysis was performed to determine the appropriate initial fuel enthalpy (fuel temperature) uncertainty factor for application to the rods (the hot assembly rods) surrounding the hot rod. For the purpose of this discussion, the term hot spot will be used as the location on the hot rod that will eventually produce or be the location of the peak cladding temperature. The probabilistic evaluation proceeded in three steps:

1. Determination of the region within the hot assembly that drives interactions (heat transfer) with the hot spot and generation of a large number of randomly distributed sets of fuel pellet enthalpy uncertainties within that region.

2. Determination and assignment of importance factors for each individual pellet and computation of the average weighted uncertainty for each set.

3. Ordering of the sets to determine the probability distribution of the average uncertainty within the region.

The premise of the separate heat structures is that certain aspects of the heat transfer process occurring at the hot spot are not controlled by hot spot conditions but rather by surrounding conditions. Locally the interaction or coupling between the hot spot and its surroundings is through heat transfer to the coolant and the physical state of the coolant. Although the hot spot influences the coolant state, preconditioning and mixing within the

entire hot assembly is far more influential. In this conditioning, however, the fuel in immediate proximity to the hot spot dominates. A proper determination of the drivers for the coolant conditions at the hot spot would reflect the varying influence of the fuel surrounding the hot spot, making remote fuel of low importance and nearby fuel of higher importance. To conservatively specify the region of influence, FTI uses only the fuel pellets within the hot rod, within the rods in contact with the four coolant subchannels directly associated with the hot rod, and within the same grid span as the hot spot. Weighting factors for each rod are determined in accordance with their association with the four subchannels. Because the average uncertainty of a group will vary inversely with the membership count of the group, this limitation will overpredict the uncertainty. This uncertainty, in the FTI approach, is then assigned to the entire hot assembly, excepting the supplemental rods, to assure a conservative representation of the coolant drivers near the hot spot.

Following the determination of the region, a series of possible uncertainty distributions is assembled by randomly assigning an enthalpy uncertainty to each fuel pellet in accordance with the TACO3 uncertainty distribution function. Each set represents a physically possible distribution of the fuel steady state enthalpies within the region but there is no assurance of conservatism. Weighting factors for the contribution of each pellet are then assigned according to the dominant physical process for the coupling. There are two of these. During periods of flow, the coupling is via convective heat transfer and the importance is assigned in accord with the individual pellet influence on the coolant temperature. During stagnant conditions, the coupling is via radiation heat transfer and the importance is assigned via the influence of pellets on cladding temperatures and the corresponding view factors. For flow periods, the region is limited to only one half of the grid span and all pellets within the region contribute according to their association with the hot subchannel. This includes the pellets in the hot rod that are assigned an importance of 1.0. For the regional uncertainty, the pellets in the hot rod below the hot spot are assigned uncertainties according to the TACO3 uncertainty distribution but those at the hot spot are forced to the TACO3 95/95 percent confidence level. For stagnant periods, none of the pellets within the hot rod are included because there is no axial radiation within a rod. However, the entire grid span is allowed because the heat transfer process is unrelated to direction. The importance factors are determined from the view factor relating the hot spot to the clad surrounding each pellet.

With the appropriate weighting factors assigned to each pellet, the average uncertainty of each set is computed. The resulting array of average uncertainties is ordered and the average uncertainty that bounds 95 percent of the values in the array (in 95 percent of all instances) is determined. If the fuel temperature uncertainty for the hot bundle heat structure is set to a value equal to or greater than this 95/95 percent bound, the fuel temperature impact of the hot assembly modeling will be suitably bounding for the LOCA calculation. For the TACO3 uncertainty distribution, the computed 95/95 percent confidence uncertainty value for flowing conditions was determined to be 2.1 percent. For stagnant conditions, the value was determined to be 2.6 percent. Within the FTI LOCA evaluations a fuel temperature uncertainty of 3 percent will be assigned for the heat structure modeling the hot assembly when the bundle exposure is up to 40

GWd/mtU and the fuel temperature prediction is generated by TACO3. Above 40 GWd/mtU, the uncertainty will be linearly increased in accordance with the extended burnup topical report [8].

3. Fuel Temperature Uncertainty for the Hot Rod

The recommended fuel temperature uncertainty factor presented in the NRC-approved, TACO3 topical report was formulated for the hot spot. The TACO3-recommended uncertainty factor, 11.5 percent, will continue to be applied to the simulation of the entire hot rod for rod average burnups up to 40 GWd/mtU. For rod average burnups above 40 GWd/mtU, the uncertainty is increased in accordance with the extended burnup topical report [8]. By preserving the application of the recommended pellet uncertainty factor to the entire hot rod, the appropriate initial fuel enthalpy will have been applied at the location of peak cladding temperature regardless of where in the hot rod that temperature occurs.

IV. Heat Transfer During Refill

The RSG- and B&W-designed EMs present slightly differing interpretations as to heat transfer from the reactor core during the refill period. Previously, this phase of the accident was mostly termed the adiabatic heatup period because minimal heat transfer from the core was possible and most evaluation models simply chose not to model any. There is actually no requirement in the regulation to restrict heat transfer during this period, other than application of the reflood restriction on convective heat transfer to steam cooling models. Recently, radiation models have been approved within the industry for heat transfer during refill/reflood. These models do not allow large amounts of heat transport, but over the course of refill small contributions accumulate and are significant. The RSG EM implies that this period is modeled as adiabatic. The B&W-design EM more correctly describes the period as nearly adiabatic. In fact, in Revision 3 of the RSG evaluation model, when RELAP5/MOD2-B&W replaced FRAP-T6-B&W for the calculation of the hot spot temperature during blowdown and the application of BEACH was expanded to initiate at the end of blowdown, heat transfer to the stagnant steam resident within the core was included. For the BEACH application, it was possible to input zero incoming flow but it was not possible to eliminate the resident steam. Therefore, for the last several years a description of nearly or essentially adiabatic is more appropriate. The NRC understood this when the FRAP-T6-B&W replacement was approved for the RSG EM.

When all rods in the hot bundle are identical, as with the previous LOCA implementations, the slight amount of heat transfer possible to the resident steam is divided equally between each rod in the assembly and the heat flow to the resident steam has an insignificant effect on an individual rod. However, when most of the rods within the hot assembly are initialized such that they will have lower temperatures than the hot rod during refill, the potential for heat transfer from the hot rod is increased and the result is noticeable. The effect is created because only about 0.5 percent of the energy transmitted to the steam is from the hot rod. Thus the steam maintains the temperature of

the hot bundle heat structure creating a temperature difference to the hot rod that leads to the transport of significant energy. To assure that this energy is not an over prediction of the actual available heat transport, the energy transfer was compared to what could have been transported by rod-to-rod radiation. The amount of energy released to the resident steam from the hot spot by the FTI model during refill amounts to approximately 2.5 percent of the decay heat rate at the hot spot. Rod-to-rod radiation would allow the transport of approximately 5 percent of the hot spot decay heat to surrounding rods. Thus, during the refill period, the heat transfer allowed by FTI's modeling remains conservative by a factor of two (2).

V. Comparisons

This section presents the results of cases that were used to assess the impact of updating from one to two hot channel heat structures and, more importantly, that of reducing the uncertainty factors. Results are shown for both B&W lowered-loop and RSG plants. Expectations for the B&W raised-loop design would fall between the results for the above mentioned plant types. The initial comparison cases are based on a uniform uncertainty of 11.5 percent. They demonstrate that the addition of a second heat structure in the hot channel has no effect of any significance whatsoever on case results. Minor noted differences result from normal computer code numerical issues—round off. The comparisons confirm proper RELAP5 implementation and no impact on prior licensing calculations.

The final comparison cases show the predictive changes achieved by reducing the self-imposed conservatism on the steady state, volume-averaged, fuel temperature, uncertainty factors. Factors of 1.0, 1.03, and 1.115 were applied to the average core, the hot assembly, and the hot rod, respectively. Primarily, the final comparison cases are discussed below.

1. Once-Through Steam Generator Plants

B&W-designed plants would be expected to show a greater sensitivity to reductions in initial stored energy than would U-tube steam generator plants. Experience indicates that the peak-clad temperature for once-through steam generator plants (notably the lowered-loop design) generally occurs late in or immediately following the end of the refill period. The refill period is the period required for the ECCS to completely fill the depleted inventory of the reactor vessel lower head and lower plenum. Since B&W plants peak early in the transient, the large break LOCA is substantially influenced by stored energy. (On the other hand, U-tube plants generally peak well past the end of the refill period. Accordingly, recirculating steam generator plants are largely controlled by decay heat and are less influenced by initial stored energy levels.)

The large break LOCA plant model used for TMI-1 nuclear plant reload licensing application was selected for the multiple core heat structure evaluation. The axial peak power at the 2.5-ft level yields the limiting PCT based on the currently licensed axial power limit (K_z). The plant configuration is presented in Table 1. The evaluation of cladding temperature transients is performed with three computer codes, interconnected as depicted

in Figure 1. The computer code models are consistent with the EM described in Reference 2. The core is radially divided into two fluid channels, hot and average fluid channels as shown in Figure 2a. Each channel consists of 22 axial volumes, numbered 325 through 346 and 425 through 446 for the hot and average fluid channels respectively. The bottom and top volumes (325 and 346 and 425 and 446) in each channel are unheated core volumes. The active core regions for the hot and average fluid channels are volumes 326 through 345 (heat structures 2 through 21) and volumes 426 through 445 respectively. The RELAP5/MOD2-B&W code [3] is used to predict the reactor coolant system thermal-hydraulic transients during the blowdown and post-blowdown core thermal analysis (BEACH). The REFLOD3B code [4] is used to generate post-blowdown hydraulic boundary conditions to be used in the core thermal analysis with the BEACH code. The initial volume-averaged fuel temperatures are calculated by the TACO3 code [6], and are adjusted to account for uncertainties for LOCA application. The following three analyses were performed to evaluate the effects of the uncertainty on the PCT.

- Case 1 (Base EM): The current licensing model has two core heat structures, one representing the hottest assembly, and the other representing the remaining 176 assemblies. The volume-averaged fuel temperatures for both heat structures have 11.5 percent uncertainty added.

- Case 2: This is Case 1 with three core heat structures. The base EM hot assembly heat structure is split into two heat structures within the hot fluid channel, one representing one (1) hot rod and the other representing the remaining 207-rod hot assembly. The temperature uncertainty remains at 11.5 percent. The average heat structure remains unchanged.

- Case 3: This is Case 2 with reduced uncertainty in the hot and average assembly heat structures. The uncertainty in the 207-rod hot assembly heat structure in Case 2 is reduced from 11.5 to 3 percent. The uncertainty for the average assembly heat structure is reduced from 11.5 to 0 percent. The hot rod heat structure remains unchanged.

The results of the B&W reduced uncertainty case are compared to the unreduced uncertainty case in Table 2 and in Figures 3 through 7. Both cases use three (3) core heat structures, one (1) in the average fluid channel, and two (2) in the hot fluid channel.

The results of the evaluation are summarized in Table 2. The peak cladding temperatures for the hot rod unruptured (node 6) and ruptured (node 7) nodes are presented in Figures 3 and 4, respectively. The cladding burst occurred near the end of blowdown due to the high peak power (16.8 kw/ft) and the low core downflow during blowdown. A brief period of enhanced local cooling following the rupture was observed. However, this is more than offset by energy addition from the metal-water reaction during the subsequent refill period. Thus, the heatup rate at the ruptured node is substantially greater than unruptured locations. In addition, high flooding rates during the early phase of the reflood transient are sufficient to provide cladding temperature turnaround a few seconds after the start of reflood. Thus, the ruptured node PCT becomes limiting. The hot spot (node 7) mass flow rate during the

blowdown in Figure 5 is relatively insensitive to the core stored energy. Figure 6 shows slightly higher flooding rates for Case 3 during the early phase of the reflood transient. The hot spot vapor temperature plots in Figure 7 show that the Case 3 vapor temperature is generally lower than those of Cases 1 and 2 due to lower energy deposition in the hot channel.

The results of Cases 1 (base EM) and 2 confirm that the multiple-core heat structure model is properly implemented in the RELAP5/MOD2 code. The clad rupture occurred at node 7 for both the hot rod and hot assembly heat structures. Case 3 with the lower hot channel fluid temperature and higher flooding rate results in a lower heatup rate. The PCT for Case 3 decreased by more than 150 F below the base EM case. The PCTs for the base EM and the revised EM (Case 3) with the reduced uncertainties are 2055 F and 1904 F respectively. Both values are substantially below 10CFR50.46 limits.

2. U-Tube Steam Generator Plants

The large break LOCA plant model used for the Sequoyah nuclear plant reload licensing application was selected for the multiple core heat structure evaluation. The axial peak power at the 9.7-ft level yields the limiting PCT based on the current licensed axial power limit (K_z). The plant configuration is presented in Table 3. The evaluation of cladding temperature transients is performed with three computer codes. Their connectivity is depicted in Figure 1. The computer code models are consistent with the EM described in Reference 1. The core is radially divided into two fluid channels, hot and average fluid channels as shown in Figure 2b. Each channel consists of 20 axial volumes, numbered 326 through 345 and 426 through 445 for the hot and average fluid channels respectively. The RELAP5/MOD2-B&W code [3] is used to predict the reactor coolant system thermal-hydraulic transients during the blowdown and post-blowdown core thermal response (BEACH). The REFLOD3B code [4] is used to generate post-blowdown hydraulic boundary conditions to be used in the core thermal analysis. The initial volume-averaged fuel temperatures are calculated by the TACO3 code [6], and are adjusted to account for uncertainties for LOCA application. The following three analyses were performed to evaluate the effects of initial fuel temperature uncertainty on PCT.

- Case 1 (Base EM): The current licensing model has two core heat structures, one representing the hot assembly and the other representing the remaining 192 assemblies. The volume-averaged fuel temperatures for both heat structures have 11.5 percent uncertainty added.

- Case 2: This is Case 1 with three core heat structures. The base EM hot assembly heat structure is split into two (2) heat structures within the hot fluid channel, one representing one (1) hot rod and the other representing the remaining 263 rods in the hot assembly. The temperature uncertainty remains at 11.5 percent. The average heat structure remains unchanged.

- Case 3: This is Case 2 with reduced uncertainty in the hot and average assembly heat structures. The uncertainty on the 263 rods in the hot assembly heat structure in Case 2 is reduced from 11.5 to 3 percent. The uncertainty for the average assembly heat structure is reduced from 11.5 to 0 percent. The hot rod heat structure remains unchanged at 11.5 percent.

The results of the evaluation are summarized in Table 4. The peak cladding temperatures for the hot rod unruptured (node 15) and ruptured (node 17) nodes are presented in Figures 8 and 9 respectively. In RSG plants with lower peak power (12.43 kw/ft), clad burst occurs during reflood and rupture-induced local cooling reduces rupture node heatup. For the unruptured node, clad temperature turnaround occurs later due to low flooding rates. Thus, the unruptured node yields the limiting PCT. The hot spot (node 15) mass flow rate during blowdown (Figure 10) is relatively insensitive to the core stored energy. Figure 11 shows slightly higher flooding rates for Case 3 during the early phase of the reflood transient (80 seconds). The hot spot vapor temperature curves in Figure 12 show that the Case 3 vapor temperature is generally lower than those in Cases 1 and 2. This is due to a lower energy deposit in the hot channel. The combined effects of lower hot channel energy and higher flooding rate in Case 3 produce a lower PCT. The effects of lower hot channel energy and higher flooding rate on the PCT in Case 3 are less pronounced than in the OTSG study due to a longer temperature turnaround time. The Case 3 PCT is 60 F less than the base EM case.

Again, the results of Cases 1 (base EM) and 2 confirm that the multiple-core heat structure model is properly implemented in the RELAP5/MOD2 code. The PCTs for the current EM (Case 1) and the revised EM (Case 3) with reduced uncertainty are 2159 F and 2098 F respectively. Both PCT values are below 10CFR50.46 limits.

VI. Conclusions

Framatome Technologies is refining the modeling of the hot rod/hot assembly in its LBLOCA EMs by separating these regions into separate heat structures. The refinements apply equally to LBLOCA licensing calculations performed with the RSG and B&W EMs. The changes affect the modeling in RELAP5 (including BEACH) and do not affect REFLOD3B modeling or usage.

First, additional modeling detail was added to the hot fluid channel. The hot channel contains two (2) heat structures, one representing the hot rod and one representing the hot assembly (less the one hot rod). Previously only one (1) heat structure was modeled in the hot fluid channel. Hot channel fluid conditions drive both heat structures and both structures are initialized at the same maximum allowable peaking or kilowatts per foot. The evaluation model results are not affected by the insertion of additional hot channel modeling detail. However, the modeling refinement allows the incorporation and simulation of differences between the hot rod and the remainder of the hot rods in the hot bundle that can affect the results of EM calculations. The added detail is appropriate for inclusion in future large break LOCA analyses and the continued licensing validity of the evaluation models is demonstrated and retained.

Secondly, unwarranted conservatism in the specification of volume-averaged fuel temperature uncertainties was removed. Previously, the TACO3-specified "hot rod" uncertainty factor was applied to all core fuel rods, substantially overestimating the initial core stored energy. Neither evaluation model [1,2] imposed the conservatism, nor was it required by TACO3 [6]. The recommended uncertainty specified in the TACO3 topical report was formulated for hot rods. Essentially the over conservatism is self-imposed and subject to removal without affecting the licensing basis of the large break LOCA evaluation models. Based on work reported in the TACO3 topical report, no volume-averaged fuel temperature uncertainty will be applied to the average core heat structure (a standard industry practice), and a three (3) percent uncertainty on TACO3 was justified and will be applied to the hot assembly heat structure. The TACO3-specified uncertainty will continue to be applied to the hot rod.

[*Note*: The future will likely hold changes to fuel code technology—the replacement of TACO3 with an improved code, COPERNIC [7], for example. Under such circumstances, fuel temperature uncertainty factors—appropriate to the new technology—for the average core, hot rod, and hot assembly heat structures will be developed. The uncertainty factors would be used in LBLOCA analyses based on the advanced fuel code. Framatome Technologies would inform the NRC of such a change.]

Comparison cases demonstrate the impact of reverting to normal industry volume-averaged fuel temperature uncertainties. Clad temperature reductions in the representative B&W plant case are substantial. This results from the transient being largely dominated by the initial stored energy. The PCT, normally occurring immediately after the end of refill, is substantially reduced. The U-tube steam generator plants generally experience a late transient peak, well after the end of the refill period. These plant transients are largely dominated by decay heat and show less impact to a reduction in initial core stored energy.

The unwarranted conservatism in setting the initial core stored energy will be removed in the next applications of either of the LBLOCA EMs. This refinement is considered to lie within the confines of the existing EMs and does not comprise a change to the EMs. The applicability and NRC licensing status of the EMs are not perturbed and the EMs incorporating the refinements remain valid for use in LBLOCA licensing applications.

VI. References

1. BAW-10168P-A, "RSG LOCA, BWNT Loss-of-Coolant Accident Evaluation Model for Recirculating Steam Generator Plants," Revision 3, December 1996.

2. BAW-10192P-A, "BWNT LOCA, BWNT Loss-of-Coolant Accident Evaluation Model for Once-Through Steam Generator Plants," Revision 0, June 1998.

3. BAW-10164P-A, "RELAP5/MOD2-B&W, An Advanced Computer Program for Light Water Reactor LOCA and Non-LOCA Transient Analysis," Revision 3, July 1996.

4. BAW-10171P-A, "REFLOD3B, Model for Multinode Core Reflooding Analysis," Revision 3, December 1995.

5. BAW-10166P-A, "BEACH, Best Estimate Analysis Core Heat Transfer, A Computer Program for Reflood Heat Transfer During LOCA," Revision 4, February 1996.

6. BAW-10162P-A, "TACO3, Fuel Rod Thermal Analysis Computer Code," Revision 0, November 1989.

7. BAW-10231P, "COPERNIC Fuel Rod Design Computer Code," Revision 0, September 1999.

8. BAW-10186P-A, "Extended Burnup Evaluation," Revision 0, June 1997.

Table 1. Initial Conditions for OTSG LBLOCA—2.5-ft Axial Peak.

Parameters	
Reactor Core Power (102 %), MWt	2827.4
Peak Linear Power, kw/ft	16.8
Total Peaking Factor, F_q	2.625
Radial Peaking Factor, $F_{\Delta H}$	1.544
Fuel Assembly	15 x 15 Mark-B9
Number Of Fuel Assemblies	177
Thermal Design Flow, lbm/hr	133.9×10^6
Bypass Flow, percentage	7.5
RCS Average Temperature, F	579.0
Pressurizer Pressure, psia	2199.0
Pressurizer Level, in	220.0
Steam Generator Tube Plugging, percentage	20.0
Accumulator Water Volume, ft^3/tank	985.0
Accumulator Gas Pressure, psia	580.0

Table 2. Summary of Results for OTSG LBLOCA—2.5-ft Axial Peak.

Parameters	Base EM	Case 2	Case 3
End of Blowdown, s	20.71	20.69	20.72
Beginning of Core Recovery, s	27.45	27.43	27.40
Hot Rod PCT, F	N/A*	2050	1904
Hot Rod PCT Node	N/A*	7	7
Hot Rod PCT Time, s	N/A*	30.7	28.1
Hot Assembly PCT, F	2055	2050	1787
Hot Assembly PCT Node	7	7	7
Hot Assembly PCT Time, s	30.8	30.7	28.1
Average Assembly PCT, F	1447	1447	1327
Average Assembly PCT Node	8	8	8
Average Assembly PCT Time, s	7.4	7.4	35.9
Hot Rod Rupture Node	N/A*	7	7
Hot Rod Rupture Time, s	N/A*	17.95	18.4
Hot Rod Rupture Node PCT, F	N/A*	2050	1904
Hot Assembly Rupture Node	7	7	7
Hot Assembly Rupture Time, s	17.9	17.95	20.2
Hot Assembly Rupture Node PCT, F	2055	2050	1787

* Note this model does not distinguish between the hot rod and the hot assembly, as such the hot rod PCT is the hot assembly PCT.

Table 3. Initial Conditions for RSG LBLOCA—9.7-ft Axial Peak.

Parameters	
Reactor Core Power (102 %), MWt	3479.2
Peak Linear Power, kw/ft	12.43
Total Peaking Factor, F_q	2.3
Radial Peaking Factor, $F_{\Delta H}$	1.471
Fuel Assembly	17 x 17 Mark-BW
Number Of Fuel Assemblies	193
Thermal Design Flow, gpm	348,000
Bypass Flow, percentage	7.0
RCS Average Temperature, F	578.2
Pressurizer Pressure, psia	2250
Pressurizer Level, percentage	60
Steam Generator Tube Plugging, percentage	15
Accumulator Water Volume, ft^3/tank	1095
Accumulator Gas Pressure, psia	614.7

Table 4. Summary of Results for RSG LBLOCA—9.7-ft Axial Peak.

Parameters	Base EM	Case 2	Case 3
End of Blowdown, s	25.69	25.69	25.76
Beginning of Core Recovery, s	46.92	46.92	46.10
Hot Rod PCT, F	N/A*	2171	2098
Hot Rod PCT Node	N/A*	15	15
Hot Rod PCT Time, s	N/A*	119.1	130.9
Hot Assembly PCT, F	2159	2173	2090
Hot Assembly PCT Node	15	15	15
Hot Assembly PCT Time, s	118.6	119.1	152.7
Average Assembly PCT, F	1653	1654	1657
Average Assembly PCT Node	15	15	17
Average Assembly PCT Time, s	122.8	123.5	122.6
Hot Rod Rupture Node	N/A*	17	17
Hot Rod Rupture Time, s	N/A*	56.7	59.5
Hot Rod Rupture Node PCT, F	N/A*	2025	1745
Hot Assembly Rupture Node	17	17	17
Hot Assembly Rupture Time, s	56.7	56.7	60.8
Hot Assembly Rupture Node PCT, F	2016	2029	1736

* Note this model does not distinguish between the hot rod and the hot assembly, as such the hot rod PCT is the hot assembly PCT.

FIGURE 1. LBLOCA EM Computer Code Interface.

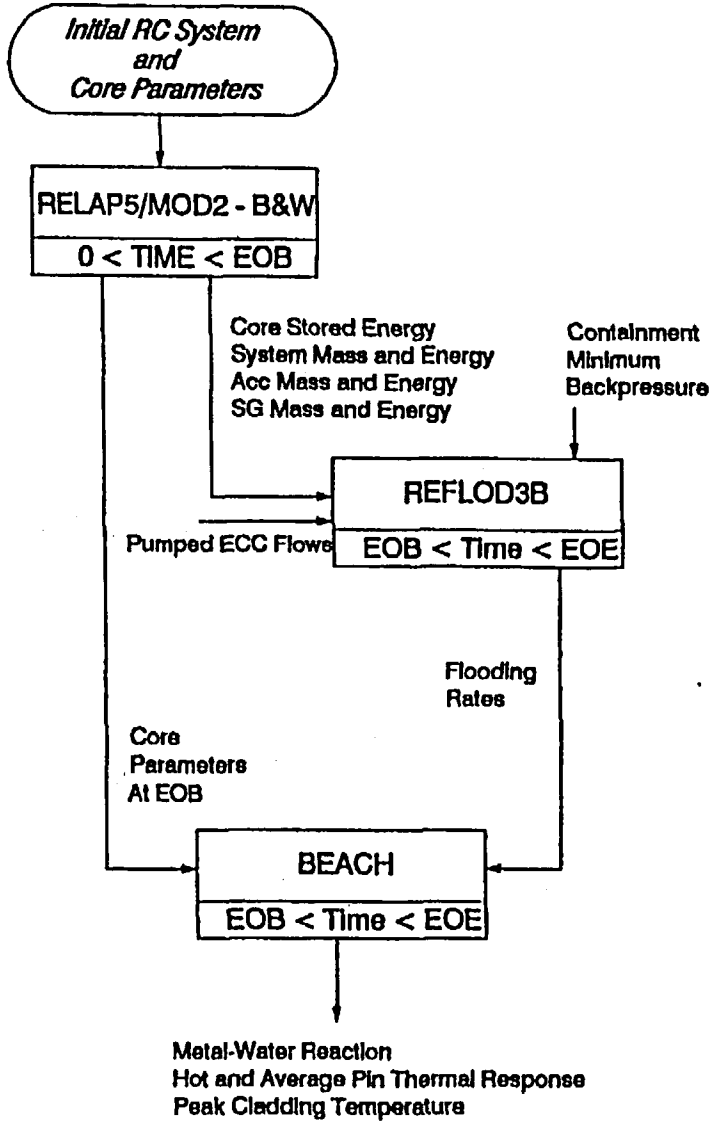

FIGURE 2a. RELAP5-BEACH Core Noding Arrangement For OTSG.

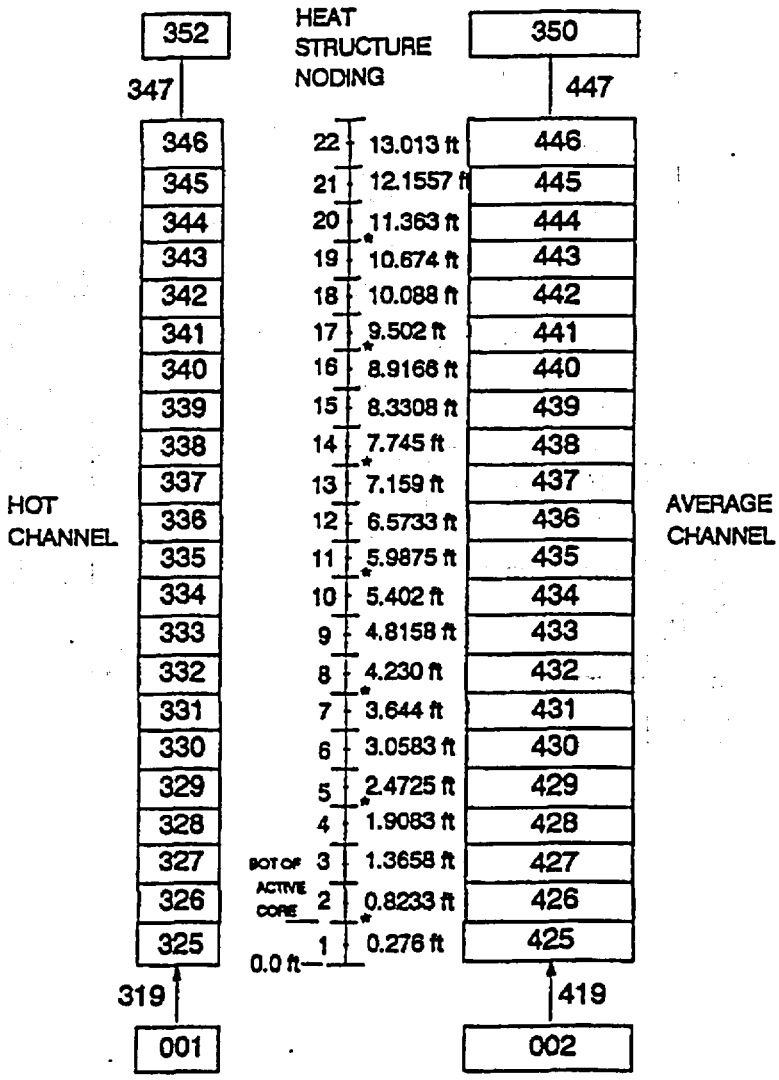

* GRID LOCATION

FIGURE 2b. RELAP5-BEACH Core Noding Arrangement For RSG.

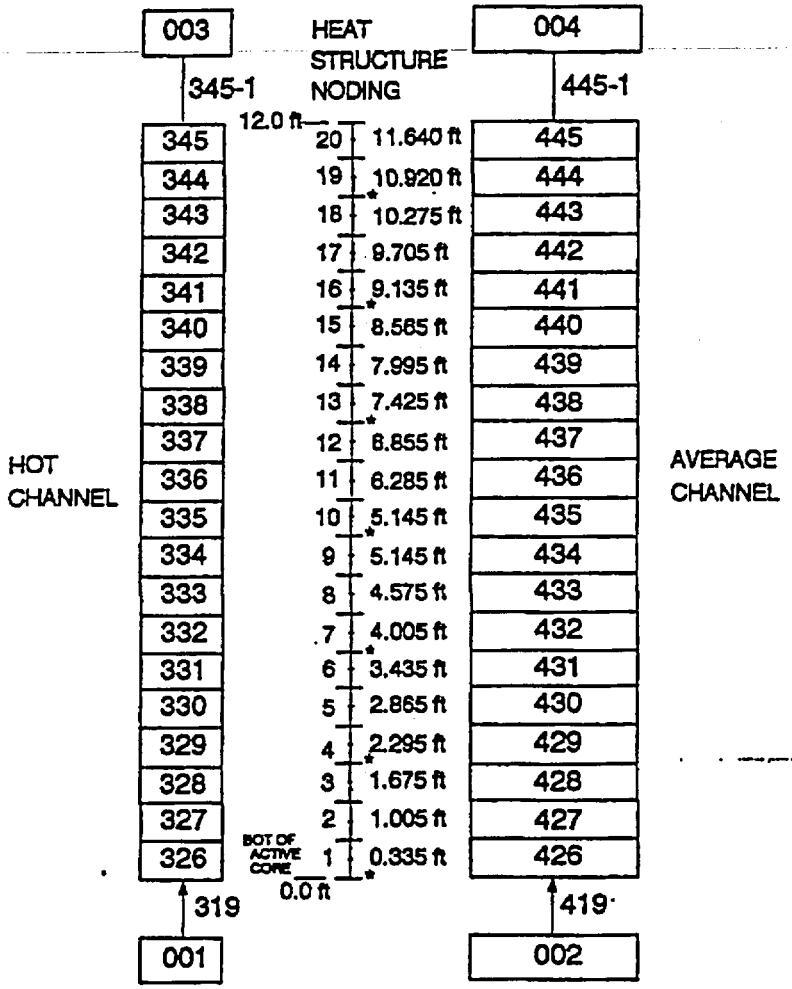

* GRID LOCATION

FIGURE 2c. Representative RELAP5-BEACH Core Heat Structure Arrangement.

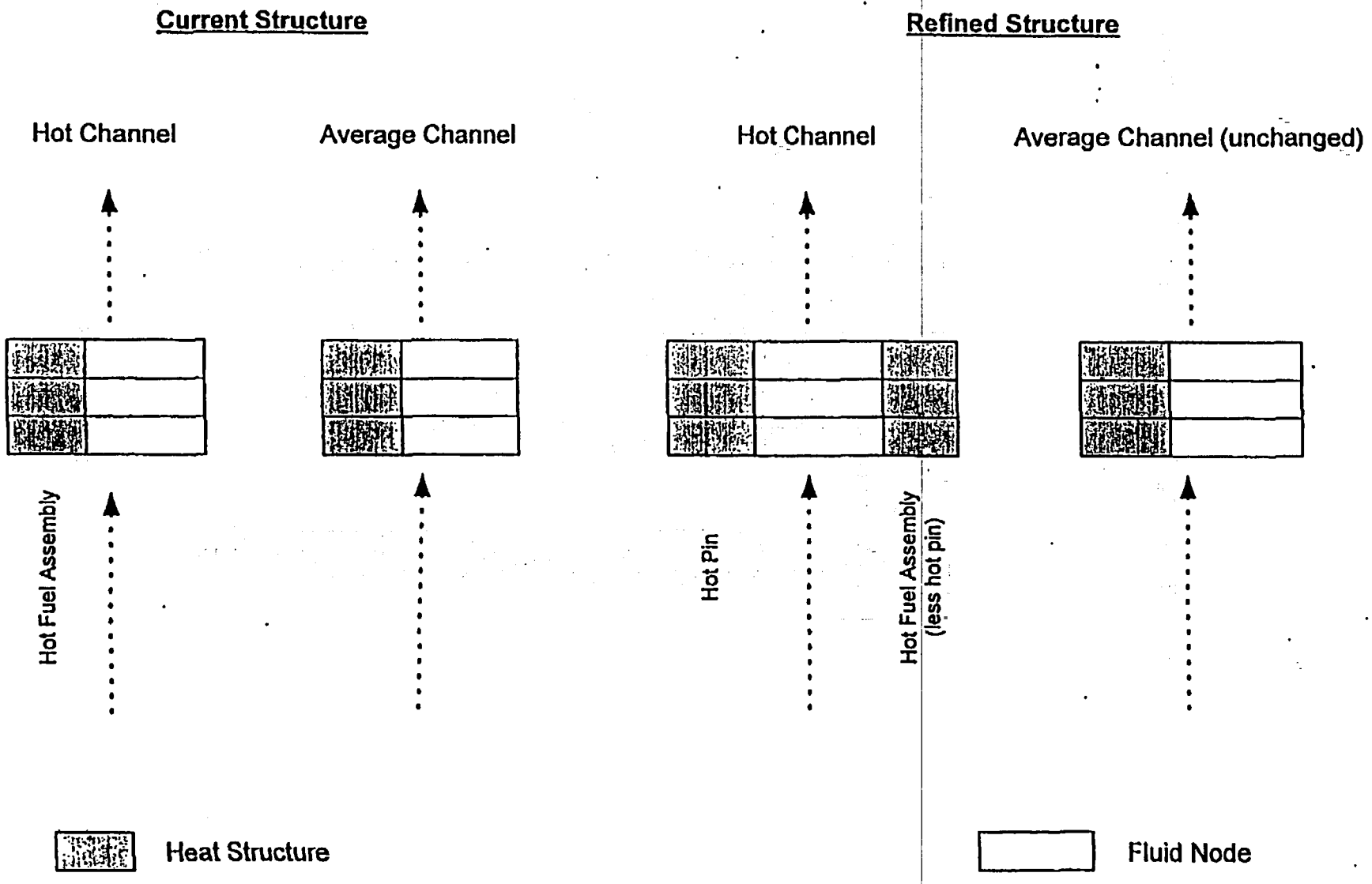

FIGURE 3. OTSG Unruptured Node PCT
2.5-ft Axial Peak.

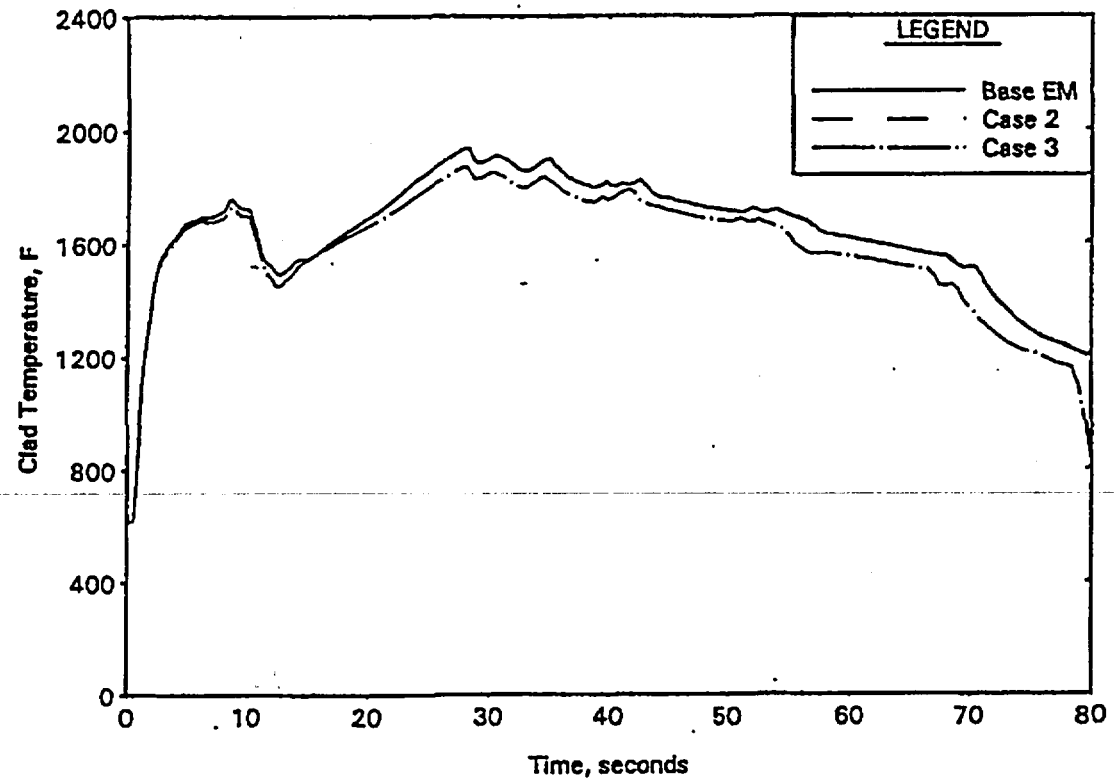

FIGURE 4. OTSG Ruptured Node PCT
2.5-ft Axial Peak.

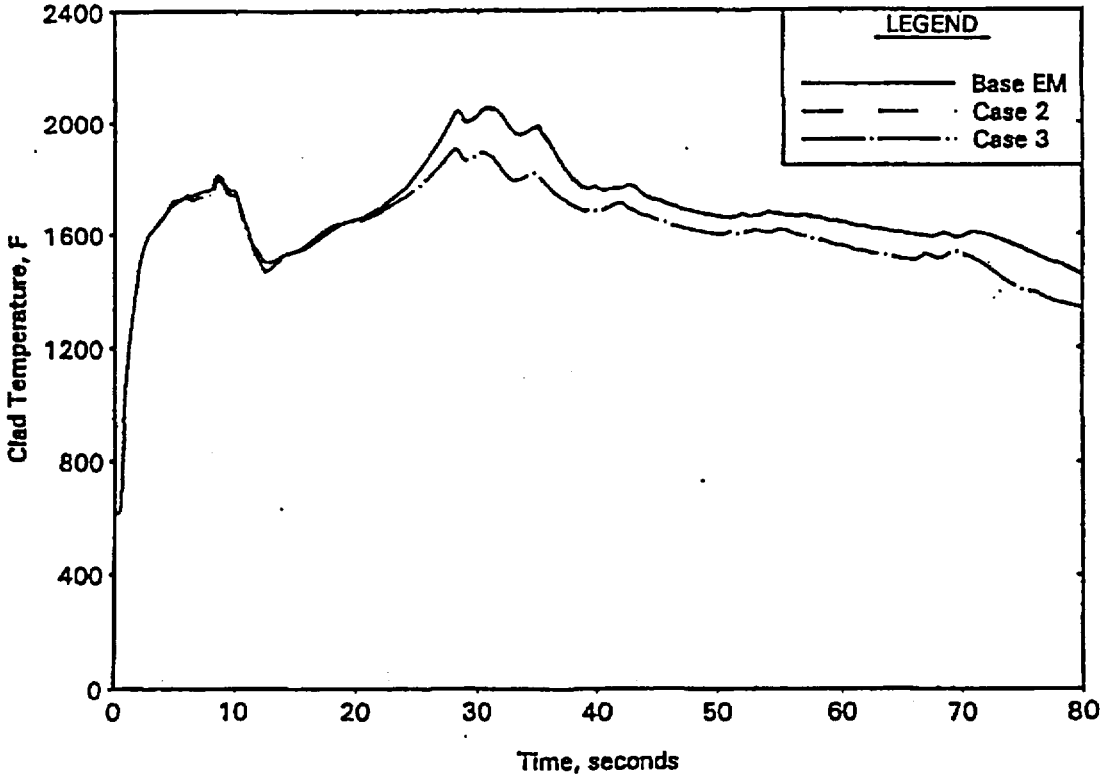

FIGURE 5. OTSG Blowdown Hot Channel Flow At PCT Location 2.5-ft Axial Peak.

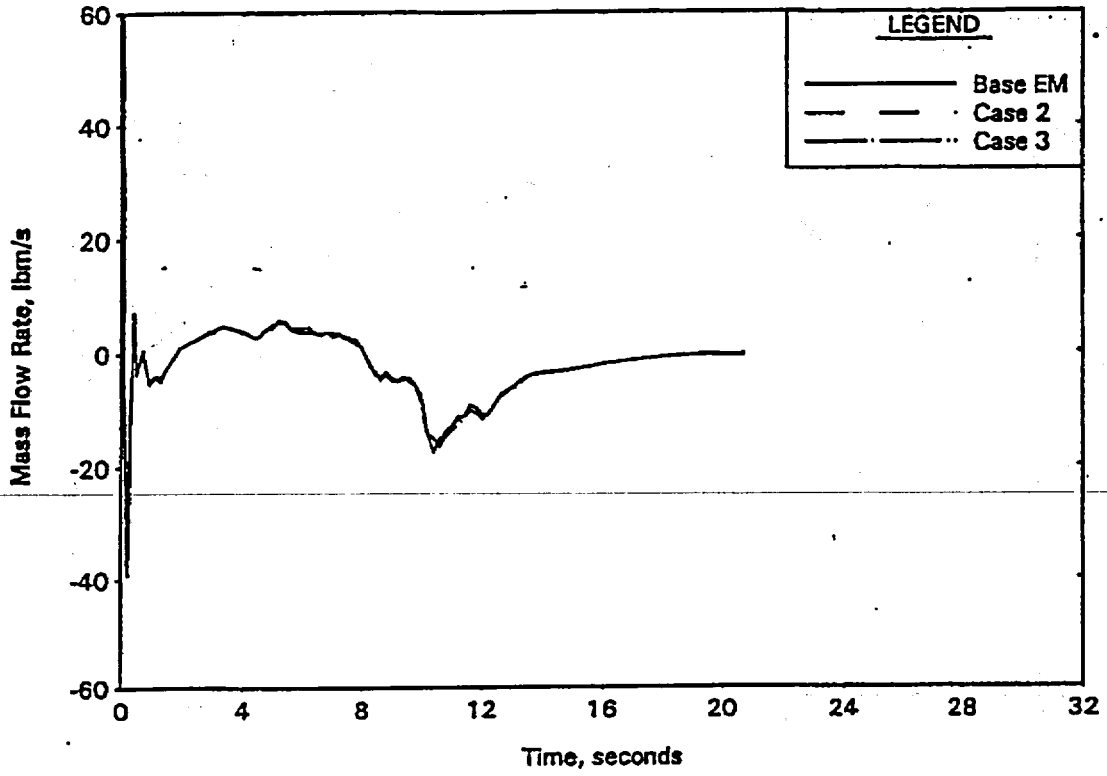

FIGURE 6. OTSG Core Flooding Rate 2.5-ft Axial Peak.

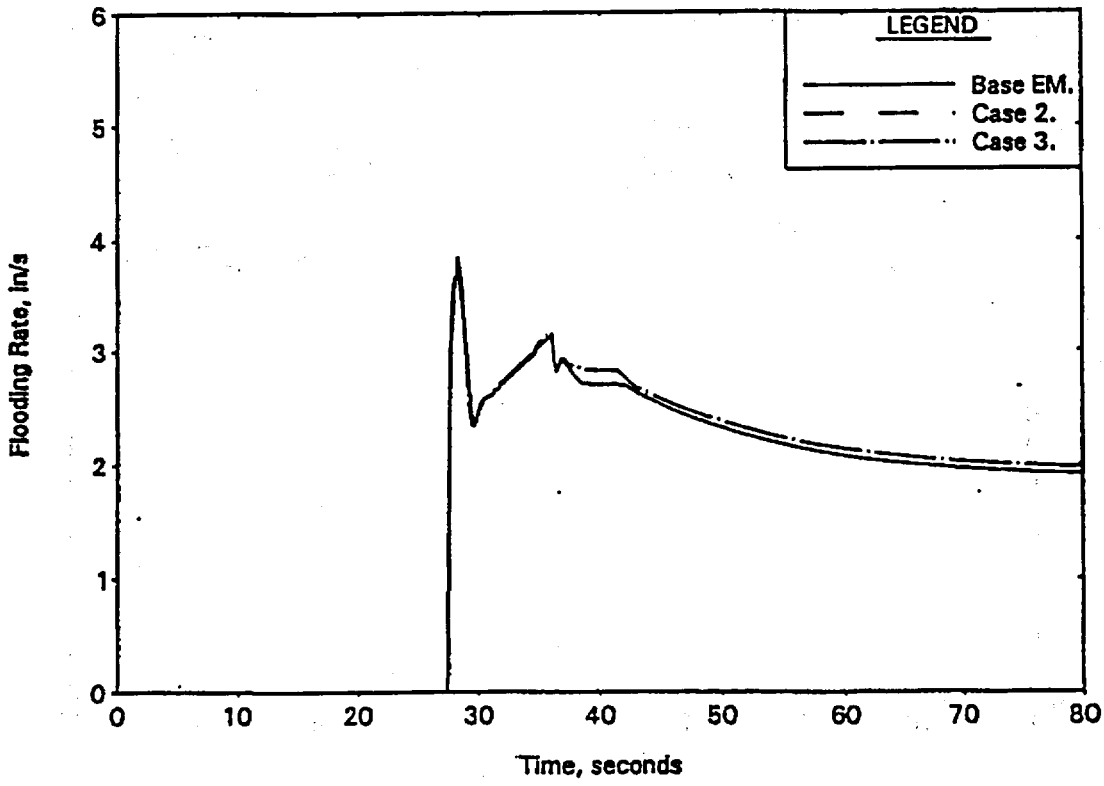

FIGURE 7. OTSG Hot Spot Vapor Temperature
2.5-ft Axial Peak.

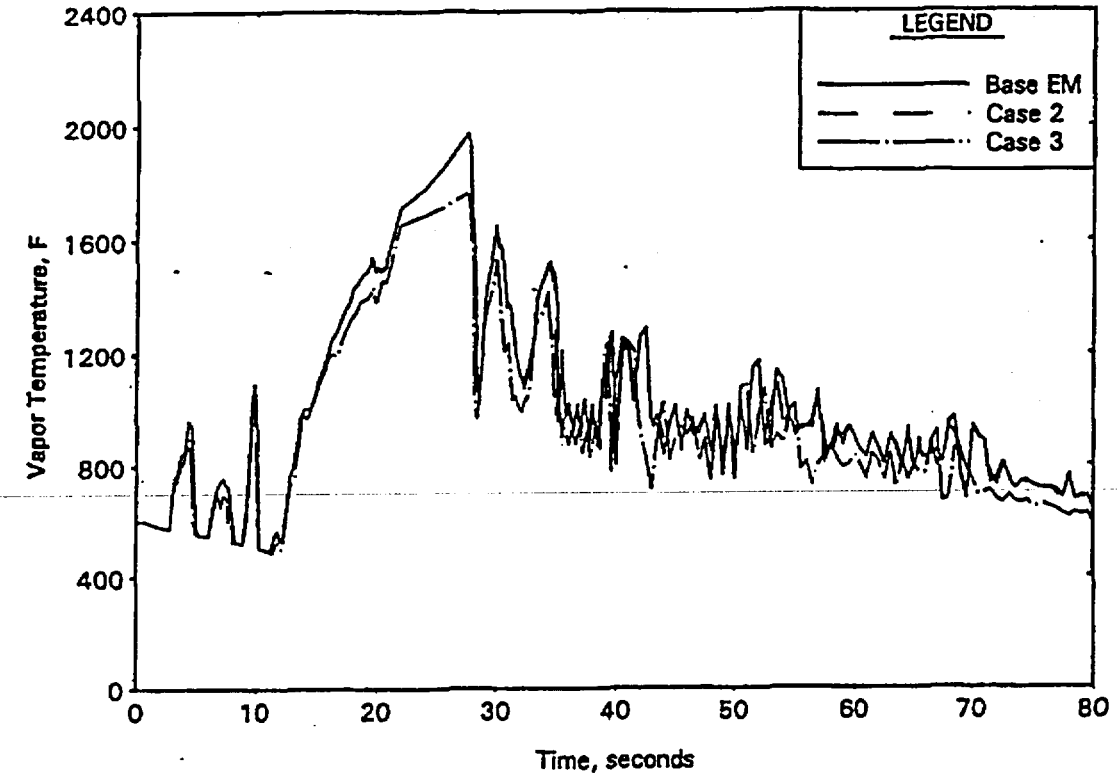

FIGURE 8. RSG Unruptured Node PCT-Node 15
9.7-ft Axial Peak.

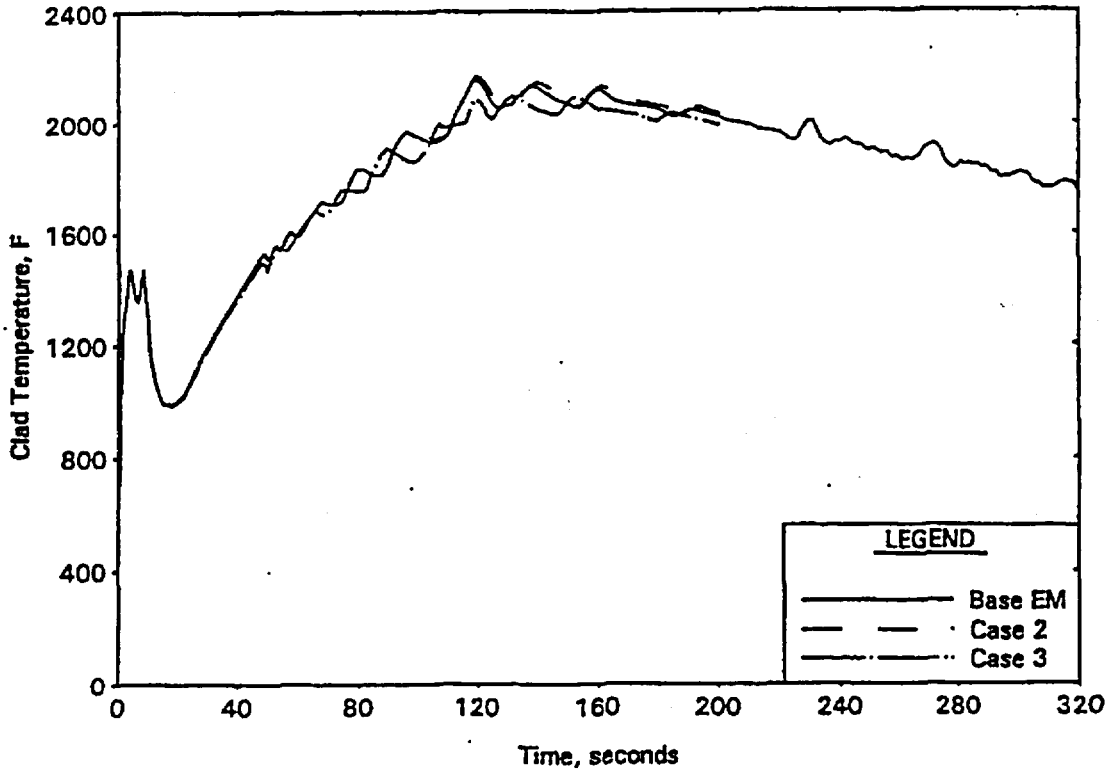

FIGURE 9. RSG Ruptured Node PCT-Node 17
9.7-ft Axial Peak.

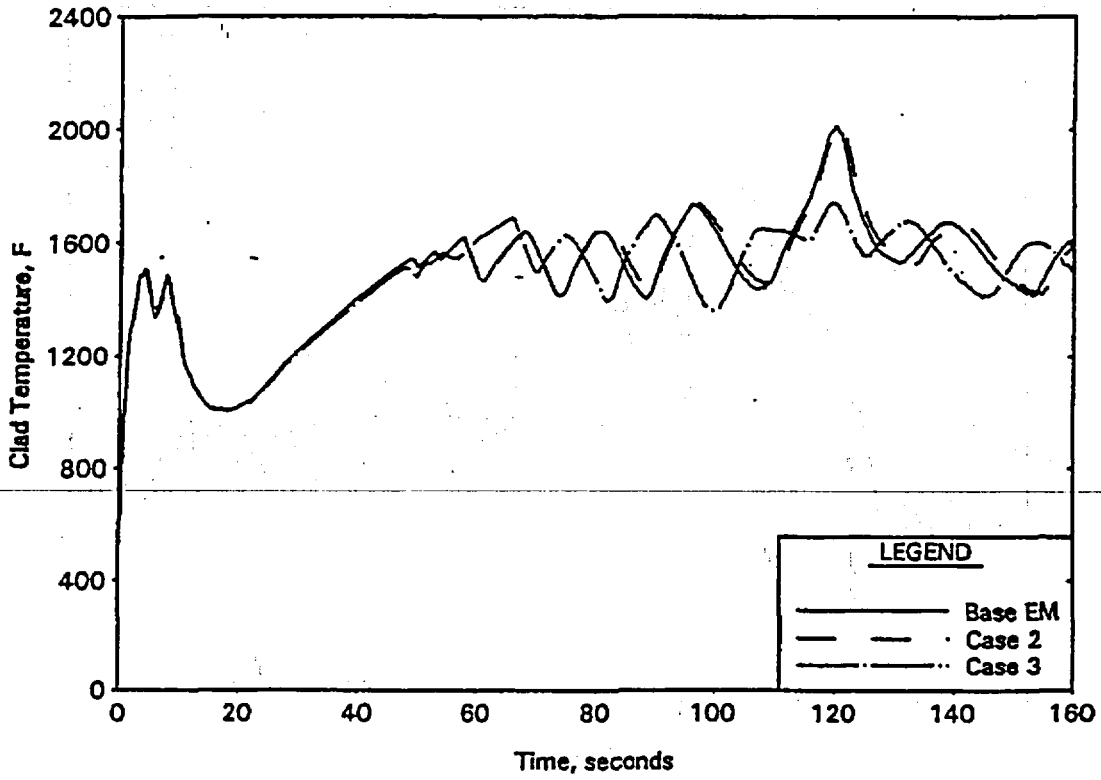

FIGURE 10. RSG Blowdown Hot Channel Flow At PCT Location
9.7-ft Axial Peak.

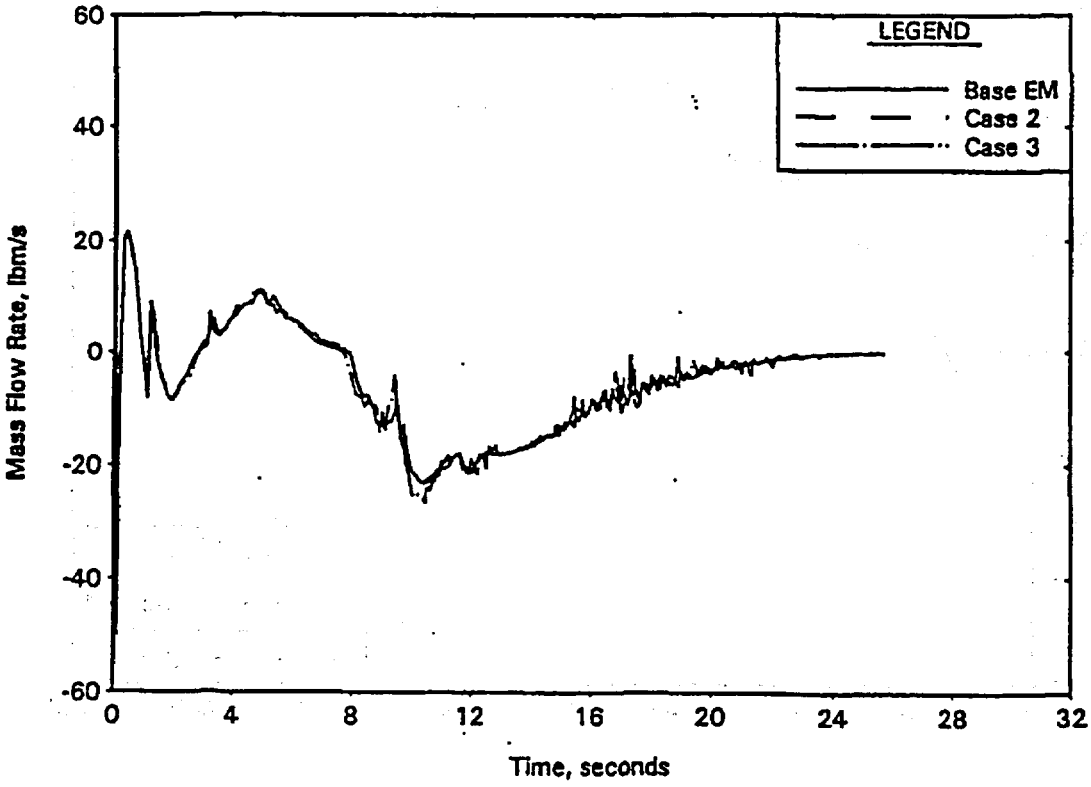

FIGURE 11. RSG Core Flooding Rate
9.7-ft Axial Peak.

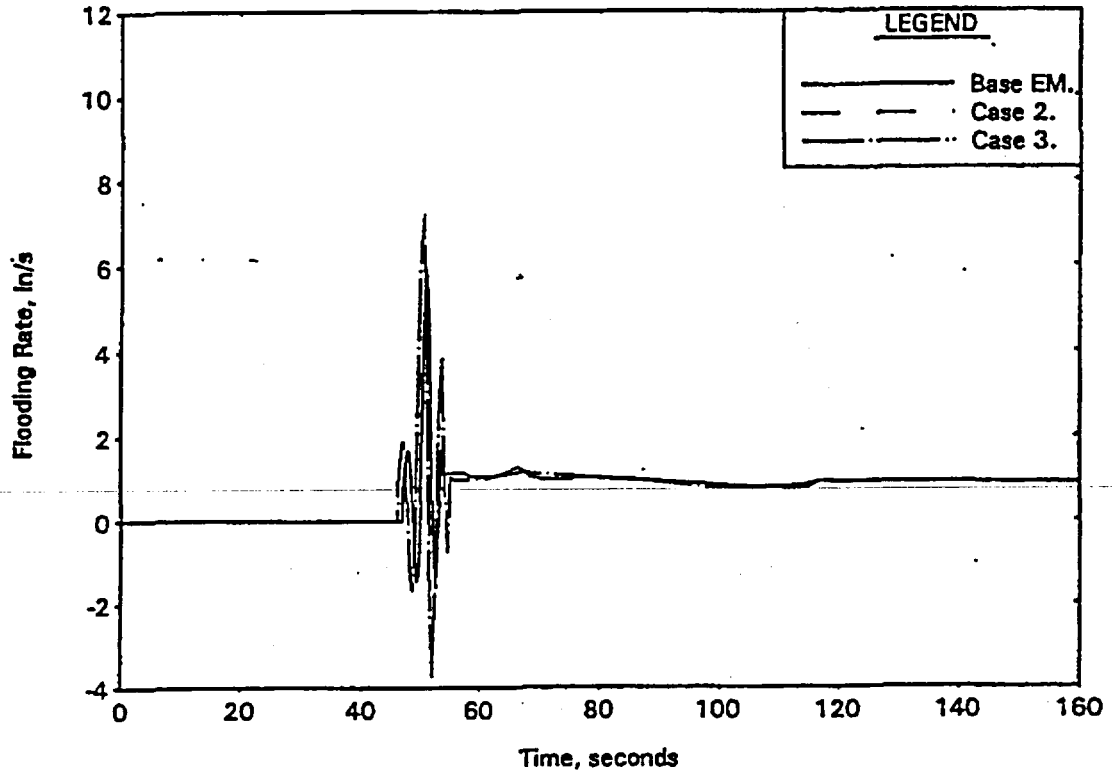

FIGURE 12. RSG Hot Spot (Node 15) Vapor Temperature
9.7-ft Axial Peak.

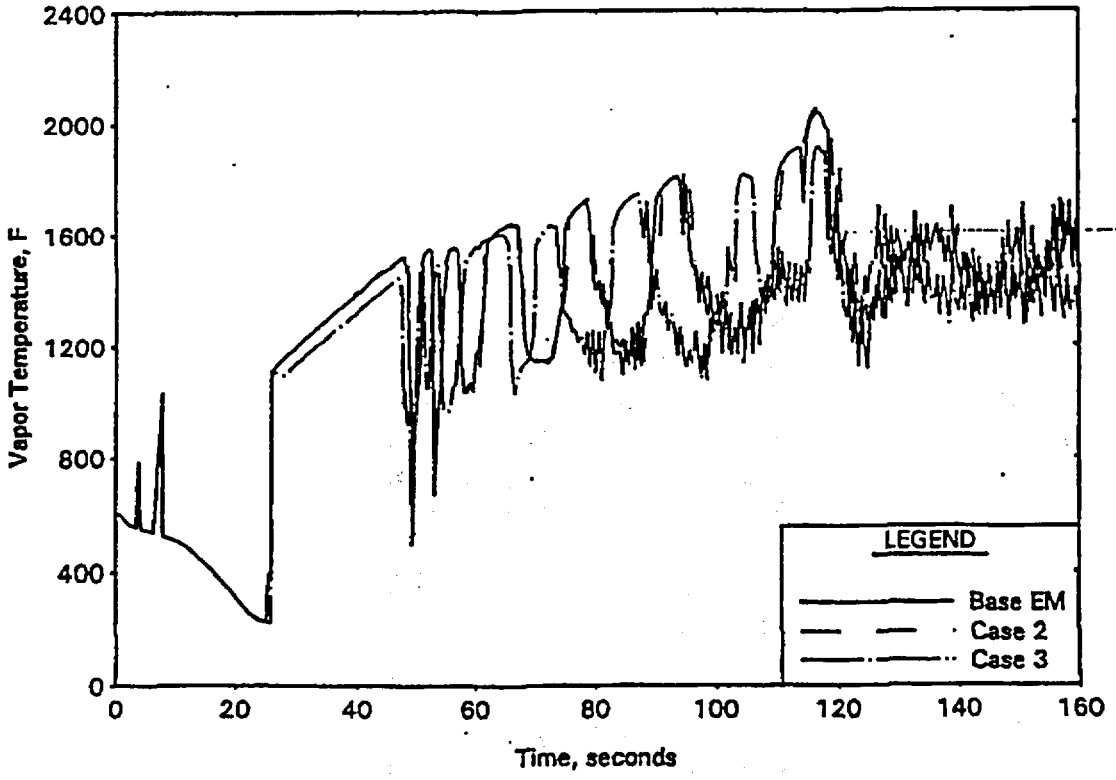

FRAMATOME
TECHNOLOGIES

September 5, 2000
FTI-00-2225

Document Control Desk
U. S. Nuclear Regulatory Commission
Washington, DC 20555-0001

Subject: Additional Information on Modeling Updates to Framatome Technologies' RELAP5-Based, Large Break LOCA Evaluation Models - BAW-10168 for Non-B&W-Designed, Recirculating Steam Generator Plants and BAW-10192 for B&W-Designed, Once-Through Steam Generator Plants

Gentlemen:

On February 29, 2000, Framatome Technologies submitted modeling updates on its large break LOCA evaluation models - BAW-10168P-A, Revision 3, December 1996 and BAW-10192P-A, Revision 0, June 1998. In discussions concerning the change in the determination of the hot assembly initial fuel temperature, the NRC staff indicated that it would be desirable if additional detail were provided on the calculation. The attachment includes such information for use in the NRC's review of our submittals.

The attachment is considered Non-Proprietary to Framatome Technologies. If you require additional information, please contact John Biller at 804/832-2600 or John Klingenfus at 804/832-3294.

Sincerely,

J. J. Kelly, Manager
B&W Owners Group Services

Attachment

c: S. N. Bailey - Nuclear Regulatory Commission
L. Lois/NRC - Nuclear Regulatory Commission
F. R. Orr/NRC - Nuclear Regulatory Commission
J. R. Biller - Framatome Technologies/OF53
B. M. Dunn - Framatome Technologies/OF53
C. K. Nithianandan - Framatome Technologies/OF53
J. A. Klingenfus - Framatome Technologies/OF53
R. N. Edwards - Framatome Technologies/MD82
M. A. Schoppman - Framatome Technologies/MD82

3315 Old Forest Road, P.O. Box 10935, Lynchburg, VA 24506-0935
Telephone: 804-832-3000 Fax: 804-832-3663
Internet: http://www.framatech.com

Attachment

Introduction

The representation of the hot fuel assemble under the Framatome LOCA evaluation models (EMs) is being refined to include better represent the cooling mechanisms acting at the hot spot. During conditions of moderate to high flows the representation of the vapor temperatures at the hot spot is being improved. Further, the adiabatic period during lower head/lower plenum refill is being replaced with an approximation of the convective and radiation heat transfer processes present during the phase. Separating the hot spot and the hot assembly, allowing heat transfer during the refill phase, and probabilistically distributing the initial fuel pellet temperatures achieve these changes.

One of the parameters that can be changed between the hot spot (the location that will eventually produce the peak cladding temperature (PCT)) and the hot assembly is the initial fuel temperature. The base uncertainty in TACO3 predictions (that applicable for exposures below 40 GWd/mtU) is obtained by benchmarking a large number of unrelated tests. There is no apparent dependency between the predicted to measured uncertainty values and particular code correlations or input parameters. (Above 40 GWd/mtU a dependency does exist and the addition of a bias is required.) Therefore, the base uncertainty applies at the pellet level and the actual to predicted temperature ratios for the fuel pellets in the immediate environment of the hot spot should be distributed according to the probability density function of the uncertainty of the prediction. For the hot spot, the initial fuel temperature should continue to be the temperature predicted by TACO3 plus the uncertainty needed to provide 95 % confidence that the modeled temperature overpredicts 95 % of the data. For TACO3, up to burnup exposures of 40 GWd/mtU, that means 111.5 % of the TACO3 prediction. For the hot assembly, however, the only requirement is that the fluid conditions, which provide cooling for the hot spot, are reasonably conservative.

If the hot pin and the remainder of the hot assembly are separated and the hot assembly fluid conditions used to cool the hot pin, the hot spot parameters can be separated from the determination of the coolant conditions. This is the refinement for the next applications of the Framatome EMs.

Current Modeling Approach and Required Revision

Currently Framatome models the hot fuel assembly and hot pin as one entity. This necessitates treating the entire hot assembly with all of the conservatisms required to assure that the hot pin or hot spot is not under-predicted. The result is a significant overprediction of the severity of the environs of the hot spot. By separating the hot pin from the hot assembly it is possible to reduce the conservatisms imposed by the hot pin environs while maintaining a conservative solution.

Convective and radiative processes govern heat transfer from the hot spot. During accident phases with relative high flow, the convective processes are dominant and primary attention is required to determine the incoming flow, its characteristics, and the convective coefficient. During accident phases with no or very low core flow, radiation to the immediate environs of the hot spot will dominate the solution. At these times, the combined heat capacity of the environs along with the radiative coefficient must be considered to assure an appropriate solution. The separation of hot spot and hot assembly assures appropriate conservatism by modeling the hot assembly such that:

1. The coolant conditions within the immediate surroundings of the hot spot during flow periods are conservatively predicted using initial fuel pellet temperatures that are at approximately the 95%/95% one sided upper tolerance limit, and

2. During stagnant conditions, the heat removal achieved by the separated model is an underprediction of that which would occur via the combined radiative and convective processes.

Under the new model the hot pin will be a separate heat structure that shares a coolant channel with the hot fuel assembly heat structure. The hot fuel assembly is comprised of all fuel pins within the hot assembly except the hot fuel pin(s). The hot pin, as implied, is comprised of one fuel pin. In some applications, MOX or gadolinium, it is anticipated that there could be more than one hot pin heat structures. Because the effect of axial heat conduction between fuel pellets in a fuel pin is small; the entire hot pin is modeled with the initial fuel temperatures applicable to the hot spot without serious over-prediction of consequences. That allows the simulation of a continuum of possible positions along the hot pin for the hot spot with a single model and computer run. Therefore, for TACO3 based evaluations, 11.5 % is added to the predicted fuel temperature for all pellets in the hot pin when the hot pin exposure is less than 40 GWd/mtU.

The initial fuel temperature within the hot assembly pellets is determined by probabilistically distributing the fuel pellet temperature prediction uncertainty throughout the immediate environs of the hot pin and determining the conservative effective average uncertainty at a 95 % confidence level. This average uncertainty is then assigned to the entire hot assembly. The result is that the hot assembly evolves in a fashion representative of the hot pin environs. This creates an over-prediction of the average fuel temperatures within the hot assembly but a reasonable representation of the hot pin coolant condition when flow is present.

The coolant heat capacity, however, is that of the entire assembly at the elevation of the hot spot and substantially larger than the region of the assembly near the hot spot. If coolant is flowing and the rise in temperature along the length of the hot spot not significant, the oversized heat capacity is not an issue. During relatively stagnant periods, vessel refill, the cladding temperatures limit the increases in vapor temperatures and the vapor heat capacity is significant in determining the vapor energy absorption. However, under these conditions, radiative heat transfer to the hot spot environs dominates energy transport away from the hot spot. This transfer mechanism occurs to the coolant and directly to the surrounding fuel pins with the surrounding pins being the far more important heat sink. The use of the entire hot assembly vapor heat capacity and the RELAP5/MOD2-B&W steam heat transfer modeling allows less than one half of the energy flow from the hot spot then would result from radiation to surrounding pins. Therefore, so long as a true pin-to-pin radiation model is not incorporated into the EMs, the use of the hot assembly vapor as a heat sink for the hot spot during refill will be conservative.

Demonstration of Fuel Temperature Distributions and Effects

To determine the appropriate fuel temperature distributions and assure a conservative prediction during refill, the following steps are required:

Fuel Temperature Distribution:

1. Determine the number and position of fuel pins and pellets, which effectively control the hot pin fluid conditions.

2. Determine a probability density function for the uncertainty of the TACO3 fuel temperature prediction.

3. Determine, with 95 % confidence, the average uncertainty for the fuel pins and pellets identified.

4. Combine this uncertainty with the hot spot uncertainty to obtain the appropriate uncertainty for the region of the hot assembly surrounding the hot spot.

Refill Heat Transfer Comparison:

1. Determine the view factors for radiative heat transfer between the hot pellet and the surrounding fuel pins/pellets.

2. Probabilistically distribute the fuel pellet initial temperature uncertainty within the significant view factor positions.

3. Determine the 95 % confidence limit for average fuel temperature uncertainty.

4. Compare the resultant radiative energy transport to the average energy removal from the hot spot with the refined model.

Fuel Temperature Distribution - Based on Flow in Assembly

Determination of the number and position of fuel pellets that control the hot pin fluid conditions

As discussed, the modeling approach will consist of a hot pin (hot spot), modeled as a separate heat structure surrounded by the remainder of the hot assembly. Because the FTI evaluation models (RELAP5) do not consider rod-to-rod radiative heat transfer, the coupling between the hot assembly and the hot spot is through the fluid conditions at which heat transfer takes place. Further, because the hot assembly heat structure and fluid nodes, not a sub-region of the hot assembly, will be used to provide the coolant conditions for the hot spot, the hot assembly must be modeled to achieve fluid conditions representative of those with which the hot spot will be cooled. Therefore, it is necessary to establish the region of the fuel assembly around the hot spot within which the heat transfer takes place. Only pins and pellets within this region can be expected to influence the fluid condition surrounding the hot spot sufficiently to warrant inclusion in the determination of those conditions.

The following diagram of fuel assembly lattice positions is useful:

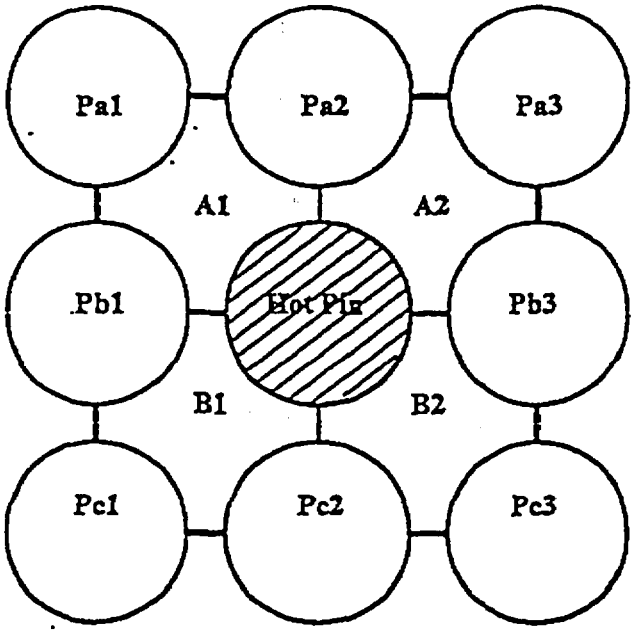

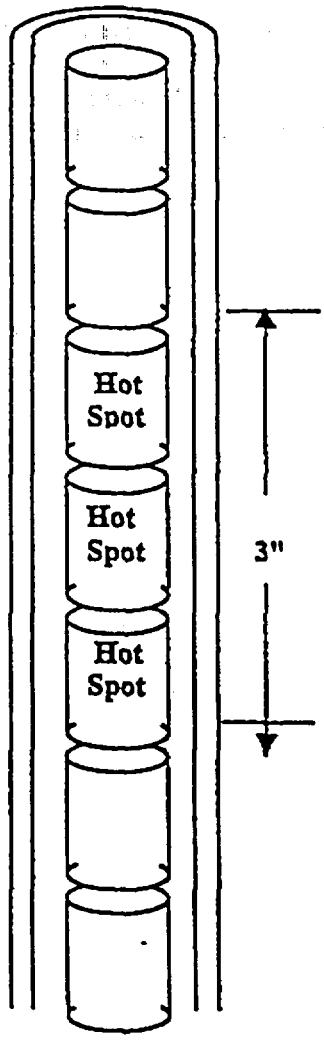

Considering the hot pin in the above drawing, the four fluid sub-channels A1, A2, B1, and B2

provide direct cooling. Realistically, the fluid sub-channels just removed from these four can be expected to mix well with the four and also be part of the cooling region. However, because expansion of the region would only lower the value of the resultant upper tolerance limit of the region uncertainty, the present calculation conservatively considers only the four sub-channels in contact with the hot pin. The pins that most govern the fluid conditions within these four sub-channels form a 9-pin array of the hot pin and its neighbors. Within the array the hot pin is fully involved, the laterally adjacent pins are only 1/2 exposed to the four flow sub-channels, and the diagonal pins only 1/4. Therefore, weighting factors, as given in the diagram below, have been assigned to the pins in determining the relative influence on the four fluid sub-channels.

1/4	1/2	1/4
1/2		1/2
1/4	1/2	1/4

Axially the cooling region will be limited to within a structural grid span which, for the purposes of this calculation, will be taken as approximately 1.5 feet (18 inches) in length. Further, only one half of that span plus one half of the length of the hot spot will be considered. This places the hot spot in the middle of the span that is a reasonable assumption and simplifies consideration of reverse flow situations. Theoretically the hot spot could be considered as having the height of one pellet (that in fact is done in establishing radiation cooling in the next section). However, a characteristic length of 3 inches, taken from the 10CFR50.46 Appendix K minimum rupture length definition, has frequently been applied within LOCA evaluations. Although 10CFR50.46 would probably not force a 3 inch height, such a length is not unreasonable. If the hot spot were not centered or if mid-span mixing grids (MSMGs) were incorporated, the hot spot would either see a larger number of pellets controlling the fluid temperature (high hot spot) or be closer to a mixer that would bring in coolant from other sub-channels (hot spot low, reverse flow hot spot high, or any MSMG application). In each case the effective mixing zone is increased, therefore, a half grid span mixing length, 10.5 inches (15/2 + 3), is acceptable or all hot spot positions and for MSMG assemblies.

The pellet height will be taken as 1/2 inch. Actual pellets vary in height from slightly greater than 0.4 inches to less than 0.5 inches. As will be shown in Section 4, the solution is not greatly affected by the actual length of the pellet and the approximation of a larger pellet height is reasonable and convenient. For the two grid span types considered, the following table provides the sets and weighting factors.

Number of pellets within each pin in region	21
Number of pellets within the Hot Spot	6
Number of pellets in Hot Pin to be probabilistically distributed	15
Number of pellets in at weighting factor of 1 and maximum uncertainty (11.5%)	6
Number of statistical pellets at weighting factor of 1	15
Number of statistical pellets at weighting factor of 1/2	84
Number of statistical pellets at weighting factor of 1/4	84

Thus, the set for which the fuel temperature uncertainty is to be determined comprises 15 pellets at full weighting, 84 pellets at 1/2 weighting, 84 pellets at 1/2 weighting, and 6 pellets forced to the TACO3 11.5 % uncertainty.

A recognized conservatism of the approach is that the existence of control rod guide tubes and the instrument tubes is ignored. Only a few of the 9 pin sets within the assembly do not include an instrument tube or a guide tube and none would be free of the influence of one of these. However, no guide tube or instrument tube is included for the evaluation.

Determination, with 95 % confidence, of the average uncertainty for the fuel pellets within the region surrounding the hot spot

To determine the average uncertainty for the group of pellets presented in Section 2.1 an EXCEL Workbook was created to randomly determine the uncertainty of each pellet in accordance with the TACO3 uncertainty distribution. By collecting groups of 15, 84, and 84 such pellets, a single possible set of uncertainties for the surrounding region is determined. The average uncertainty of each set is then determined through application of the weighting factors and the result stored in an array. The process is repeated 50,000 times with the average uncertainty of each set added to the array to give a large number of samples. The array is then ordered and the uncertainty values at selected percentage positions within the array reported. The value at the 95 % position is the uncertainty that bounds 95 % of the results and will be used to determine the average fuel temperature for the environs of the hot spot.

The result for the pellet distribution selection is that approximately 95 percent of the time the average uncertainty for fuel pellets in the environs surrounding the hot spot will be bounded by an uncertainty of 1.4 % including the TACO3 .5 % bias.

Combination of surrounding pellet uncertainty with the hot spot 95 percent uncertainty (Gives the appropriate uncertainty for the hot spot/hot pin region)

The average uncertainty for the pellets in the region surrounding the hot spot was determined to be 1.4 percent. However, the region which determines the coolant properties by which the hot spot is cooled should also include the hot spot. These pellets will be considered to be at the upper 95%/95% tolerance level (11.5 %) for the TACO3 measured to predicted ratio. Combining these uncertainties and averaging gives a hot spot region initial fuel temperature uncertainty of:

$$Hot\ \ Spot\ \ Region\ \ FTU = \left[\frac{6 \bullet 1.115 + 78 \bullet 1.014}{84}\right] = 1.021$$

Thus, if the entire hot fuel assembly is initialized with an uncertainty of 2.1 percent, the fluid conditions, to the extent that they are influenced by the fuel pin thermal response, will be representative of the region immediately surrounding the hot spot during LOCA phases wherein flow induced cooling is significant (blowdown and reflood).

Refill Heat Transfer Comparison - Very Low Flow Conditions

For the proposed model, the hot pin and the hot assembly will be simulated at the same normalized power. Because both regions are cooled by the same coolant, the only difference between these regions then is comprised of the initial fuel temperature. From experience the difference in fuel temperatures during refill between pins initialized at different temperatures is about half the initial difference. A similar difference can be expected across the fuel pellet to its outer surface and within the cladding. Therefore, an approximate evaluation of the amount of energy transport possible by radiant heat transfer can be made based on the initial fuel temperatures for pellets within a region.

The first step in specifying the radiative heat transfer is to determine to what pins and pellets radiative heat transfer can take place and the relative importance of each. The next step is to probabilistically distribute pellets to these locations, generate a large number of possible distributions and compute the average effective fuel temperature uncertainty. The final step is to use the expected temperature differences in the radiative heat transfer model to compute a representative energy transport.

Determine the view factors for radiative heat transfer between the hot pellet and the surrounding fuel pins/pellets

An examination of the earlier diagram shows that direct radiative heat transfer from the hot pin can only take place to the pins in the immediate surrounding ring and selected pins of the next outer ring. Within the half quadrant formed by the hot pin (Pb2), Pb3 and Pa3, only a small widow is available to pass radiant energy on to the next outer most pin lattice. Pa4 will intercept radiation passing through this window. Thus, it is only necessary to evaluate view factors for the pins at lattice points Pa3, Pb3, and Pa4 and apply symmetry around the hot pin. The following diagrams show the planner view angles occupied by each of these lattice points for both the Mark-B (15x15) assembly and the Mark-BW (17x17) assemblies. Although representative dimensions have been used, the dimensions do vary slightly within the design covered. However, as can be seen there is negligible difference between the view factors of the 15x15 and 17x17 assemblies and no significant difference is expected for the small dimensional changes possible from on design to another.

Using the Mark-BW assembly as the base, the three pins occupy the following view angles from the center of the hot pin within the half quadrant: the adjacent pin occupies 22.4°, the diagonal pin in the close ring 15.4°, and the diagonal pin in the far ring 7.2°. From these angles and the distance of the pin from the center of the hot spot, the base of the area occluded by a pin segment can be calculated. When the base is combined with the height of a pin segment and the resultant area projected to a sphere, the fraction of sphere area or the solid angle occupied by a given segment can be calculated. This sphere fraction or solid angle gives the relative importance of the segment within the radiative process.

To facilitate the calculations an occlusion factor defined as the portion of the pin seen by the hot spot is defined for each pin position. For the adjacent and the diagonal pins the factor is 1. For the diagonal pin in the far ring the factor is $7.2/(36.2-16.9) = 0.373$.

MARK-B Pin View Diagram

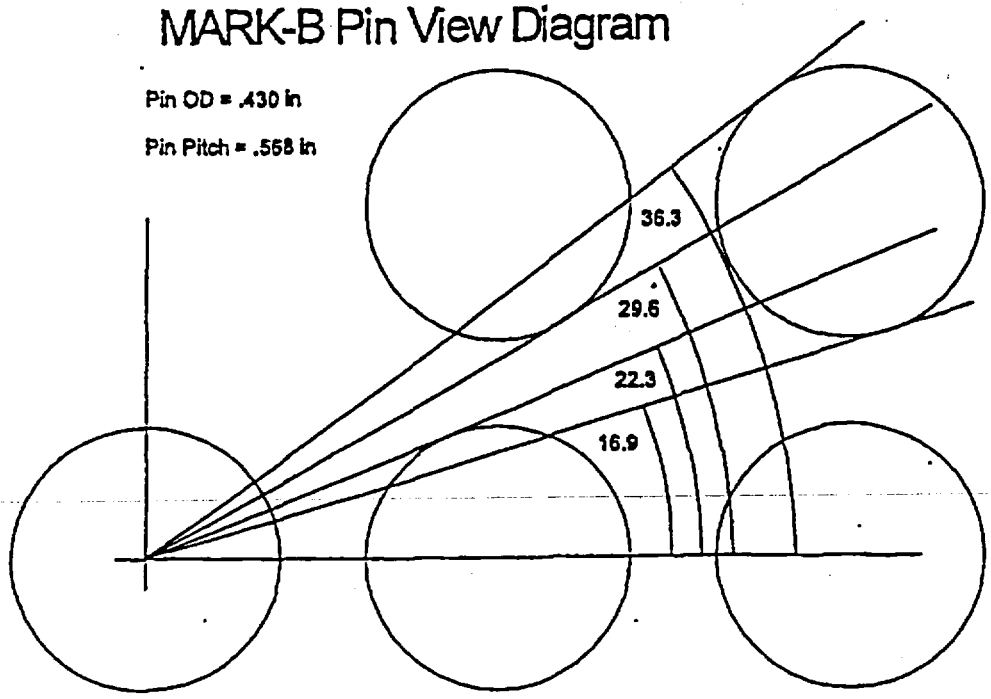

Dimensions from Reference 8, pages 5 and 11.

Mark-BW Pin View Diagram

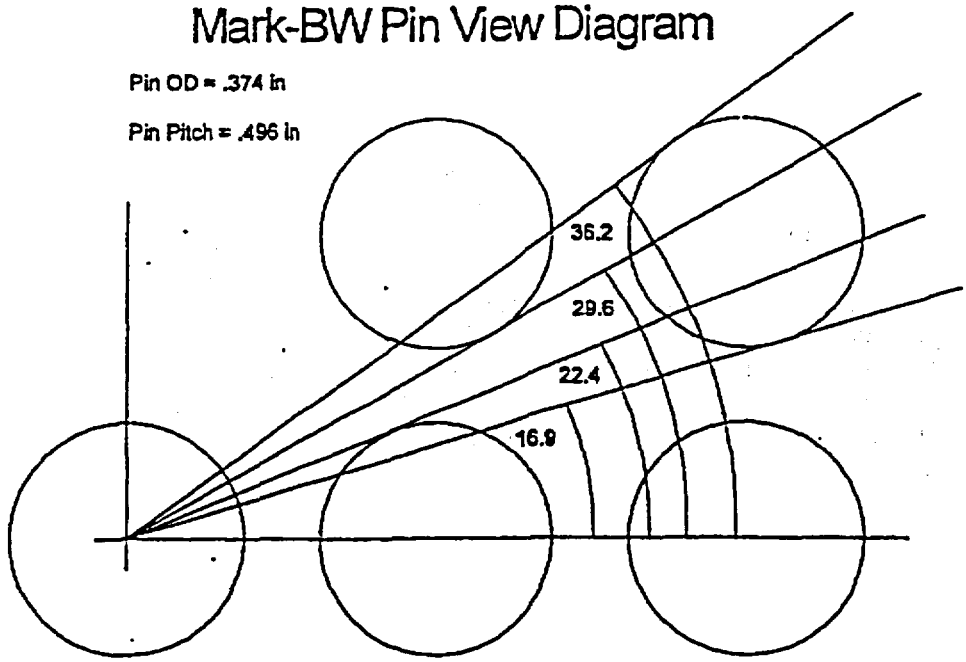

Dimensions from Reference 9, page 24.

The pin segments considered are one pellet in height because the fuel temperature uncertainty is assigned pellet by pellet. For convenience the pellet height is taken as 0.5 inches. Actual heights range between 0.4 and 0.5 inches. Using 0.5 minimizes the number of pellet segments to consider and increases, just slightly, the average uncertainty of the resulting sets. The height of each segment can be determined from the following diagram.

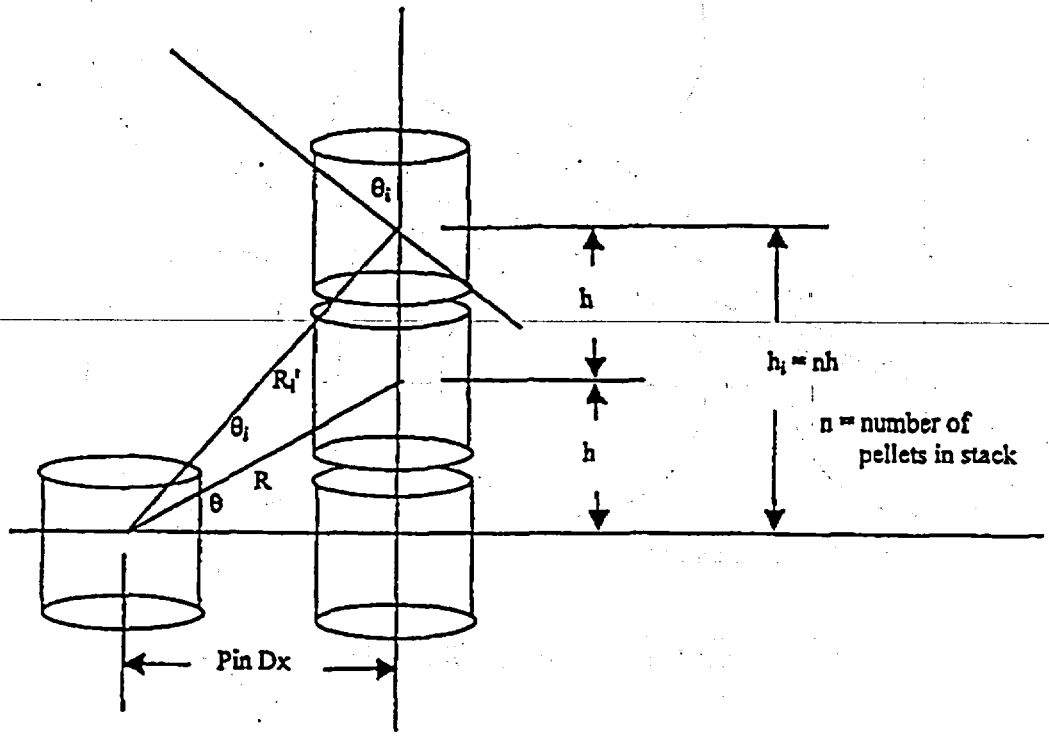

For radiation heat transfer, the pellet stacks run above and below the hot spot location because there is no preferential radiation direction. For the evaluation only one pellet is considered and the view areas or factor are evaluated as if radiation emitted from the center of that pellet. A more accurate determination would involve integration over the surface of the initiating pellet or pellets and, because the energy will be transported uniformly to the surface of the hot pin, not alter the results beyond the margins achieved. The area of sink is taken at the center line of each pellet and then projected onto a sphere at that radius. The solid angle or sphere surface fraction is computed from the projected area and a sphere area at the calculated radius (actually the calculation takes credit for symmetry and works on a hemisphere).

$R_i = (\text{Pin Dx}^2 + h_i^2)^{0.5}$

$\text{Cos}\ \theta_i = \text{Pin Dx}/R_i$

Area of Segment = h • Pin Diameter

Projected Area seen by the hot spot @ R_i = Cos θ_i • Area of Segment • Occlusion Factor

Sphere Area @ $R_i = 4 \bullet \pi \bullet R_i^2$

Fraction of Sphere @ R_i = Relative View Factor = Projected Area @ R_i / Sphere Area @ R_i

This development has been placed in the XL workbook. Each of the 3 pin positions are evaluated separately and then combined in a summary sheet. The summary sheet also contains the grouping and averaging of the number of segments and their individual importance factors into 8 groups. Two of these groups have no members for the configurations studied herein and the group with the lowest importance is arbitrarily assigned a 0.0 average importance.

Applicability to Other Hot Spot Locations and to MSMG Designs

The evaluation performed places the hot spot in the middle of a normal grid span. If the hot spot is located above or the mid-plane of a grid span or if MSMGs were present the view of some of the fuel locations credited in this evaluation would be occluded by the closer grid or the MSMG. As will be shown only the very close neighbor pin positions are significant in determining the radiation heat transfer. Therefore, even if these locations were removed from the evaluation the result would not change appreciably. Further, the view would still be present except that it would now be occupied by an unheated structure, some kind of grid. This would undoubtedly result in an effective increase in radiative heat transport. Therefore, the central position is acceptable for the demonstration for all hot spot positions or for application to an MSMG design.

Probabilistically distribute the fuel pellet initial temperature uncertainty within the significant view factor positions

The relative importance for the pin segments that receive radiation form the hot pellet are:

Group	Number of Pin Segments/Pellets	Relative Importance
1	4	.0605
2	12	.0242
3	8	.0163
4	24	.0052
5	24	.0030

The group numbers have been revised to be consecutive. These groups are now assigned fuel temperature uncertainties randomly in accordance with the TACO3 uncertainty distribution to achieve a 95 % confidence limit the set average uncertainty. The pin segments that will receive radiation from the hot spot are evaluated and the hot spot is not a member of that group. Using the above table for input and setting the forced (hot spot) pellets to 0, the 95 % confidence level for the set average is 2.5 % fuel temperature uncertainty.

For the evaluations conducted herein, the fuel temperature uncertainty for all receptor regions will be considered

2.5 % (note that in the LOCA calculations a 3 % uncertainty is used for conservatism.)

Note should be made that some of the possible receptors, 520 of them, are not included. These receptors, however, have a low average uncertainty and if included would only decrease the uncertainty. Also the evaluation conducted is only for one pellet as the source while the hot spot is treated as 6 pellets. Each of these 6 will have a replication of the sink evaluated here in and

thus the same uncertainty result can be applied.

Compare the resultant radiative energy transport to the average energy removal from the hot spot with the revised model

To demonstrate that the model as implemented achieves a conservative solution during refill the heat flux actually achieved for a representative calculation is herein compared to that which would have been achieved with radiation heat transfer.

The following is a simplified equations for radiant heat transfer.

$$q = 0.172 \bullet A \bullet \left[\left(\frac{T_s}{100} \right)^4 - \left(\frac{T_r}{100} \right)^4 \right] \bullet e \bullet F_a \qquad \text{and}$$

$$e = \frac{1}{1/e_s + 1/e_r - 1} \quad ;$$

where

q	= heat flow from interior object, Btu/hr	
A	= Area of source for an enclosed body	
T_s	= Source temperature, R	
T_r	= receptor temperature, R	
e_s	= emissivity of source	
e_r	= emissivity of receptor	
F_a	= Geometric factor	= 1 for enclosed bodies

Within the core $e_s = e_r \approx 0.7$ $e = 0.54$.

As in the determination of importance, we will assume a pellet height of 0.5 in, but because the reference run to which we will compare heat exchange is for a 15x15 design we will use the Mark-B pin diameter of 0.43 in.

The area of source "A" is therefore becomes 0.675 in^2 or 0.00469 ft^2.

The following calculation was conducted with the proposed RELAP5 standalone hot pin model transferring energy to a hot bundle controlled fluid channel. The fuel temperature initialization of the hot bundle included 3 % uncertainty. The following figures provide the hot pin temperature and heat flux extracted from case "FDAF WJGF" at the position of the peak cladding temperature, level 6. Refill for this case was between 22 and 27.5 seconds.

Figures from "refill_radiation.xls"

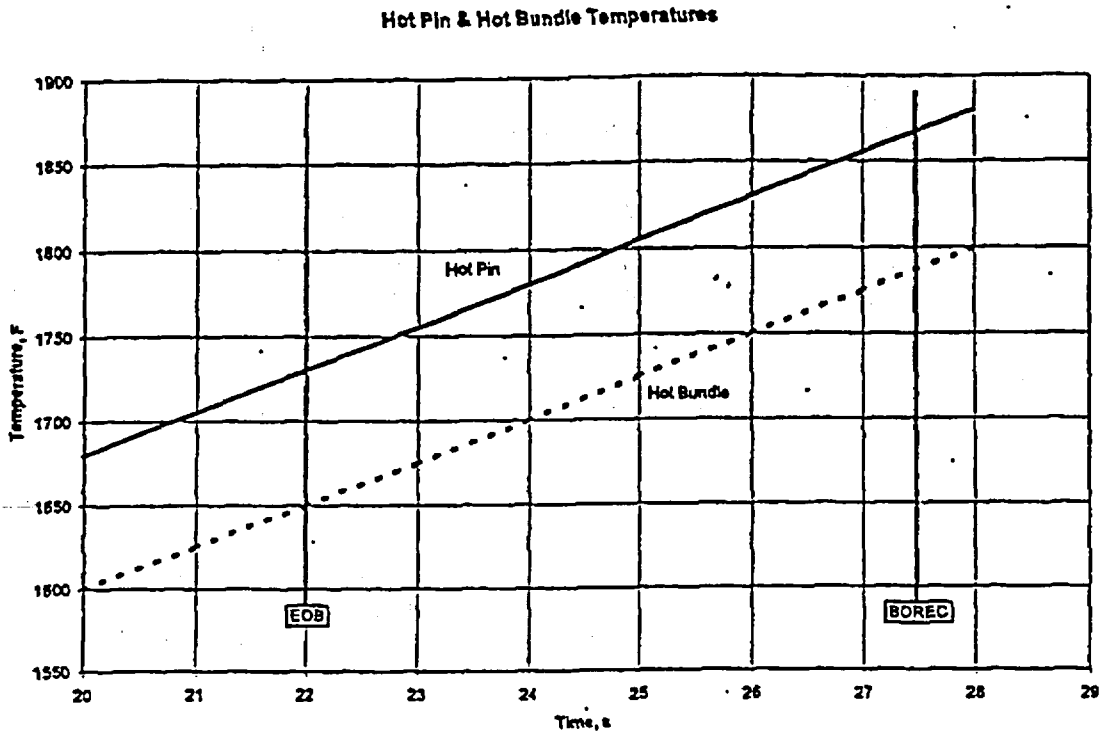

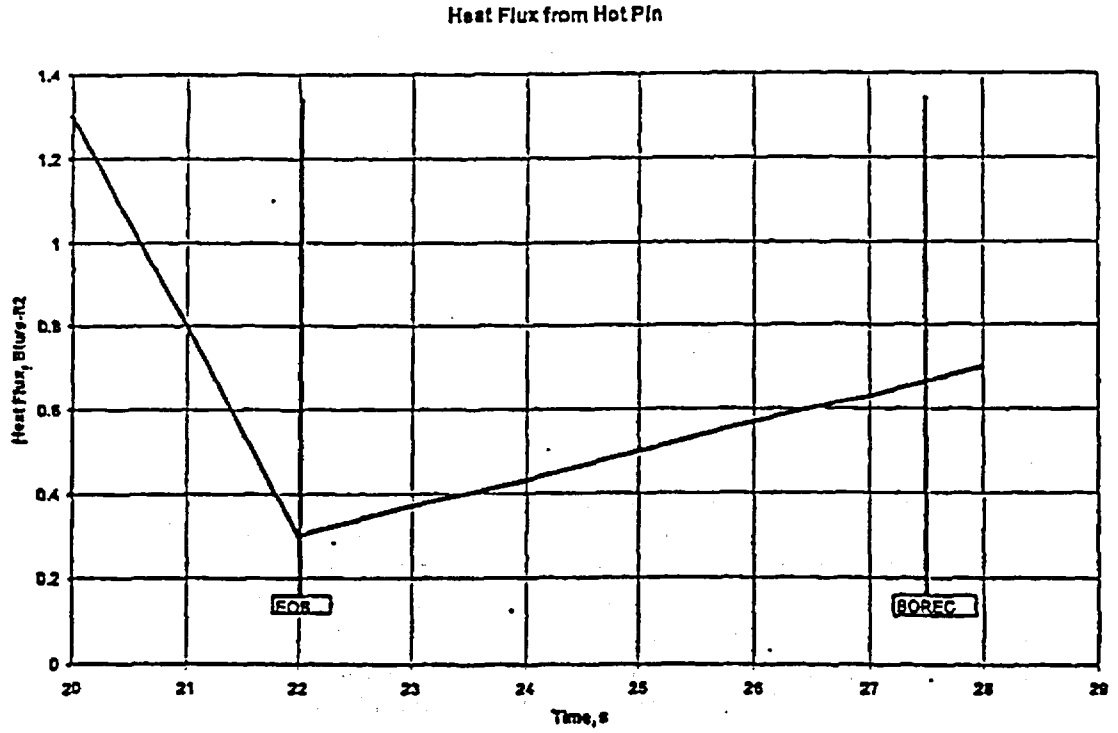

From this data and the prior equations a workbook comparing the heat flow achieved during refill and that which would have been possible with a radiation heat transfer model was constructed. The output shows that heat fluxes achieved were conservative by a factor of 2 during refill.

radiation.xls Jennings worksheet

Radiation Heat Transfer Calculation — The data in columns a, b, d, f is from 32-5003556-00

Data Source

Tsource	Simplified characterization of hot bundle temperature transient on page 217 of 32-5003556-00
Tsink	Simplified characterization of hot rod temperature transient on page 207 of 32-5003556-00
Heat Flux	Simplified characterization of heat flux transient taken from plot of FDAFWJGF in 32-5003556-00
	This plot is not recorded in 32-5003556-02 and is therefore reproduced herein as Figure 2

Length of Source	0.5	in	Diameter of Source	0.43	in	Fa	1
Area of Source	0.675	in^2		0.00469	ft^2	EOB	22 s
Emissivity	0.7		Effective Emissivity	0.538		BOCR	27.5 s

Time	Tsource, T_s		Tsink, T_r		$(T_s/100)^4$ - $(Tr/100)^4$	Radiation Qr		Model Heat Flux	Q	Ratio Model/Radiation
s	F	R	F	R		Btu/Hr	Btu/s	Btu/s-ft^2		
20	1680	2140	1600	2060	29646	12.9	0.00358	1.3	0.00610	1.704501
21	1705	2165	1625	2085	30717	13.3	0.00371	0.8	0.00375	1.012345
22	1730	2190	1650	2110	31814	13.8	0.00384	0.3	0.00141	0.366543
23	1755	2215	1675	2135	32936	14.3	0.00397	0.37	0.00174	0.436663
24	1780	2240	1700	2160	34085	14.8	0.00411	0.43	0.00202	0.490373
25	1805	2265	1725	2185	35260	15.3	0.00425	0.5	0.00235	0.5512
26	1830	2290	1750	2210	36462	15.8	0.00440	0.57	0.00267	0.607658
27	1855	2315	1775	2235	37690	16.4	0.00455	0.63	0.00296	0.649728
28	1880	2340	1800	2260	38946	16.9	0.00470	0.7	0.00328	0.698639

Average Net Hot Pellet Loss During Refill 22 - 27 s 0.004188

Plant Power	2772	MWT	Plant	2627856.0	Btu/s
Relative Power EOB	0.05		@ EOB	131392.8	Btu/s
# of FA	177		per FA	742.3	Btu/s
# of pins/FA	208		per pin	3.568905	Btu/s
Length of each pin	12				
# of segments in pin	288		per segment	0.012392	Btu/s
Local Peaking	2.5		peak segment	0.030980	Btu/s
Average Heat to sink	0.004188		Average heat to sink	0.00419	Btu/s
# sink pellets/source	3		To each sink pellet	0.00140	

Ratio Radiation heat to generated heat 0.045

One item of concern is the effect that the real, radiative, heat flux would have on the temperatures of the hot bundle pins if the transfer actually took place. This would only be a concern if the radiation heat load was significant relative to other heat loads. At the bottom of the worksheet a comparison between radiation heat load on the sink pins to decay heat energy is made. This comparison shows that the radiation load is only about 5 % of the decay heat and from the model half of that 5 % was present. Therefore, the comparison is valid and the use of the standalone hot pin model is a conservative approximation of the heat transfer to be expected from the hot spot during the refill or other low flow periods.

Hot Rod Hot Spot Heat Flux from FDAFWJGF.

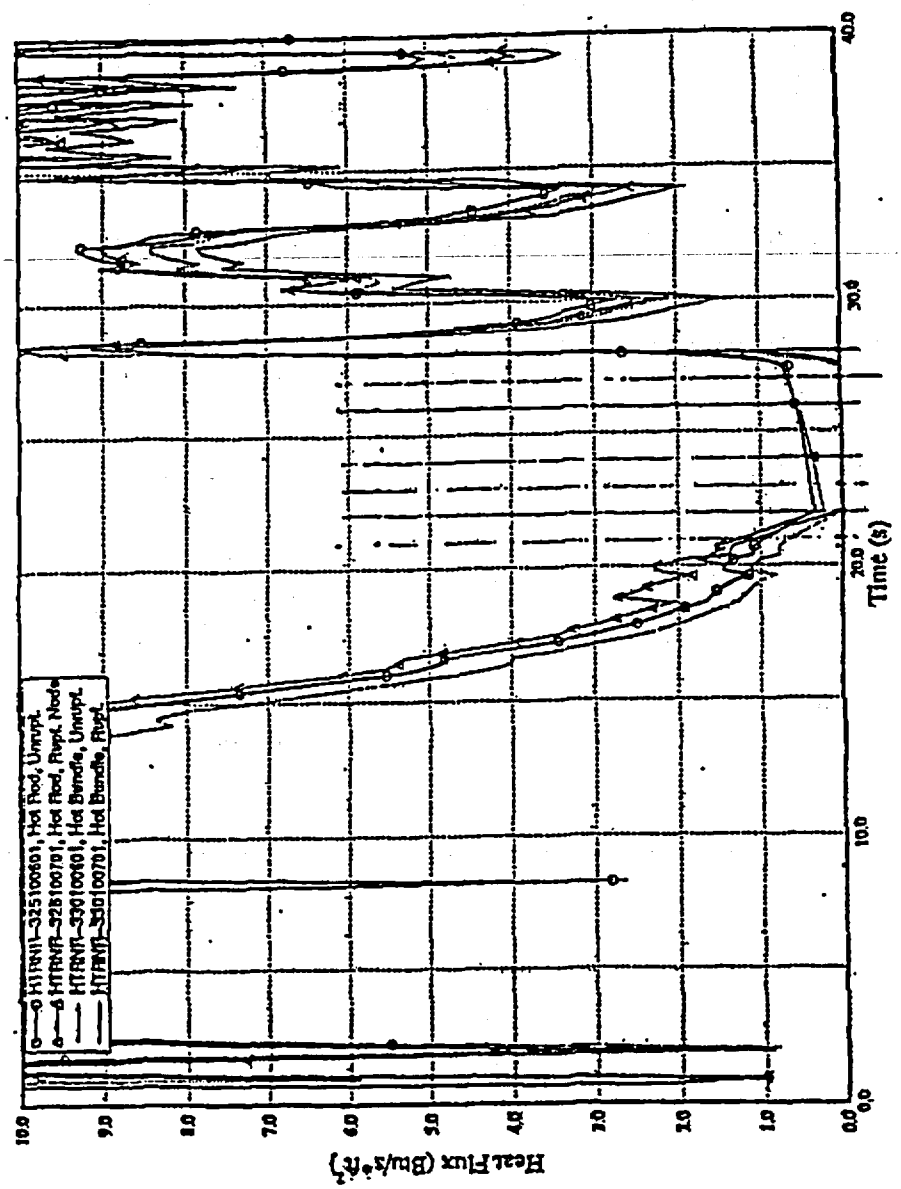

Conclusions

The FTI LOCA evaluation models are being upgraded to use a two region approach to determination of the heat transfer processes around the hot spot. The hot bundle is modeled as a heat structure with an associated coolant channel. The hot pin is modeled as a separate heat structure that uses the hot bundle coolant channel as its heat sink. This allows a more accurate determination of the coolant conditions for the hot pin. This calculation was to determine what the appropriate fuel temperature uncertainty was for the initialization of the hot bundle fuel. The method was to randomly distribute the fuel temperature uncertainty within the effective regions of the hot bundle according to the uncertainty distribution curve for the fuel temperature prediction, TACO3 code. 50,000 sets of such distributions were generated and sorted in order. The final distribution used was that which bounded 95 % of those sets. This provides assurance that the fluid temperatures achieved in the hot bundle are appropriately conservative for the evaluation of peak cladding temperature as far as the initialization of fuel temperature is concerned.

Heat transfer from the hot spot is governed by either convective transfer or radiant transfer during the course of an accident.

For convective heat transfer conditions a fuel temperature uncertainty of 2.1% for the hot bundle initialization is appropriate.

For radiative heat transfer a fuel temperature uncertainty of 2.5% for the hot bundle initialization is appropriate.

For pin average burnups below 40 GWd/mtU, the proposed model will use an uncertainty of 3 % to initialize the fuel temperature in the hot bundle and is therefore conservative beyond the 95 % level used to determine the appropriate values for initialization.

For pin average burnups greater than 40 GWd/mtU but less than 65 GWd/mtU, a bias will be added to both the hot pin and the hot bundle temperatures in accordance with the approval of TACO3 for those burnups.

FRAMATOME ANP

March 23, 2001
FANP-01-915

Document Control Desk
U. S. Nuclear Regulatory Commission
Washington, DC 20555-0001

Subject: Additional Information on Use of the Void-Dependent Cross-Flow Model Implemented in RELAP5/MOD2-B&W Code (BAW-10164, Rev. 4 P) for B&W-Plant SBLOCA Applications Performed Using the BWNT LOCA EM (BAW-10192PA)

Gentlemen:

The attached response addresses a verbal request for additional information from Frank Orr of the Nuclear Regulatory Commission. It was prepared to clarify use of a code automation feature in the new RELAP5/MOD2-B&W code topical revision (BAW-10164 Revision 4). This material clarifies the development and future use of the RELAP5/MOD2 void-dependent cross-flow model for SBLOCA applications performed for the B&W-designed plants in accordance with the BWNT LOCA Evaluation Model (EM) (BAW-10192 PA). This new code model automates the user implementation of the core cross-flow modeling approach used in this NRC-approved LOCA EM topical.

Some of the material in the attachment is considered Proprietary to Framatome ANP (FRA-ANP) as sworn by me as Vice President, Engineering and Licensing, FRA-ANP, presented as an enclosure within this submittal. All the proprietary material, which is enclosed in [brackets], is classified as categories "c" and "e" based on the FRA-ANP proprietary criteria given in the enclosure.

If clarification of any of the provided information is needed, please contact John Klingenfus at (804) 832-3294.

Very truly yours

R. W. Ganthner
Vice President
Engineering and Licensing

cc: Frank Orr/NRC
John Klingenfus, OF53
R. J. Schomaker, OF57
J. R. Biller, OF53

3315 Old Forest Road P.O. Box 10935 Lynchburg, VA 24506-0935 Tel: 804-832-3000 www.framatech.com

AFFIDAVIT OF RAYMOND W. GANTHNER

A. My name is Raymond W. Ganthner. I am Vice-President of Engineering & Licensing for Framatome ANP, Inc. (FRA-ANP), and as such, I am authorized to execute this Affidavit.

B. I am familiar with the criteria applied by FRA-ANP to determine whether certain information of FRA-ANP is proprietary and I am familiar with the procedures established within FRA-ANP to ensure the proper application of these criteria.

C. In determining whether an FRA-ANP document is to be classified as proprietary information, an initial determination is made by the Unit Manager, who is responsible for originating the document, as to whether it falls within the criteria set forth in Paragraph D hereof. If the information falls within any one of these criteria, it is classified as proprietary by the originating Unit Manager. This initial determination is reviewed by the cognizant Section Manager. If the document is designated as proprietary, it is reviewed again by me to assure that the regulatory requirements of 10 CFR Section 2.790 are met.

D. The following information is provided to demonstrate that the provisions of 10 CFR Section 2.790 of the Commission's regulations have been considered:

(i) The information has been held in confidence by FRA-ANP. Copies of the document are clearly identified as proprietary. In addition, whenever FRA-ANP transmits the information to a customer, customer's agent, potential customer or regulatory agency, the transmittal requests the recipient to hold the information as proprietary. Also, in order to strictly limit any potential or actual customer's use of proprietary information, the substance of the following provision is included in all agreements entered into by FRA-ANP, and an equivalent version of the proprietary provision is included in all of FRA-ANP's proposals:

"Any proprietary information concerning Company's or its Supplier's products or manufacturing processes which is so designated by Company or its Suppliers and disclosed to Purchaser incident to the performance of such contract shall remain the property of Company or its Suppliers and is disclosed in confidence, and Purchaser shall not publish or otherwise disclose it to others without the written approval of Company, and no rights, implied or otherwise, are granted to produce or have produced any products or to practice or cause to be practiced any manufacturing processes covered thereby.

Notwithstanding the above, Purchaser may provide the NRC or any other regulatory agency with any such proprietary information as the NRC or such other agency may require; provided, however, that Purchaser shall first give Company written notice of such proposed disclosure and Company shall have the right to amend such proprietary information so as to make it non-proprietary. In the event that Company cannot amend such proprietary information, Purchaser shall prior to disclosing such information, use its best efforts to obtain a commitment from NRC or such other agency to have such information withheld from public inspection.

Company shall be given the right to participate in pursuit of such confidential treatment."

(ii) The following criteria are customarily applied by FRA-ANP in a rational decision process to determine whether the information should be classified as proprietary. Information may be classified as proprietary if one or more of the following criteria are met:

a. Information reveals cost or price information, commercial strategies, production capabilities, or budget levels of FRA-ANP, its customers or suppliers.

b. The information reveals data or material concerning FRA-ANP research or development plans or programs of present or potential competitive advantage to FRA-ANP.

c. The use of the information by a competitor would decrease his expenditures, in time or resources, in designing, producing or marketing a similar product.

d. The information consists of test data or other similar data concerning a process, method or component, the application of which results in a competitive advantage to FRA-ANP.

e. The information reveals special aspects of a process, method, component or the like, the exclusive use of which results in a competitive advantage to FRA-ANP.

f. The information contains ideas for which patent protection may be sought.

The document(s) listed on Exhibit "A", which is attached hereto and made a part hereof, has been evaluated in accordance with normal FRA-ANP procedures with respect to classification and has been found to contain information which falls within one or more of the criteria enumerated above. Exhibit "B", which is attached hereto and made a part hereof, specifically identifies the criteria applicable to the document(s) listed in Exhibit "A".

(iii) The document(s) listed in Exhibit "A", which has been made available to the United States Nuclear Regulatory Commission was made available in confidence with a request that the document(s) and the information contained therein be withheld from public disclosure.

(iv) The information is not available in the open literature and to the best of our knowledge is not known by General Electric, Westinghouse-CE, or other current or potential domestic or foreign competitors of FRA-ANP.

(v) Specific information with regard to whether public disclosure of the information is likely to cause harm to the competitive position of FRA-ANP, taking into account the value of the information to FRA-ANP; the amount of effort or money expended by FRA-ANP developing the information; and the ease or difficulty with which the information could be properly duplicated by others is given in Exhibit "B".

E. I have personally reviewed the document(s) listed on Exhibit "A" and have found that it is considered proprietary by FRA-ANP because it contains information which falls within one or more of the criteria enumerated in Paragraph D, and it is information which is customarily held in confidence and protected as proprietary information by FRA-ANP. This report

comprises information utilized by FRA-ANP in its business which affords FRA-ANP an opportunity to obtain a competitive advantage over those who may wish to know or use the information contained in the document(s).

RAYMOND W. GANTHNER

State of Virginia)
) SS. Lynchburg
City of Lynchburg)

Raymond W. Ganthner, being duly sworn, on his oath deposes and says that he is the person who subscribed his name to the foregoing statement, and that the matters and facts set forth in the statement are true.

RAYMOND W. GANTHNER

Subscribed and sworn before me
this 23rd day of March 2001.

Brenda C. Maddox
Notary Public in and for the City
of Lynchburg, State of Virginia.
(I was commissioned a notary public
as Brenda C. Cardoza.
My Commission Expires July 31, 2003

EXHIBITS A& B

EXHIBIT A

Response to a Verbal Request for Additional Information on Use of the Void-Dependent Cross-Flow Model Implemented in RELAP5/MOD2-B&W Code (BAW-10164, Rev. 4P) for B&W-Plant SBLOCA Applications Performed Using the BWNT LOCA EM (BAW-10192PA).

EXHIBIT B

The above listed document contains information, which is considered Proprietary in accordance with Criteria c and e of the attached affidavit.

Attachment

Response to a Verbal Request for Additional Information on the RELAP5/MOD2-B&W Void-Dependent Core Cross-Flow Model Used in B&W-Plant SBLOCA Applications

Table of Contents

List of References

1. FTI Topical Report BAW-10192PA-00, "BWNT LOCA – BWNT Loss-of-Coolant Accident Evaluation Model for Once-Through Steam Generator Plants", June 1998.

2. FTI Topical Report BAW-10164PA-03, "RELAP5/MOD2-B&W An Advanced Computer Program for Light Water Reactor LOCA and Non-LOCA Transient Analysis," July 1996.

3. FCF Topical Report BAW-10227P-A, "Evaluation of Advanced Cladding and Structural Material (M5) in PWR Reactor Fuel," February 2000.

1. Background and Introduction

Framatome Advanced Nuclear Power (FRA-ANP), previously Framatome Technologies Inc., has used the BWNT LOCA Evaluation Model (EM) documented in BAW-10192P-A (Reference 1) for small break loss of coolant accident (SBLOCA) licensing analyses for the B&W-designed 177-fuel assembly lowered-loop (177-FA LL) and raised-loop (177-FA RL) plants. These analyses have been performed in accordance with the EM descriptions and they have complied with the EM and code limitations and restrictions imposed via the NRC safety evaluation reports (SERs). During the course of analysis, FRA-ANP has discovered that the SBLOCA core cross-flow form loss modeling requirements are cumbersome for the analysts to use when analyzing the spectrum of SBLOCA transients with core uncovering. FRA-ANP has remedied these problems by standardizing the current EM cross-flow implementation methods via RELAP5/MOD2-B&W code automation improvements. The extent of the FRA-ANP code improvements and plans for using this improved implementation are provided to the NRC through this documentation.

The EM describes the philosophy and physical cross-flow modeling approach used in SBLOCA analyses (Reference 1, Volume II, Section A.4). A high cross-flow resistance is used in the pool region to stabilize the void gradients or mixture levels between the hot and average channels. This pool void gradient results in a slightly higher hot channel

mixture level than that of the average core. Above the mixture level, the cross-flow resistance from the hot-to-average channel is conservatively reduced to allow steam flow diversion out of the hot channel. The average-to-hot channel resistance is increased in the steam region to restrict the flow of cooler steam from the average channel. The cross-flow resistance model that represents this stated approach is shown as the "Base Case" model in Table A-3 of the SBLOCA EM (Reference 1). Demonstration cases provided characteristic behavior when this segmented flow resistance model is used with low resistances in the upper core region and a high resistance in the lower core or pool region. Section A.4 of the SBLOCA EM (Volume II) states that the discontinuity in the resistances must be near or below the elevation of the minimum core mixture level obtained in the analysis. If the user specifies the transition elevation between the wrong two volumes, then an iteration on the cross-flow resistance input model might be required. This iteration is both burdensome to the user and it can introduce a variation of roughly +/- 40 F in the maximum peak clad temperature (PCT) prediction related to the degree of conservatism that the user imposed via specification of the elevation of the cross-flow resistance step change. This type of variation has been noted in SBLOCA analyses with limiting PCTs in the 1300 to 1450 F range for B&W-designed plants.

FRA-ANP reviewed the EM modeling philosophy and devised a simple code model that could be made responsive to the SBLOCA cross-flow resistance model requirements and change dynamically with the actual mixture levels. This variable resistance model will eliminate any potential user iteration associated with the specification of the fixed cross-flow resistance change. This standardization of the resistance modeling will also eliminate any PCT variations associated with the user's specification of the fixed-resistance transition elevation.

The new RELAP5/MOD2-B&W code (Reference 2) cross-flow model option alters the cross-flow resistance based on the local volume upstream conditions. At void fractions less than the pool region cutoff, the high cross-flow loss coefficients are used. At void fractions greater than the steam region cutoff, the low form loss coefficients are used. A smoothing region with linear interpolation between the two cutoff values is included to smooth the transition between the two resistance factors. This improved implementation method remains consistent with current EM discussions, therefore it is not considered to be an EM change. Nonetheless, FRA-ANP has notified the NRC of the implementation method differences, because of the slight alteration of the interpolation region and code automation of the cross-flow resistance model. The RELAP5/MOD2-B&W cross-flow code formulation changes were included in the documentation provided in the Revision 4 code updates supplied with the M5 licensing documentation in Appendix K of Reference 3. That information, with the void fractions at which the transitions occur, clearly defines the model that Framatome ANP will use in BAW-10192 SBLOCA EM applications.

2. Void-Dependent Cross-Flow Model

The basic principles described in Section A.4 of the SBLOCA EM volume describe a relationship between the cross-flow form loss and the upstream fluid conditions. If the upstream fluid is representative of the pool region (i.e. below the mixture level), then the

resistance should be high. Use of the higher pool resistance supports the variations in the mixture region void fraction related to power differences between the hot and average channels. These resistances are reduced [c, e] above the top of the mixture region to allow for steam flow diversion out of the hot channel. The steam region resistance factor from the average-to-hot channel is increased [c, e] to restrict steam flow from the average-to-hot channel. The pool or steam region can be defined within the code via use of an upstream volume void fraction. Based on simple changes in code logic, the cross-flow resistance was modified based on the upstream void fraction for any junction that is designated as a void-dependent cross-flow junction.

The new code option allows the user to specify the core cross-flow junctions as void-dependent cross-flow paths via a specialized flag on the junction-input cards. The user also provides the void fractions that define the steam region and the pool region. The pool region cross-flow resistance is specified for the junctions. If the upstream volume void fraction is below the pool region void fraction, then the high void fraction form loss factor [c, e] is unmodified. If the upstream volume void fraction is above the steam region void fraction, then the hot-to-average pool resistance is reduced [c,e] to the steam form loss [c, e] for the hot-to-average resistance. A lower multiplicative factor [c, e] is used to adjust the pool resistance value to the average-to-hot steam form loss [c, e]. All of these form loss coefficients are unmodified from the original fixed cross-flow EM modeling concepts. The only difference with the void-dependent model implementation is that a smoothing integral is used when the void fraction falls between the pool and steam void fractions. A linear interpolation on upstream void fraction will be used to define the multiplicative adjustments for both the forward and reverse form loss coefficients under these conditions.

This new code option forces the cross-flow resistance to be similar to that described in the EM at the time of minimum core inventory. It has the added benefit of providing a smooth transition from the higher pool region resistance to that of the steam region both during both the uncovering and refill phases. Without this new code option, the user was limited to a fixed cross-flow resistance specification at a predefined core elevation. This fixed modeling could be modified via code restarts in the transient, although this approach provides another way that the user can affect the overall calculation of PCT.

The new void-dependent user-input options for the pool void fraction cutoff value are obtained by observing the maximum pool-region void fraction in the worst break size range for the SBLOCA spectrum analyses. Generally, the highest PCT is predicted for B&W-plant analyses when the break size is between 0.024 and 0.15 ft^2. The highest core void fractions in the pool regions vary [c, e] for these break sizes, with the void fraction increasing with break size. The pool-region cutoff void fraction [c, e] will cover all of these break sizes and should be reasonable for the typically non-limiting analyses at larger break sizes. In fact, its use on the largest SBLOCAs will likely reduce the cross-flow over the entire channel, causing the PCTs to increase slightly for these break sizes. These breaks should remain non-limiting, however, because the uncovering duration is short.

The steam-region void-fraction cutoff should be set close to 1.0 during the core-uncovering phase. Consideration of the refill phase suggests that the steam-region void-fraction cutoff should be slightly less than 1.0 to prevent an increase in the resistance before there is a mixture level re-established in the volume. Accordingly, a void fraction [c, e] was selected as a reasonable value that is appropriate for both the initial uncovering and refill periods for all SBLOCA transients.

In equation form, the form losses are defined for the positive flow direction (forward flow) from the average channel to the hot channel (i.e. Volume K is the average channel volume, Volume L is the hot channel volume).

Void fraction Check		Form Loss Factor	For Flow From
$\alpha_g(K) \le \alpha_{pool}$	Then,	$K_{forward} = K_{forward\ input}$ [c, e]	average-to-hot
$\alpha_g(L) \le \alpha_{pool}$	Then,	$K_{reverse} = K_{reverse\ input}$ [c, e]	hot-to-average
$\alpha_g(K) \ge \alpha_{stm}$	Then,	$K_{forward} = K_{forward\ input} * M_{forward\text{-}stm}$ [c, e]	average-to-hot
$\alpha_g(L) \ge \alpha_{stm}$	Then	$K_{reverse} = K_{reverse\ input} * M_{reverse\text{-}stm}$ [c, e]	hot-to-average
$\alpha_{pool} \le \alpha_g(K) \le \alpha_{stm}$	Then,	$K_{forward} = K_{forward\ input} * M^{Interpolated}_{forward-stm}$	average-to-hot
$\alpha_{pool} \le \alpha_g(L) \le \alpha_{stm}$	Then,	$K_{reverse} = K_{reverse\ input} * M^{Interpolated}_{reverse-stm}$	hot-to-average

where

$$M^{Interpolated}_{forward-stm} = 1-(1-M_{forward-stm})*\left[\frac{\alpha_{pool}-\alpha_g(K)}{\alpha_{pool}-\alpha_{stm}}\right],$$

$$M^{Interpolated}_{reverse-stm} = 1-(1-M_{reverse-stm})*\left[\frac{\alpha_{pool}-\alpha_g(L)}{\alpha_{pool}-\alpha_{stm}}\right],$$

[c, e](average-to-hot)

[c, e] (hot-to-average)

[c, e]

[c, e]

3. Summary and Conclusion

The void-dependent cross-flow option implemented in RELAP5/MOD2-B&W Revision 4 standardizes the SBLOCA cross-flow modeling approach used in BAW-10192PA. It is an improved code implementation that was developed from the original EM methods with a resistance model that responds mechanistically to the actual core mixture level. It preserves the three major conservatisms that were targeted or imposed by the EM cross-flow model selections. These conservatisms entailed (1) limiting the difference in the hot and average mixture levels to roughly one volume height or less, (2) forcing a low cross-flow resistance in the uncovered or steam region to maximize flow diversion out of the hot channel, and (3) restricting the average-to-hot channel steam region flow. These three conservatisms are preserved with the new void-dependent model.

A small set of limiting SBLOCA plant cases have been run with the new void-dependent cross-flow option, and these have been compared with the original fixed-resistance method application results. The PCTs have increased in some cases and decreased in others, but the general variation in PCTs is primarily influenced by the degree of conservatism imposed by the user-specified fixed cross-flow resistance step change location in the original application. The representative plant cases examined showed that the void-dependent cross-flow model PCT falls within the PCT range that can be produced by different user-selected locations of the fixed cross-flow resistance model. Therefore, based on this examination of these current SBLOCA application cases, FRA-ANP has concluded that this new void-dependent standardization will not provide any significant increase or decrease in the BAW-10192PA calculated SBLOCA PCTs for limiting SBLOCA analyses performed with a loss of offsite power (LOOP). Therefore, the void-dependent model will be included in future B&W-designed EM applications performed with Reference 1.

The new model has the added benefit in that it is responsive to faster transients with dynamic mixture level transitions and applications such as those with manual reactor coolant pump trip within the first several minutes after loss of subcooling margin. These applications, which are being performed as a result of Preliminary Safety Concern (PSC) 2-00, were not considered when the fixed resistance model was developed. The void dependent cross-flow model is well suited for applications such as these; therefore it was used for the PSC 2-00 analyses that will be submitted to the NRC in April, 2001.

The void-dependent cross-flow model with the inputs prescribed in this letter represents an automated form of the fixed core cross-flow resistance model that the NRC approved for use for SBLOCA applications with BAW-10192PA. The automated model retains the prescribed EM conservatisms from the original SBLOCA EM approach and standardizes the PCT predictions for LOOP or no LOOP transients for B&W-designed plants. Therefore, FRA-ANP intends to use the void-dependent model in all future SBLOCA applications performed with the BAW-10192PA EM.

FRAMATOME

June 15, 2001
NRC:01:026

Document Control Desk
ATTN: Chief, Planning, Program and Management Support Branch
U.S. Nuclear Regulatory Commission
Washington, D.C. 20555-0001

NRC Review and Approval of BAW-10164P Revision 4, RELAP5/MOD2-B&W, An Advanced Computer Program for Light Water Reactor LOCA and Non-LOCA Transient Analysis

Framatome ANP (FRA-ANP) Lynchburg maintains two NRC-approved large break loss-of-coolant accident (LBLOCA) evaluation models (EMs). The EM described in BAW-10168P-A, Revision 3, December 1996, applies to recirculating steam generator (RSG) plants and the EM described in BAW-10192P-A, Revision 0, June 1998, is applied to B&W plants. These EMs use the RELAP5 code described in BAW-10164P-A Revision 3.

The EMs are being modified as described in the attachment. The modifications have been under review by the NRC for the past year. The purpose of the attachment to this letter is to summarize the changes and the documentation provided to the NRC to support the changes. A copy of this letter and the enclosures has been provided directly to those on distribution.

The NRC has been requested to approve these changes by issuance of a Safety Evaluation for the report BAW-10164 Revision 4. Framatome ANP would appreciate completion of the NRC review of these changes and the issuance of the Safety Evaluation by July 31, 2001.

Framatome ANP considers some of the information contained in the attachment and enclosures to this letter to be proprietary. The proprietary information in the attachment is enclosed within brackets [ ]. As required by 10 CFR 2.790(b) an affidavit is enclosed to support the withholding of this information from public disclosure.

Very truly yours,

Gerald S. Holm Jr.

James F. Mallay, Director
Regulatory Affairs

Enclosure

cc: F. M. Akstulewicz (w/enclosures)
S. N. Bailey (w/enclosures)
F. Orr (w/enclosures)

Framatome ANP Richland, Inc.

2101 Horn Rapids Road
Richland, WA 99352

Tel: (509) 375-8100
Fax: (509) 375-8402

The modeling changes are 1) subdivision of the hot bundle modeling and hot pin versus hot bundle fuel temperature uncertainty, 2) void dependent cross flow model for small breaks, and 3) implementation of the BEACH blockage limitation.

Subdivision of the Hot Bundle Modeling and Hot Pin versus Hot Bundle Fuel Temperature Uncertainty

The modeling of the hot rod/hot assembly is broken into two heat structures to improve the simulation of the LOCA cooling process. The changes apply to the large break LOCA EMs for both RSG and the B&W plants.

References 1, 2, and 3 were provided to the NRC to describe this modification. The previously provided references are enclosed with this letter to facilitate the NRC review. A copy of these references has been provided directly to Frank Akstulewicz.

RELAP5 Changes for This Modification

In order to model the hot pin and the hot assembly as separate heat structures, an option was added to RELAP5/MOD2-B&W to specify the pin channel (rod) as a primary or supplemental channel. The supplemental pin capability allows multiple pin channels within a single hydrodynamic fluid channel (i.e., a fuel assembly, for example). The changes to RELAP5/MOD2-B&W are documented in Revision 4 of RELAP5/MOD2-B&W topical report (Reference 1) on the following pages.

Page 2.3-26, Item 2

Page 2.3-27

Pages 2.3-46, 2.3-46.1 and 2.3-46.2

All changes are identified with a vertical line in the left or right margin

Further discussion of these changes is given in Section II of Reference 2.

Reactor Modeling Changes

These changes are documented in Reference 2, which describes the application of this model in the RSG and B&W plant EMs. Reference 2 describes the division of the heat structures simulating the hot rod and hot assembly, the calculation of steady state volume averaged fuel temperatures for each, and the sensitivity of the changes for both RSG and B&W designs.

The average core heat structure will be initialized with no uncertainty. The hot assembly heat structure will be initialized at a statistical-based uncertainty providing 95 percent confidence in 95 percent of all instances that the average fuel temperature in the assembly is bounded. The maximum 95/95, fuel temperature uncertainty will be imposed only on the hot rod heat structure. (Note that a correction to TACO3 predictions at high burnup will still be applied.)

Additional supporting information describing the calculation of the initial fuel temperature within the hot assembly was provided in Reference 3.

Void-Dependant Cross Flow Model for Small Breaks

The cross flow resistance model used within the core simulation for small break evaluations of B&W-designed plants is automated. The changes apply only to the small break LOCA EMs for the B&W plants.

This revised model is described in more detail in Reference 4. The change is also described briefly in BAW-10164P Revision 4 (Reference 1). A copy of the previously provided Reference 4 is enclosed with this letter to facilitate the review.

RELAP5 Changes for This Modification

The void-dependant cross flow model is an automation of the procedure outlined in Section A.4 of the BWNT LOCA evaluation model BAW-10192P-A, Revision 0, June 1998. Different cross flow resistances are required above and below the mixture height for the proper simulation of small break core uncovering. The current procedure is manual alteration of the resistances during the transient using code restarts. The automation divides the core region into three segments: a mixture region where the void fraction is less than the user input value $\alpha_{min\text{-}Kcross}$; a steam or in the misty region where the void fraction is larger than the user input value $\alpha_{max\text{-}Kcross}$; and a transition zone where the void fraction is between the two user input values. User input values for the K-factors and multipliers are selected so that the resulting form loss coefficients in the mixture region and in the steam or misty region will be the same as those specified in BAW-10192. In the transition zone, linear interpolation is used to calculate the form loss coefficients. A void fraction of [c,e,] typically represents the slug-to-annular flow transition boundary and therefore it is used as $\alpha_{min\text{-}Kcross}$. A void fraction of about [c,e] is a reasonable value for the lower boundary of the mist flow regime and therefore it is used as $\alpha_{max\text{-}Kcross}$. The changes to RELAP5/MOD2-B&W are documented in Revision 4 of the RELAP5/MOD2-B&W topical report (Reference 1) on the following pages.

Pages 2.1-126.1 and 2.1-126.2

All changes are identified with a vertical line in the left or right margin.

Reactor Modeling Changes

No changes to the reactor modeling are required because this is an automation of a technique already described in the approved BWNT LOCA evaluation model, BAW-10192. Although the modeling is general in its applicability, Framatome ANP only intends to apply it within the BWNT evaluation model for small breaks.

Implementation of the BEACH Blockage Limitation

The third change is the implementation of an SER limitation on the amount of blockage that can be credited in evaluating rupture induced cooling effects. The SER for the BEACH topical report

Revision 2 (this SER is documented on pages 5-226 through 5-230 of BAW-10166P-A, Revision 4, February 1996) limits the credited blockage to 60 percent of the flow channel. This limitation was previously verified by the user. The code logic that calculates rupture induced cooling effects was modified by limiting the maximum value of the credited blockage to 60 percent to assure implementation of the limit.

This modification is described in Reference 1.

RELAP5 Changes for This Modification

The logic changes to implement the limitation automatically are described in Revision 4 of the RELAP5/MOD2-B&W topical report (Reference 1) on the following pages.

Pages 2.1-126.1 and 2.1-126.2

All changes are identified with a vertical line in the left or right margin.

Ref.: 1. BAW-10164P Revision 4, *RELAP5/MOD2-B&W An Advanced Computer Program for Light Water Reactor LOCA and Non-LOCA Transient Analysis*, September 1999. This reference was provided with the letter GR99-194.doc, September 24, 1999.

Ref.: 2. Letter, J. J. Kelley (Framatome Technologies) to Document Control Desk (NRC), "Modeling Refinements to Framatome Technologies' RELAP-5 Based, Large Break LOCA Evaluation Models-BAW-10168 for Non-B&W-Designed, Recirculating Steam Generator Plants and BAW-10192 for B&W -Designed, Once-Through Steam Generator Plants," FTI-00-551, February 29, 2000.

Ref.: 3. Letter, J. J. Kelley (Framatome Technologies) to Document Control Desk (NRC), "Additional Information on Modeling Updates to Framatome Technologies' RELAP-5 Based, Large Break LOCA Evaluation Models-BAW-10168 for Non-B&W-Designed, Recirculating Steam Generator Plants and BAW-10192 for B&W-Designed, Once-Through Steam Generator Plants," FTI-00-2225, September 5, 2000.

Ref.: 4. Letter, R. W. Ganthner (Framatome Technologies) to Document Control Desk (NRC), "Additional Information on Use of the Void-Dependent Cross-Flow Model Implemented in RELAP5/MOD2-B&W Code (BAW-10164, Rev. 4 P) for B&W-Plant SBLOCA Applications Performed Using the BWNT LOCA EM (BAW-10192PA), FANP-01-915, March 23, 2001.

AFFIDAVIT

STATE OF WASHINGTON)
) ss.
COUNTY OF BENTON)

1. My name is Jerald S. Holm. I am Manager, Product Licensing, for Framatome ANP ("FRA-ANP"), and as such I am authorized to execute this Affidavit.

2. I am familiar with the criteria applied by FRA-ANP to determine whether certain FRA-ANP information is proprietary. I am familiar with the policies established by FRA-ANP to ensure the proper application of these criteria.

3. I am familiar with the FRA-ANP information included in the attachment and enclosures to the letter NRC:01:026, dated June 2001, from James F. Mallay to Document Control Desk. This letter is referred to herein as "Document." Information contained in this Document has been classified by FRA-ANP as proprietary in accordance with the policies established by FRA-ANP for the control and protection of proprietary and confidential information.

4. This Document contains information of a proprietary and confidential nature and is of the type customarily held in confidence by FRA-ANP and not made available to the public. Based on my experience, I am aware that other companies regard information of the kind contained in this Document as proprietary and confidential.

5. This Document has been made available to the U.S. Nuclear Regulatory Commission in confidence with the request that the information contained in the Document be withheld from public disclosure.

6. The following criteria are customarily applied by FRA-ANP to determine whether information should be classified as proprietary:

(a) The information reveals details of FRA-ANP's research and development plans and programs or their results.

(b) Use of the information by a competitor would permit the competitor to significantly reduce its expenditures, in time or resources, to design, produce, or market a similar product or service.

(c) The information includes test data or analytical techniques concerning a process, methodology, or component, the application of which results in a competitive advantage for FRA-ANP.

(d) The information reveals certain distinguishing aspects of a process, methodology, or component, the exclusive use of which provides a competitive advantage for FRA-ANP in product optimization or marketability.

(e) The information is vital to a competitive advantage held by FRA-ANP, would be helpful to competitors to FRA-ANP, and would likely cause substantial harm to the competitive position of FRA-ANP.

7. In accordance with FRA-ANP's policies governing the protection and control of information, proprietary information contained in this Document has been made available, on a limited basis, to others outside FRA-ANP only as required and under suitable agreement providing for nondisclosure and limited use of the information.

8. FRA-ANP policy requires that proprietary information be kept in a secured file or area and distributed on a need-to-know basis.

9. The foregoing statements are true and correct to the best of my knowledge, information, and belief.

Gerald S Holm

SUBSCRIBED before me this 15th day of June, 2001.

Valerie W. Smith

Valerie W. Smith
NOTARY PUBLIC, STATE OF WASHINGTON
MY COMMISSION EXPIRES: 10/10/04

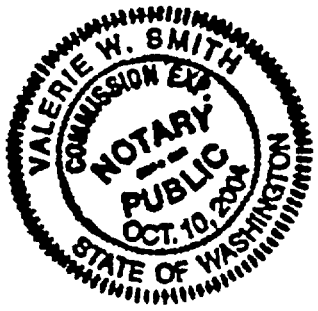

Note on Attachments

References 1, 2, 3, and 4 were provided to the NRC as part of the letter dated June 15, 2001. Each of these references were also submitted individually and have been included in this document on pages 5-404 through 5-462, 5-463 through 5-493, 5-494 through 5-510, and 5-511 through 5-524 respectively.

5.9 Revision 4 SER

This section contains the SER transmitted to FRA-ANP by Leslie W. Barnett of the NRC in their letter dated April 9, 2002.

UNITED STATES
NUCLEAR REGULATORY COMMISSION
WASHINGTON, D.C. 20555-0001

April 9, 2002

Mr. James F. Mallay
Director, Regulatory Affairs
Framatome ANP, Richland, Inc.
2101 Horn Rapids Road
Richland, WA 99352

SUBJECT: SAFETY EVALUATION OF FRAMATOME TECHNOLOGIES TOPICAL REPORT BAW-10164P REVISION 4, "RELAP5/MOD2-B&W, AN ADVANCED COMPUTER PROGRAM FOR LIGHT WATER REACTOR LOCA AND NON-LOCA TRANSIENT ANALYSES" (TAC NOS. MA8465 AND MA8468)

Dear Mr. Mallay:

By letters dated September 24, 1999 and February 29, 2000, Framatome submitted BAW-10164P, Revision 4, "RELAP5/MOD2-B&W, An Advanced Computer Program for Light Water Reactor LOCA and Non-LOCA Transient Analyses," for review by the NRC staff. By letters dated September 5, 2000, March 23, 2001, and June 15, 2001, Framatome provided additional information.

Framatome proposed the following changes to BAW-10164P-A (as Revision 4) and refinements to the loss of coolant accident (LOCA) evaluation models (EMs):

1. A change that will model the hot channel modeling to treat the hot pin and the hot assembly as two heat structures for large break LOCA (LBLOCA) evaluations of recirculating steam generator (RSG) and once through steam generator (OTSG) plants,

2. A change to the initial fuel stored energy uncertainty that will apply a lower uncertainty in the initial fuel stored energy, derived from TACO3, to the hot assembly and core average heat structures for LBLOCA evaluations of RSG and OTSG plants,

3. A change to automate the void-dependent cross-flow model and to interpolate the inter-channel void-dependent cross-flow for small break LOCA (SBLOCA) evaluations for OTSG plants, and

4. Automation of the core heat BEACH blockage limitation that will automate flow-blockage limit in BEACH, used for LBLOCA and SBLOCA analyses of RSG and OTSG plants.

The staff has completed its review of the subject topical report (TR) and finds it is acceptable for referencing in licensing applications to the extent specified and under the limitations delineated in the report and in the associated safety evaluation (SE). The SE defines the basis for acceptance of the report.

Pursuant to 10 CFR 2.790, we have determined that the enclosed SE does not contain proprietary information. However, we will delay placing the SE in the public document room for a period of 10 working days from the date of this letter to provide you with the opportunity to comment on the proprietary aspects only. If you believe that any information in the enclosure is proprietary, please identify such information line by line and define the basis pursuant to the criteria of 10 CFR 2.790.

We do not intend to repeat our review of the matters described in the subject report, and found acceptable, when the report appears as a reference in license applications, except to ensure that the material presented applies to the specific plant involved. Our acceptance applies only to matters approved in the report.

In accordance with the guidance provided in NUREG-0390, we request that Framatome publish an accepted version of this TR within 3 months of receipt of this letter. The accepted version shall incorporate this letter and the enclosed safety evaluation between the title page and the abstract. It must be well indexed such that information is readily located. Also, it must contain in appendices historical review information, such as questions and accepted responses, and original report pages that were replaced. The accepted version shall include an "-A" (designated accepted) following the report identification symbol.

Should our criteria or regulations change so that our conclusions as to the acceptability of the report are invalidated, Framatome and/or the applicants referencing the TR will be expected to revise and resubmit their respective documentation, or submit justification for the continued applicability of the TR without revision of their respective documentation.

Sincerely,

Leslie W. Barnett, Acting Director
Project Directorate IV
Division of Licensing Project Management
Office of Nuclear Reactor Regulation

Project No. 693

Enclosure: Safety Evaluation

UNITED STATES
NUCLEAR REGULATORY COMMISSION
WASHINGTON, D.C. 20555-0001

SAFETY EVALUATION BY THE OFFICE OF NUCLEAR REACTOR REGULATION

TOPICAL REPORT BAW-10164P, REVISION 4, "RELAP5/MOD2-B&W, AN ADVANCED COMPUTER PROGRAM FOR LIGHT WATER REACTOR LOCA AND NON-LOCA TRANSIENT ANALYSES"

PROJECT NO. 693

1.0 INTRODUCTION

Framatome ANP proposed several changes to its loss-of-coolant accident (LOCA) evaluation models (EMs) and methodologies in letters dated September 24, 1999 and February 29, 2000. Framatome provided additional information by letters dated September 5, 2000, March 23, 2001, and June 15, 2001.

Framatome ANP maintains several LOCA EMs to cover the conditions of small break LOCAs (SBLOCAs) and large break LOCAs (LBLOCAs) in once-through steam generator (OTSG) plants and recirculating steam generator (RSG) plants. The LOCA EMs are described in several Framatome topical reports, including the following:

BAW-10168P-A, "RSG LOCA, BWNT Loss-of Coolant Accident Evaluation Model for Recirculating Steam Generator Plants," Revision 3, December 1996.

BAW-10192P-A, "BWNT LOCA, BWNT Loss of Coolant Accident Evaluation Model for Once-Through Steam Generator Plants," Revision 0, June 1998.

BAW-10164P-A, "RELAP5/MOD2-B&W, An Advanced Computer Program for Light Water Reactor LOCA and Non-LOCA Transient Analyses," Revision 3, July 1996.

BAW-10166P-A, "BEACH, Best Estimate Analysis Core Heat Transfer, A Computer Program for Reflood Heat Transfer During LOCA," Revision 4, February 1996.

BAW-10162P-A, "TACO3, Fuel Rod Thermal Analysis Computer Code," Revision 0, November 1989.

Framatome proposed the following changes to BAW-10164P-A (as Revision 4) and refinements to the LOCA EMs:

1. A change that will model the hot channel modeling to treat the hot pin and the hot assembly as two heat structures for LBLOCA evaluations of RSG and OTSG plants.

2. A change to the initial fuel stored energy uncertainty that will apply a lower uncertainty in the initial fuel stored energy, derived from TACO3, to the hot assembly and core average heat structures for LBLOCA evaluations of RSG and OTSG plants,

3. A change to automate the void dependent crossflow model and to interpolate the inter-channel void-dependent cross-flow for SBLOCA evaluations for OTSG plants, and

4. Automation of the core heat BEACH blockage limitation that will automate flow-blockage limit in BEACH, used for LBLOCA and SBLOCA analyses of RSG and OTSG plants.

2.0 STAFF EVALUATION

The staff reviewed the above proposed changes for acceptability in the context of the previously approved LOCA EMs listed above (e.g., Revision 3 to BAW-10164P-A, Revision 3 to BAW-10168P-A, and Revision 0 to BAW-10192P-A). These EMs will use the RELAP 5 code described in BAW-10164P, Revision 4.

The staff's review of the changes to the hot channel modeling, fuel initial stored energy uncertainty, cross-flow modeling, and flow blockage limit automation, in the context of the previously approved LOCA EMs, is presented below.

2.1 Changes to the Hot Channel Modeling in the LBLOCA Methodology

By letters dated September 24, 1999, and February 29, 2000, Framatome described the changes to the hot assembly modeling. Additional information was provided in letters dated September 5, 2000, March 23, 2001, and June 15, 2001. The changed modeling applies to the RELAP5/MOD2-B&W LBLOCA EMs for OTSG (BAW-10192P-A, Revision 0) and RSG (BAW-10168P-A, Revision 3) plants. The principal amended changes are: (a) replacing the hot rod/hot assembly channel with one channel containing two heated surfaces, one representing the hot rod and the other representing the other rods in the hot assembly, and (b) using the fuel initial stored energy uncertainty, and corresponding initial fuel rod conditions, as discussed in Section 2.2.

Currently, the Framatome model for peak cladding temperature (PCT) calculations does not differentiate between the hot fuel assembly and the hottest pin. This modeling scheme causes the entire hot assembly to incorporate all of the conservatisms required for the hot pin or hot spot to assure that the hot pin or hot spots are not under predicted. In the present model, Framatome assumes that the hot assembly consists of all hot rods at the peak rod power and peaking factors, and at the hottest rod initial temperature (stored energy) uncertainty. Framatome contends that this model results in a significant overprediction of the severity of the hot pin or hot spot conditions, and a very conservative prediction of the PCT. Framatome also contends that this conservative modeling did not represent the actual physical phenomenon in that there are cooling mechanisms affecting the hot spot. Framatome contends that these cooling mechanisms include convective heat transfer when there is high coolant flow, and a radiative heat transfer process to the immediate surroundings of the hot spot during low coolant flow. The cooling mechanisms govern heat transfer between the hot spot and the hot fuel assembly.

Therefore, Framatome proposed a new model which separates hot pin and hot spots from the hot fuel assembly. In the proposed model, the power of the rods in the core is assumed to be the same as in the present model, with all rods in the hot assembly at the same limiting power. However, in the proposed version, the initial conditions of temperature uncertainties for the fuel rods in the hot assembly are changed based on TACO3 calculations. The hottest rod uncertainty remains the same as assumed in the present model. The remainder of the rods in the hot assembly have an initial temperature uncertainty, derived from TACO3 calculations, statistically based on the fuel rods immediately surrounding the hottest rod. This lowers the temperature uncertainty assumption for all the fuel rods in the hot assembly except for the hottest rod. In addition, the average core heat structure will be initialized with no uncertainty, consistent with the above statistical approach. The fuel temperature uncertainty is discussed in more detail in Section 2.2 of this safety evaluation. The rest of the rods in the core are modeled the same as in the present model.

The changes would not affect the hot rod directly. The hot rod would be represented the same as it is in the present model. However, the changes to the initial conditions including the stored energy of the other rods, would in turn change the transient effects of the other rods. The transient effects of the other rods would affect the transient coolant conditions of the hot channel, and thereby affect the transient behavior of the hot rod. The overall result of the reduced conservatism of the non-hot rod initial conditions is a lowering of the calculated peak cladding temperature.

The staff concludes that the change to two heat surfaces in the hot channel and the changes in assumed initial fuel temperature uncertainty are acceptable because the methodology continues to assume that all the fuel rods in the hot assembly are at the same limiting power and peaking factors as the hottest rod. The staff expects the assumed power level in the hot assembly to be sufficiently conservative such that the EM, using the initial fuel temperature uncertainty discussed below, will provide conservative results.

In summary, the staff concludes that the hot channel modeling changes are acceptable for the proposed version of the methodology because the Framatome assumption that all the hot assembly fuel rods are at the hottest rod's power assures that the methodology will continue to be conservative when changes reducing the conservatism of the initial fuel temperature uncertainty are included.

2.2 Changes to Initial Fuel Stored Energy Uncertainty

By letter dated February 29, 2000, Framatome proposed changes to the uncertainty applied to the fuel initial stored energy. As previously discussed, the current Framatome model for PCT does not differentiate between the hot fuel assembly and the hottest pin. This modeling scheme causes the entire hot assembly to incorporate all of the conservatisms required for the hot pin or hot spot to assure that the hot pin or hot spot is not underpredicted. As a result, in the current EM, Framatome applies an uncertainty that is applicable to the hot spot to the entire hot assembly and hot pin. The stored energy in the fuel is derived from the approved TACO3 fuel performance code.

Framatome's proposed new model includes a hot pin modeled as a separate heat structure that shares a coolant channel with the hot fuel assembly. The hot fuel assembly is comprised of all fuel pins within the hot assembly except the hot pin. For the hot pin, Framatome will use an initial fuel temperature uncertainty of 11.5 percent, which is based on the hot spot. This is the same uncertainty value as is used for the hot rod/assembly in the current model. Thus, the stored energy for the hot pin is identical for both current and proposed models. The staff considers this approach acceptable.

The initial fuel temperature uncertainty for the hot fuel assembly is determined by a probability distribution of the fuel pellet temperature predictions such that the temperature is overpredicted 95 percent of the time at the 95 percent confidence level. To deduce the average fuel temperature uncertainty for the hot fuel assembly, Framatome described a flow channel that shows a hot pin surrounded by eight fuel pins to form four subchannels. Framatome contended that only pins and pellets within these subchannels can be expected to affect the heat transfer from the hot spot. This approach effectively shields the hot pin from influence by those pins outside the channel, thereby conservatively predicting fuel temperature uncertainty. Framatome assigned weighting factors for those eight pins surrounding the hot pin that contribute heat to the subchannels. These weighting factors are based on a conservative geometrical consideration that maximizes the heat added to the subchannels. Framatome notes that there is an additional conservatism because the control rod guide tubes and instrument tubes are not considered in the hot fuel assembly. To determine the average uncertainty for the fuel pellets surrounding the hot pin, Framatome applied a statistical method to randomly determine the uncertainty of each pellet, according to the TACO3 uncertainty distribution, and considered the applicable heat transfer mechanisms at the hot spot. This process was repeated until a 95/95 confidence level was reached. The result showed that the average uncertainty for the hot fuel assembly is 2.1 percent for conditions with coolant flow and 2.3 percent for conditions without coolant flow. For conservatism, Framatome will assign an average uncertainty of 3 percent for the hot assembly. Based on this average uncertainty, Framatome can calculate the stored energy for the hot fuel assembly. The staff agrees with this approach.

Similar to the calculation of hot assembly uncertainty, Framatome evaluated the average uncertainty to be applied to the average core heat structure. Framatome determined that, core wide, the average uncertainty is zero (e.g., no bias in the TACO3 results). Framatome noted, however, that a correction to the TACO3 results is applied for high burnup fuel (greater than 40 GWd/mtU), consistent with the high burnup Topical Report, BAW-10186P-A, "Extended Burnup Evaluation," Revision 0, June 1997.

The staff has reviewed Framatome's proposed stored energy model for hot pin, hot fuel assembly, and average core heat structures. Based on the approved TACO3 code and conservative approach in the modeling and statistical method, the staff finds the proposed changes to be acceptable.

2.3 Changes to Void-Dependent Cross-Flow Model

Framatome proposed to change its small break LOCA analysis methodology as described in their September 24, 1999, letter. The staff also consulted BAW-10192P-A, Volume 2, which described the previous SBLOCA methodology for B&W designs. The previous methodology provides coefficients controlling cross-flow in the core between the hot channel and the average channel in both directions for both below the water surface and the steam space above the water surface. The values of the coefficients used in the approved model were determined by analytical sensitivity studies to assure relative conservatism and consistent calculated behavior. No formal comparisons to test data were performed. The time-dependent variance of the fluid condition at any given level determines the values of these coefficients at that level. In the present methodology, coefficient values were entered by the analyst in an iterative process of interpretation of the calculated time- and level-dependent fluid conditions.

The existing core cross-flow model provides flow coefficients between the hot channel and the average channel. The coefficients are fixed-valued, but specific to the flow location (above and below the water surface) and the flow direction (out of the hot channel or into the hot channel from the average channel). In the previous model, the values of the time-dependent coefficient values were determined by the analyst's assessment of the time variance of fluid conditions in the channels. The specific values were initially checked against large break data, and then tuned with sensitivity studies to give qualitatively credible results and identify the bounding case of those studied. This was considered by the staff in its previous review and approval of the model.

The proposed model change adds a void-dependent transition zone (which varies in elevation with the time-dependent change in core water level) to interpolate the coefficients, providing greater continuity to the calculations. In the updated methodology, the interpretation of time- and level-dependent fluid condition is automated, avoiding the possible inconsistencies introduced by different interpretations between analysts.

In a letter dated March 23, 2001, Framatome stated that it examined the relative effect of this change for a limited number of cases that they considered representative. In comparisons of results using the previous model and results using the proposed model, the calculated results using the proposed model are consistent and fall within the range of variance between different analysts using the previous model. This demonstrates that, for SBLOCA analyses representative of B&W-design licensing cases, use of the proposed model yields results within the range of results using the previously approved model.

The staff concludes that the proposed treatment of cross-flow is acceptable for the proposed version of the SBLOCA methodology because the proposed automated cross-flow model provided more consistent results than the previously approved analyst-controlled model, and because the results using the proposed model fell within the range of variance of the results using the previously approved analyst-controlled model in comparisons performed by Framatome.

Future changes to the Framatome SBLOCA methodology could significantly affect either the form of the cross-flow model or the cross-flow coefficient values. Because the staff only considered the proposed cross-flow model within the context of the Framatome SBLOCA

methodology as it is presently configured, and for scenarios represented in a limited sensitivity study, future modifications of the SBLOCA methodologies could compromise any conservatism remaining in the methodology. The staff will in future reviews of SBLOCA model changes, request additional empirical data comparisons supporting the cross-flow model discussed in this safety evaluation to confirm that sufficient conservatism remains in the future methodologies in accordance with 10 CFR Part 50, Appendix K.

Plant design and fuel differences, and discovered errors or changes, could affect the results, both quantitative and qualitative, due to the form of the cross-flow model or the cross-flow coefficient values. Differences in the results could indicate different compensatory or remedial actions. Deviations from the versions of the LOCA methodologies containing the cross-flow model discussed in this safety evaluation are subject to the requirements of 10 CFR 50.46.

2.4 Automation of BEACH Blockage Limitation

The approved version of the BEACH methodology contains a credited flow blockage limitation of 60 percent, which is implemented by the analyst inspecting the analytical results. In the September 24, 1999, letter, Framatome proposed to automate this limit in the BEACH coding. This automation is more convenient, and makes implementation of the limitation and calculated results more reliable and consistent. For these reasons, the staff finds this change acceptable.

3.0 CONCLUSIONS

Based on reviews discussed in Section 2, the staff finds the following Framatome proposed methodology changes (BAW-10164P, Revision 4) acceptable within the stated terms and limitations:

1. A change that will model the hot channel modeling to treat the hot pin and the hot assembly as two heat structures for LBLOCA evaluations of RSG and OTSG plants.

2. A change to the initial fuel stored energy uncertainty that will apply a lower uncertainty in the initial fuel stored energy, derived from TACO3, to the hot assembly and core average heat structures for LBLOCA evaluations of RSG and OTSG plants.

3. A change to automate the void dependent crossflow model and to interpolate the inter-channel void-dependent cross-flow for SBLOCA evaluations for OTSG plants.

4. Automation of the core heat BEACH blockage limitation that will automate the flow-blockage limit in BEACH, used for LBLOCA and SBLOCA analyses of RSG and OTSG plants.

For reasons discussed in Section 2, in its review of future changes to the LBLOCA and SBLOCA methodologies beyond the context discussed in this safety evaluation, the staff will closely examine the impacts of the proposed changes with respect to the TACO3 stored energy model, the hot channel modeling changes, and the cross-flow model discussed in this safety evaluation.

As discussed in Section 2, the methodology changes addressed in this safety evaluation are significant. They involve both LBLOCA and SBLOCA, and a variety of plant designs, including recirculating steam generator and once-through steam generator designs. The methodology changes would likely affect the various plant designs differently. Identified errors and changes, and compensatory and remedial actions could be different between the plants. Deviations from the versions of the LOCA methodologies containing the items discussed in this safety evaluation (BAW-10164P, Revision 4) are subject to the requirements of 10 CFR 50.46.

Principal Contributor: F. Orr

Date: April 9, 2002

5.10 Pages removed for Revision 4

The following pages have been replaced in revision 3 to create revision 4.

BAW-10164-A
Topical Report
Revision 3
October 1996

- RELAP5/MOD2-B&W -

An Advanced Computer Program for Light Water Reactor LOCA and Non-LOCA Transient Analysis

B&W Nuclear Technologies
P. O. Box 10935
Lynchburg, Virginia 24506

B&W Nuclear Technologies
Lynchburg, Virginia

Topical Report BAW-10164-A
Revision 3
October 1996

RELAP5/MOD2-B&W

An Advanced Computer Program for Light Water Reactor LOCA and Non-LOCA Transient Analysis

Key Words: RELAP5/MOD2, LOCA, Transient, Water Reactors

Abstract

This document describes the physical solution technique used by the RELAP5/MOD2-B&W computer code. RELAP5/MOD2-B&W is a B&W Nuclear Technologies adaption of the Idaho National Engineering Laboratory RELAP5/MOD2. The code developed for best estimate transient simulation of pressurized water reactors has been modified to include models required for licensing analysis. Modeling capabilities are simulation of large and small break loss-of-coolant accidents, as well as operational transients such as anticipated transient without SCRAM, loss-of-offsite power, loss of feedwater, and loss of flow. The solution technique contains two energy equations, a two-step numerics option, a gap conductance model, constitutive models, and component and control system models. Control system and secondary system components have been added to permit modeling of plant controls, turbines, condensers, and secondary feedwater conditioning systems. Some discussion of the numerical techniques is presented. Benchmark comparison of code predictions to integral system test results are presented in an appendix.

This page is intentionally left blank.

Topical Revision Record

Documentation Revision	Description	Program Change?	Program Version
0	Original issue	———	8.0
1	Typographical corrections Replace CSO correlation with Condie-Bengston IV	yes	10.0
2	SBLOCA modifications Miscellaneous corrections	yes	18.0
3	EM Pin Enhancements Filtered Flows for Hot Channel Heat Transfer Rupture Area Enhancement for Surface Heat Transfer OTSG Improvements and Benchmarks using the Becker CHF, Slug Drag, and Chen Void Ramp	yes	19.0

TABLE OF CONTENTS (cont'd)

LIST OF FIGURES (Cont'd)

1. INTRODUCTION

RELAP5/MOD2 is an advanced system analysis computer code designed to analyze a variety of thermal-hydraulic transients in light water reactor systems. It is the latest of the RELAP series of codes, developed by the Idaho National Engineering Laboratory (INEL) under the NRC Advanced Code Program. RELAP5/MOD2 is advanced over its predecessors by its six-equation, full nonequilibrium two-fluid model for the vapor-liquid flow field and partially implicit numerical integration scheme for more rapid execution. As a system code, it provides simulation capabilities for the reactor primary coolant system, secondary system, feedwater trains, control systems, and core neutronics. Special component models include pumps, valves, heat structures, electric heaters, turbines, separators, and accumulators. Code applications include the full range of safety evaluation transients, loss-of-coolant accidents (LOCAs), and operating events.

RELAP5/MOD2 has been adopted and modified by B&W for licensing and best estimate analyses of PWR transients in both the LOCA and non-LOCA categories. RELAP5/MOD2-B&W retains virtually all of the features of the original RELAP5/MOD2. Certain modifications have been made either to add to the predictive capabilities of the constitutive models or to improve code execution. More significant, however, are the B&W additions to RELAP5/MOD2 of models and features to meet the 10CFR50 Appendix K requirements for ECCS evaluation models. The Appendix K modifications are concentrated in the following areas: (1) critical flow and break discharge, (2) fuel pin heat transfer correlations and switching, and (3) fuel clad swelling and rupture.

Since the connecting K and L volumes are assumed to be predominately axial-flow volumes, the crossflow junction momentum flux (related to the axial volume velocity in K and L) is neglected along with the associated numerical viscous term. In addition, the horizontal stratified pressure gradient is neglected.

All lengths and elevation changes in the one-dimensional representation are based upon the axial geometry of the K and L volumes and the crossflow junction is assumed to be perpendicular to the axial direction and of zero elevation change, thus, no gravity force term is included.

The resulting vapor momentum finite difference equation for a crossflow junction is

$$\left[\alpha_g \rho_g\right]_j^n \left[v_g^{n+1} - v_g^n\right]_j \Delta x_j = - \alpha_{g,j}^n (P_L - P_K)^{n+1} \Delta t$$
$$- \left[\alpha_g \rho_g\right]_j^n \text{HLOSSG}_j^n \, v_{g,j}^{n+1} \Delta t$$
$$- \left[\alpha_g \rho_g\right]_j^n \text{FIG}_j^n \left[v_{g,j}^{n+1} - v_{f,j}^{n+1}\right] \Delta x_j \Delta t$$
$$+ \text{ADDED MASS} + \text{MASS TRANSFER MOMENTUM} . \qquad 2.1.4\text{-}72$$

A similar equation can be written for the liquid phase. In Equation 2.1.4-72, HLOSSG_j^n contains only the user input crossflow resistance. The Δx_j term that is used to estimate the inertial length associated with crossflow is defined using the diameters of volumes K and L,

$$\Delta x_j = \frac{1}{2} \left[D(K) + D(L)\right] . \qquad 2.1.4\text{-}73$$

The crossflow option can be used with the crossflow junction perpendicular to the axial flow in volume L (or K) but parallel

2.3.2. Core Heat Structure Model

The ordinary RELAP5 heat structures are general in nature and can be used for modeling core fuel pins; however, licensing calculations require special treatment of the fuel pin heat transfer. To accommodate these requirements, two additional models, commonly referred to as the EM (Evaluation Model) pin and core surface heat transfer model were added to the code. The EM pin model calculates dynamic fuel-clad gap conductance, fuel rod swell and rupture using NUREG-0630[117] options, and cladding metal-water reaction. The core fuel pin surface heat transfer is calculated with a flow regime-dependent set of correlations that include restrictions on which correlations can be selected per NRC licensing requirements. These new models are independent and mutually exclusive of the original system heat transfer model (described in section 2.2.2) and the existing simple gap conductance model[118] (referenced in Appendix A). The new models are explicitly coupled to the solution scheme though the modification of the gap conductance term, addition of fluid hydraulic resistance upon rupture, deposition of metal-water reaction energy in the clad, and determination of fuel pin surface heat transfer. The new EM pin model calculations are described in this section, while the EM heat transfer description is contained in section 2.3.3.

The EM pin model consists of three basic parts:

1. Dynamic fuel-clad gap conductance,
2. Fuel rod swell and rupture using NUREG-0630 options, and
3. Clad metal-water reaction,

which couple explicitly to the heat structure solution scheme or add fluid hydraulic resistance upon rupture. The model may be executed either in a steady-state initialization or transient mode determined by user input.

The pin calculations are performed on single fuel rod which represent the average behavior of a large number of rods. Each rod (also termed channel) can be broken into up to ninety heat structures, each having an associated pin segment. The gap conductance, deformation mode, and metal-water reaction are determined for each individual segment based on the channel specific pin pressure.

2.3.2.1. Transient Dynamic Fuel-Clad Gap Conductance

The RELAP5 heat structure conduction scheme uses cold, unstressed geometrical dimensions for its solution technique. The dynamic gap conductance, h_{gap}, is calculated from hot stressed conditions from which an effective gap thermal conductivity, $\bar{K}_{gap}$, based on cold gap size, $r_{g_{cold}}$, is determined for each pin segment.

$$\bar{K}_{gap} = h_{gap} \cdot r_{g_{cold}} . \qquad 2.3.2\text{-}1$$

The gap conductance is determined by calculating the gap gas conductivity, temperature jump gap distance, radiation component, and dynamic fuel-clad gap from the deformation models. An additive fuel-clad contact conductance term has also been included as an option to simulate the closed gap contribution for high fuel rod burn-up applications. Two options are provided to calculate the conductance. The first option assumes that the fuel pellet is concentric within the clad, while the second option assumes the fuel pellet is non-concentric within the clad as illustrated in Figure 2.3.2-1.

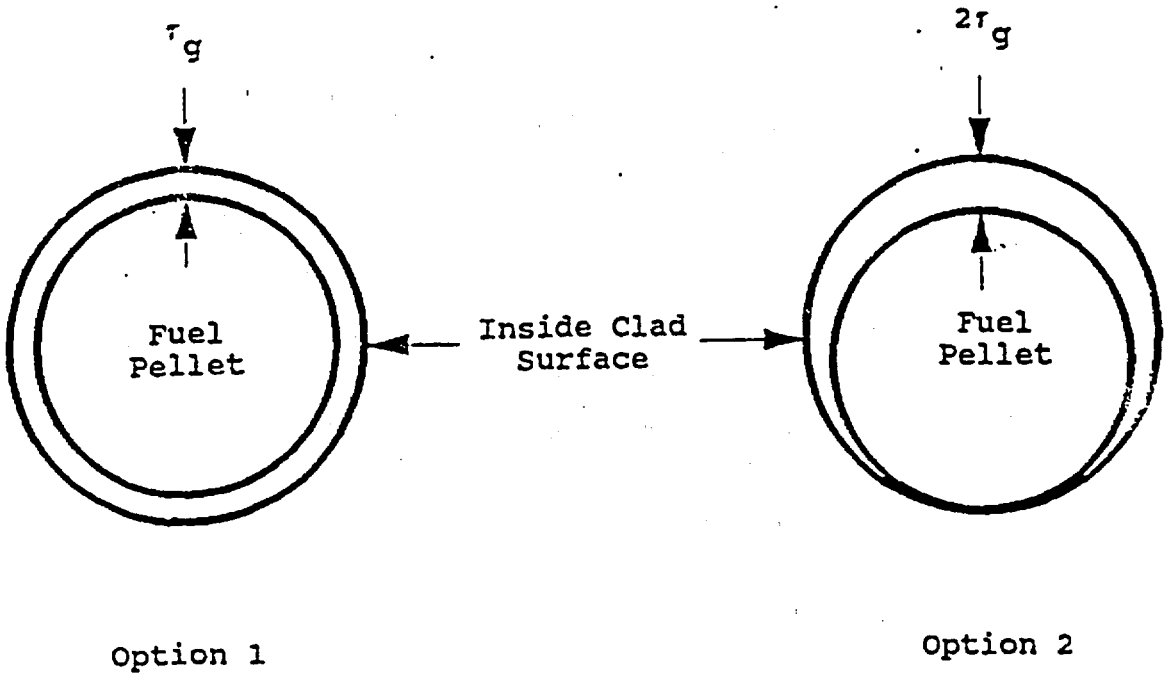

Figure 2.3.2-1. Gap Conductance Options.

Eight half-symmetrical azimuthal sections are used for determining the overall conductance for the second option without calculating an azimuthal temperature gradient. The total gap conductance is determined by

$$h_{gap} = M_g \, h_{\substack{gap \\ gas}} + h_{rad} + h_{fcc} \qquad 2.3.2\text{-}2$$

with

h_{gap} = conductance through gap gas (w/m^2-K),

M_g = user input multiplier used to acquire correct initial temperature within fuel,

$h_{gap\ gas}$ = gap gas conductance contribution (w/m^2-K),

h_{rad} = conductance due to radiation contribution from fuel to clad (w/m^2-K), and

h_{fcc} = gap contact conductance contribution due to fuel-cladding mechanical interaction (w/m^2-K).

The radiation gap conductance contribution is calculated by

$$h_{rad} = \frac{\sigma}{\frac{1}{e_f} + \frac{r_f}{r_{ic}}\left(\frac{1}{e_c} - 1\right)} \left[\frac{T_{fs}^4 - T_{ics}^4}{T_{fs} - T_{ics}}\right]$$

$$= \frac{\sigma(T_{fs}^2 + T_{ics}^2)(T_{fs} + T_{ics})}{\frac{1}{e_f} + \frac{r_f}{r_{ic}}\left(\frac{1}{e_c} - 1\right)}, \qquad 2.3.2\text{-}2.1$$

where

σ = Stefan-Boltzmann constant,

= 5.6697×10^{-8} (w/m^2-K^4),

e_f = emissivity of fuel surface,

e_c = emissivity of clad-inside surface,

T_{fs} = fuel outside surface temperature (K), and

T_{ics} = clad-inside surface temperature (K).

$$C_1 = 1.0 \cdot 10^{-5} \ (K^{-1}),$$
$$C_2 = -3.0 \cdot 10^{-3},$$
$$C_3 = 4.0 \cdot 10^{-2}, \text{ and}$$
$$C_4 = -5.0 \cdot 10^{3} \ (K).$$

The fuel is defined by the first material type specified in the heat structure input, with the next material type being the gap and the third the clad as shown in Figure 2.3.2-2. Any deviation from the geometry will result in an error or misinterpretation of the information by the pin model. The gap can only be one mesh interval wide, while fuel or clad must be greater than or equal to one mesh interval. Currently no provisions are made for annular fuel pellets.

The calculation of the inside clad radius is not as straightforward as the fuel outside radius. Seven different calculational modes are required to cover the possible clad conditions. They are defined as:

1. Elastic and thermal expansion within an unruptured channel,
2. Elastic and thermal expansion within 166.7K (300°F) of the clad rupture temperature within an unruptured channel,
3. Plastic deformation within an unruptured channel,
4. Elastic thermal expansion within a ruptured channel,
5. Plastic deformation in a ruptured channel,
6. Ruptured segment, and
7. Fuel-cladding mechanical iteration (closed gap).

Each mode is related to the NUREG-0630 calculated rupture temperature.

$$T_{rupt} = 4233 - \frac{20.4\sigma_h}{1 + H} - \frac{(8.51 \cdot 10^6)\sigma_h}{100(1 + H) + 2790\sigma_h}, \qquad 2.3.2\text{-}17$$

where

T_{rupt} = NUREG-0630 rupture temperature (K),

σ_h = clad hoop stress (kpsi), and

H = dimensionless clad heating ramp rate, $0 \leq H \leq 1$.

The clad hoop stress for any pin segment is given by

$$\sigma_h = C_p \, (P_g \, r_{ic_{cold}} - P_f \, r_{oc_{cold}})/(r_{oc_{cold}} - r_{ic_{cold}}), \quad 2.3.2\text{-}18$$

with

$r_{ic_{cold}}$ = cold unstressed inside clad radius (m),

$r_{oc_{cold}}$ = cold unstressed outside clad radius (m),

P_g = internal fuel rod pin pressure for that channel (Pa), and

P_f = external fluid pressure of the right-hand side heat structure associated volume (Pa).

$C_p = 1 / 6.894757 \times 10^6$

The heating rate can be either a user input constant or one of three additional transient-dependent algorithms discussed in detail later in this section.

At the beginning of each new time step following a successful RELAP5 time step advancement, the hoop stress and normalized heating ramp rate are computed for each pin segment. The clad average temperature is also known at this time. If the clad average temperature is greater than the rupture temperature, then rupture occurs. Should the segment still be elastic and the rupture minus the clad temperature is less than 166.7K (300 F), then the segment stays elastic. Between these two temperatures the clad can be either elastic or plastic depending upon this

temperature difference and the burst strain as described in the following paragraphs for ruptured or unruptured channels.

Mode 1: Unruptured Elastic and Thermal Deformation

Within an unruptured channel, the clad is considered purely elastic if it has never gone plastic, ruptured, or the temperature difference between rupture and clad average temperatures is less than 166.7 K (300 F). The inside clad radius for this pure elastic mode is determined by

$$r_{ic} = r_{ic_{cold}} + u_{TC} + u_{CC} + u_e \ , \qquad 2.3.2\text{-}19$$

where

u_{TC} = clad radial displacement due to thermal expansion (m),

u_{CC} = clad radius over-specification factor (m), determined during pin transient initiation, and

u_e = clad radial displacement due to elastic deformation (m).

The clad thermal expansion is determined similarly to that for the fuel.

$$u_{TC} = (r_{N_{HS}+1} - r_{N_f+2})\ \epsilon_{TC} / 2 \ , \qquad 2.3.2\text{-}20$$

with

N_{HS} = total number of mesh intervals in the heat structure,

r_n = heat structure radius at the inside of mesh interval n or outside of n-1 (m), and

ϵ_{TC} = radial strain function defining fuel thermal expansion as a function of clad average temperature.

The radial strain function is defined by either a user input cubic fit

$$\epsilon_{TC} = C_1 T^3 + C_2 T^2 + C_3 T + C_4 , \qquad 2.3.2\text{-}21$$

or a built in code correlation set[119]

$$\epsilon_{TC} = -2.0731 \cdot 10^{-3} + 6.721 \cdot 10^{-6} T_C \qquad 2.3.2\text{-}22$$

for $T_C < 1073K$ (α phase), and

$$\epsilon_{TC} = -9.4495 \cdot 10^{-3} + 9.7 \cdot 10^{-6} T_C \qquad 2.3.2\text{-}23$$

for $T_C > 1273K$ (β phase), where T_C is the average cladding temperature (K). In the α phase to β phase transition zone, $1073K < T_C < 1273K$, a table lookup is used. Some selected values are listed in Table 2.3.2-2.

Table 2.3.2-2. Thermal Strain of Zircaloy for 1073 K < T < 1273 K.

T(K)	Radial Strain ϵ_{TC}	Axial Strain ϵ_{ATC}
1073.	$5.14 \cdot 10^{-3}$	$3.53 \cdot 10^{-3}$
1093.	$5.25 \cdot 10^{-3}$	$3.50 \cdot 10^{-3}$
1103.	$5.28 \cdot 10^{-3}$	$3.46 \cdot 10^{-3}$
1123.	$5.24 \cdot 10^{-3}$	$3.33 \cdot 10^{-3}$
1143.	$5.15 \cdot 10^{-3}$	$3.07 \cdot 10^{-3}$
1183.	$4.45 \cdot 10^{-3}$	$1.50 \cdot 10^{-3}$
1223.	$2.97 \cdot 10^{-3}$	$1.10 \cdot 10^{-3}$
1273.	$2.90 \cdot 10^{-3}$	$1.40 \cdot 10^{-3}$

Young's modulus is given either by the code for zircaloy cladding as

$$E = \begin{cases} 1.088 \cdot 10^{11} - 5.475 \cdot 10^{7}\, T_c & 1090K \geq T_c \\ 1.017 \cdot 10^{11} - 4.827 \cdot 10^{7}\, T_c & 1240K \geq T_c > 1090K \\ 9.21 \cdot 10^{10} - 4.05 \cdot 10^{7}\, T_c & 2027K \geq T_c > 1240K \\ 1.0 \cdot 10^{10} & T_c > 2027K, \end{cases} \qquad 2.3.2\text{-}28$$

or by a user specified cubic equation

$$E = C_1 T_c^{\,3} + C_2 T_c^{\,2} + C_3 T_c + C_4 \,. \qquad 2.3.2\text{-}29$$

Poisson's ratio is a constant which is defined as 0.30 for zircaloy by the code, however, the user can over-ride this value.

The normalized heating ramp rate for the elastic mode is determined by one of two methods. One method calculates an instantaneous heating rate and normalizes it with respect to a rate of 28K/s.

$$H = \left[\frac{dT_c}{dt}\right] / 28.0$$

$$= \left[\frac{T_c^{\,n} - T_c^{\,n-1}}{\Delta t}\right] / 28.0 \,. \qquad 2.3.2\text{-}30$$

The normalized value is then limited to $0 \leq H \leq 1$ before using it for subsequent checking and calculations. The superscripts reflect the current and old time values. The second method defines the normalized heating rate as a constant between 0 and 1 based on user input.

Mode 2: Unruptured Elastic and Thermal Deformation Within 166.7K (300 F) of the Rupture Temperature

When the clad average temperature is within 166.7K (300 F) of the rupture temperature, the elastic inside clad radius is calculated as shown in Mode 1. This radius is compared against the plastic inside clad radius calculated in Mode 3. If the elastic radius is greater than the plastic radius, then Mode 2 is retained and the inside clad radius is set to the elastic radius. If not, the clad becomes plastic (Mode 3) and the plastic clad calculations are used. An informative message is printed when a segment first becomes plastic. No return to elastic Modes (1 or 2) is permitted once the clad becomes plastic.

$$r_{ic} = MAX(r_{ic_{elastic}}, r_{ic_{plastic}}) . \qquad 2.3.2\text{-}31$$

If $r_{ic_{elastic}} \geq r_{ic_{plastic}}$, Mode = 2 .

If $r_{ic_{elastic}} < r_{ic_{plastic}}$, Mode = 3 .

Mode 3: Unruptured Plastic Deformation

The unruptured plastic deformation is determined by the plastic strain, ϵ_p.

$$r_{ic} = r_{ic_{cold}}(1 + \epsilon_p), \qquad 2.3.2\text{-}32$$

with

$$\epsilon_p = 0.2\epsilon_B \exp[-0.02754(T_{rupt} - T_c)], \qquad 2.3.2\text{-}33$$

where ϵ_B is the clad burst strain determined by a double interpolation relative to H and T_{rupt} in the user input or default NUREG-0630 burst strain Tables 2.3.2-3 and 2.3.2-4. The

plastic strain behaves as a ratchet. Once a given plastic strain is reached, no decrease in its value is allowed. In other words, for plastic mode calculations

$$r_{ic} = \text{MAX}(r_{ic}^{n}, r_{ic}^{n-1}), \qquad 2.3.2\text{-}34$$

where the superscripts refer to the current and old time values.

If the plastic mode is selected, the normalized heating ramp rate is calculated from any of three user options: user input constant, average ramp rate, or plastic weighted ramp rate. The normalized average ramp rate is calculated from

$$H = \left[\frac{T_c^{n} - T_c^{p}}{t^{n} - t^{p}}\right] \Big/ 28.0 , \qquad 2.3.2\text{-}35$$

where

t = time (s),

n = superscript defining the current time, and

p = superscript defining the time in which the clad first went plastic.

The normalized plastic weighted ramp is calculated by

$$H = \left[\frac{\int_{t^p}^{t^n} W(T) \left[\frac{dT_c}{dt}\right] dt}{\int_{t^p}^{t^n} W(T)\, dt}\right] \Big/ 28.0 , \qquad 2.3.2\text{-}36$$

noding options) chosen by the user. The fine mesh noding option computes the inside radius as

$$r_{ic} = r_{ic_{cold}}(1 + \epsilon_B) \ . \qquad 2.3.2\text{-}39$$

With this option, the gap conductance is calculated as though there is steam in the gap. The steam thermal conductivity is evaluated at the gap temperature and used with the hot gap size to compute the conductance. This option also calculates inside metal-water reaction for the ruptured segment.

The coarse mesh noding option computes the inside clad radius as

$$r_{ic} = r_{ic_{cold}}(1 + 0.2\ \epsilon_B) \ . \qquad 2.3.2\text{-}40$$

This option uses the regular gap gas conductance and does not consider inside metal-water reaction. It is intended for use nominally when the expected rupture length is small when compared to the total segment length. The microscopic effects at the rupture site considered with the fine mesh option are expected to be negligible when compared to the longer segment behavior. With the coarse mesh option, the overall behavior will be more closely controlled by the entire segment rather than just the rupture site conditions.

Within the ruptured channel various calculations are modified at the time of rupture. Each segment within that channel undergoes a mode change. The pin pressure becomes that of the hydrodynamic volume associated with the ruptured segment. An additive form loss coefficient is calculated at rupture based on the clad flow blockage by a simple expression for an abrupt contraction-expansion.

$$K_{add} = \frac{0.5(1 - \beta^2) + (1 - \beta^2)^2}{(\beta^2)^2} \ , \qquad 2.3.2\text{-}41$$

where

β^2 = fraction of the channel flow area blocked,

= $(1.0 - A_{blocked}/A_{channel})$.

The flow blockage is obtained via a double table interpolation relative to the normalized heating ramp rate and rupture temperature similarly to the clad burst strain. The table is either user supplied or default NUREG-0630 values listed in Tables 2.3.2-3 and 2.3.2-4. The additive value of the loss coefficient is edited at the time of rupture. The flow blockage loss coefficient is added automatically to the problem unless the user overrides via a new optional input. If added, the form loss is applied to the forward flow direction for the inlet (bottom) junction and the reverse flow direction for the exit (top) junction attached to the volume in which the clad ruptured. The user option to exclude this form loss addition from the junctions has been included for certain non-licensing specialized applications (such as in models that use a single fluid channel in the core with multiple radial heat structure channels).

Another option has been added to the EM Pin model help to minimize user burden when running EM reflooding heat transfer analyses with BEACH (BAW-10166 Section 2.1.3.8.4). This user-controlled option automatically includes code-calculated pin rupture, droplet break-up and convective enhancement adjustments. The input grid parameters are modified with the ruptured values and will be retained for use in the reflooding heat transfer calculations. This model is optional and requires input to activate the calculations. If no input is specified the default is that no rupture enhancements will be calculated.

When this option is selected several sets of calculations will be performed following cladding rupture. The first calculation

performed determines the midpoint elevation of ruptured segment, referenced from the bottom of the pin channel (which coincides with the bottom of the heat structure geometry or reflood stack). This midpoint elevation, Z_{grid}, is the location where the new "grid" is inserted. This elevation is used to determine the droplet break-up effects for the ruptured segment.

$$Z_{grid} = 0.5 \cdot \Delta Z_{rupt_{seg}} + \sum_{j=1}^{rupt\ seg-1} \Delta Z_{seg_j} , \qquad 2.3.2\text{-}41.1$$

where

ΔZ_{seg} = elevation change of pin segment.

The second set of calculations is to calculate rupture droplet breakup efficiency. These calculations are identical to those described in Sections 2.1.3.7. and 2.1.3.8. of Reference 123. The rupture atomization factor, η_{etamax}, is calculated as

$$\eta_{etamax} = \frac{1}{[\ 1 + (n^{1/3} - 1)\epsilon_b\ ]} , \qquad 2.3.2\text{-}41.2$$

where

n = number of equal size droplets resulting from the split-up of the larger droplets,

[b,c,d,e]

ϵ_b = flow blockage fraction.

The increase in the droplet surface area from that used for interface heat transfer is defined in Equation 2.1.3-105[123] as

$$\Delta a_{gf} = C_{maxDB}\ \theta\ a_{gf} .$$

The proportionality constant, C_{maxDB}, is determined from the constant, C_1, the rupture flow blockage fraction, and the length of the ruptured segment.

$$C_{maxDB} = \frac{C_1\ \epsilon_b}{\Delta Z_{rupt_{seg}}} . \qquad 2.3.2\text{-}41.3$$

[b,c,d,e]

The velocity of the fluid at the ruptured location increases because of the flow area reduction. The physical area in the code calculations is not modified, but a velocity multiplier, used for determining the droplet Weber number, is calculated from

$$VELMULT = \frac{1}{1 - \epsilon_b} \quad . \qquad 2.3.2\text{-}41.4$$

The cladding rupture results in an increase in the pin outside heat transfer surface area. The increase in area is not directly included in the conduction solution in the code calculations. It is accounted for by using the rupture convective enhancement factor and applying it to the grid wall heat transfer enhancement factor, F_{gg}. The rupture enhancement, M_{RAR}, is an multiplicative contribution determined by

$$M_{RAR} = \text{Rupture Area Ratio}$$

$$= \frac{2\pi\, r_{rupt_{oc}}\, L}{2\pi\, r_{oc_{cold}}\, L} = \frac{r_{rupt_{oc}}}{r_{oc_{cold}}} \quad , \qquad 2.3.2\text{-}41.5$$

where

$r_{rupt_{oc}}$ = outside clad radius of the ruptured node given by

$$= r_{ic} + \left[r_{oc_{cold}} - r_{ic_{cold}}\right]\left[r_{ic_{cold}}/r_{ic}\right]. \qquad 2.3.2\text{-}41.6$$

The total wall heat transfer convective factor then becomes

$$F_{gq_{tot}} = F_{gq_{grid}} \cdot M_{RAR} \, . \qquad 2.3.2\text{-}41.7$$

These droplet break-up and convective enhancement terms are optionally calculated and edited at rupture by the EM pin model.

L_j = axial length of the jth segment (m),

ϵ_{ATF} = fuel strain function of Equation 2.3.2-15, evaluated at fuel volume weighted average temperature $\bar{T}_f$ of Equation 2.3.2-25, (dimensionless), and

ϵ_{ATC} = axial strain function defining clad axial thermal expansion as a function of clad volume average temperature, (dimensionless).

The axial strain function for clad is defined by either a user input cubic fit

$$\epsilon_{ATC} = C_1 T^3 + C_2 T^2 + C_3 T + C_4 \qquad 2.3.2\text{-}51.8$$

or a built in code correlation set[119]

$$\epsilon_{ATC} = -2.506 \times 10^{-5} + (T_C - 273.15)\ 4.441 \times 10^{-6}$$
$$= -1.2381 \times 10^{-3} + 4.441 \times 10^{-6}\ T_C \qquad 2.3.2\text{-}51.9$$

for $T_C < 1073.15K$ (α phase), and

$$\epsilon_{ATC} = -8.3 \times 10^{-3} + (T_C - 273.15)\ 9.7 \times 10^{-6}$$
$$= -1.0950 \times 10^{-2} + 9.7 \times 10^{-6}\ T_C \qquad 2.3.2\text{-}51.10$$

for $T_C \geq 1273K$ (β phase), where T_C is the volume average cladding temperature (K) of Equation 2.3.2-24. In the α phase to β phase transition zone, $1073K < T_C < 1273K$, a table lookup is used. Some selected values are listed in Table 2.3.2-2.

Using the assumption that both the slope of the fuel mesh point temperatures and the overall gap conductance will not change significantly, the last gap multiplier (1.0 for the first iteration) can be adjusted via a ratio to give a new multiplier,

$$M_g^{\eta+1} = \frac{\Delta T_{gap}}{(\Delta T_{gap} + \Delta \bar{T}_f)} M_g^{\eta} \quad . \qquad 2.3.2\text{-}52.3$$

After calculation of the new gap multiplier, another conduction solution iteration step is taken. The fuel volume average temperature differential is recalculated via Equation 2.3.2-52.1. If the absolute value is greater than 2 K, then another iteration step is taken after recalculating a new multiplier via Equations 2.3.2-52.2 and 2.3.2-52.3. If the absolute value is less than 2 K, then the iteration has converged and the last multiplier calculated is edited and used during the steady-state and transient EM pin calculations. Up to six iterations are allowed. If convergence is not obtained in six iterations, then the code will stop at the end of the initialization process and appropriate failure messages will be edited. Failure of the iteration to converge is generally related to poor estimates given for the initial mesh point temperature distribution. An improved estimate will normally allow the iteration to converge properly. If convergence is still a problem, user specification of the multiplier is also available.

At the completion of the EM pin steady-state calculations (i.e., after EM pin steady-state trip becomes true or during the first time step if there is no trip) several calculations are required to initiate the pin transient calculations. The user-supplied cold unstressed pin geometry input via the heat structure cards is elastically expanded using the final code calculated temperature and mechanical stresses.

5.0 LICENSING DOCUMENTS

This section contains documents generated as a result of U.S. Nuclear Regulatory Commission (NRC) review of previous versions of this topical report. Sections 5.1 and 5.2 contains responses to rounds one and two questions, respectively, for revision 1 of this report. These documents were previously issued in the approved proprietary and non-proprietary versions as appendices H and I. Section 5.3 contains the Safety Evaluation Report (SER) issued for revision 1.

Sections 5.4 and 5.5 contain responses to NRC questions on revisions 2 and 3, respectively, of this report. Section 5.6 contains supplemental information to revisions 2 and 3. Section 5.7 contains the SER issued for revisions 2 and 3.

5.11 SER Directed Changes and Typographical Corrections

The SER for Revisions 2 and 3 of the RELAP5/MOD2-B&W topical requested that changes be made to portions of the text based on typographical changes identified in the RAIs. These changes were not incorporated in the approved version of Revision 3 per the SER direction. They are being included in the Approved Revision 4 Topical to ensure that the incorrect information given previously is not used in completing future analyses, references, or evaluations.

Some of the incorrect material was crossed out while other simple typos were fixed. Underlined, italicized text was added to denote the corrections or to direct the reader to the corrected information provided based on the response to the RAI. The information is marked in the margin with a change bar and a letter "t" to denote the requested typographical corrections identified in the Revision 2 & 3 SER Table 2. These SER directed changes were located on pages 2.3-36, 2.3-46, 2.3-83.1, H-6, H-7, I-5, I-11, I-12, J-8, and L-13.

In addition, two typographical errors have been discovered in two other text descriptions versus what is contained in the actual code formulation. The first error is in the two-phase head degradation table (first HAD head degradation point) on page 2.1-149. The topical has the incorrect sign for the head difference given in Subroutine RPUMP. The second error is in the steam heat transfer coefficient Equation 2.2.2-76 in the B&W high AFW model on page 2.2-40. The equation was corrected to match the correct formulation used in Subroutine HTFILM. These two errors could result in inappropriate code input to analyses or incorrect hand calculations based on the equation given. Therefore, corrected information has been provided in the approved topical version by replacing these two pages. The incorrect material was replaced with underlined, italicized text to indicate the corrected information. The information is marked in the margin with a change bar and a letter "s" to denote the supplemental typographical correction.

Each of the replaced pages (12 in all) with the incorrect information are attached following this page. These pages

have been updated with the correct information in the main body of the Revision 4 topical text.

Table 2.1.5-1. Semiscale Dimensionless Head Ratio Difference (single-phase minus two-phase) Data.

$$x = \frac{v}{\alpha} \text{ or } \frac{\alpha}{v}$$

$$y = \frac{h}{\alpha^2}\bigg|_{1\phi} - \frac{h}{\alpha^2}\bigg|_{2\phi} \text{ - or } \frac{h}{v^2}\bigg|_{1\phi} - \frac{h}{v^2}\bigg|_{2\phi}$$

Curve Type	x	y
1 (HAN)	0.00	0.00
	0.10	0.83
	0.20	1.09
	0.50	1.02
	0.70	1.01
	0.90	0.94
	1.00	1.00
2 (HVN)	0.00	0.00
	0.10	-0.04
	0.20	0.00
	0.30	0.10
	0.40	0.21
	0.80	0.67
	0.90	0.80
	1.00	1.00
3 (HAD)	-1.00	1.16
	-0.90	-1.24
	-0.80	-1.77
	-0.70	-2.36
	-0.60	-2.79
	-0.50	-2.91
	-0.40	-2.67
	-0.25	-1.69
	-0.10	-0.50
	0.00	0.00
4 (HVD)	-1.00	-1.16
	-0.90	-0.78
	-0.80	-0.50
	-0.70	-0.31
	-0.60	-0.17
	-0.50	-0.08
	-0.35	0.00
	-0.20	0.05
	-0.10	0.08
	0.00	0.11
5 (HAT)	0.00	0.00
	0.20	-0.34
	0.40	-0.65
	0.60	-0.95
	0.80	-1.19
	1.00	-1.47
6 (HVT)	0.00	0.11
	0.10	0.13
	0.25	0.15
	0.40	0.13
	0.50	0.07
	0.60	-0.04
	0.70	-0.23
	0.80	-0.51
	0.90	-0.91
	1.00	-1.47
7 (HAR)	-1.00	0.00
	0.00	0.00
8 (HVR)	-1.00	0.00
	0.00	0.00

For $(T_{sat} - 4.0) < T_\ell < T_{sat}$,

$$\Gamma_{wf} = \Gamma_{wChen} - [(\Gamma_{wChen} - 0.0)(T_{sat} - T_\ell)/4.0] \qquad 2.2.2\text{-}73$$

and

$$\Gamma_{wg} = 0.0 \ . \qquad 2.2.2\text{-}74$$

In the cases where $(T_{sat} - 4.0) > T_\ell$, there is an additional limit applied to Γ_{wf}. If Γ_{wf} calculated by Equations 2.2.2-70 or 2.2.2-72 exceeds 80% of the liquid available for boiling within a control volume, then the wetted area is reduced accordingly to give a value which can only equal 80%. This limit avoids the possibility of introducing an artificial mass error by vaporizing more liquid than is available.

Average Heat Flux and Heat Transfer Coefficients

The average values of heat flux and heat transfer coefficients are calculated as follows

$$h_{fff} = h_\ell \, A_{wet}/A_{slab} \ , \qquad 2.2.2\text{-}75$$

$$h_{ffg} = h_g \, A_{wet}/A_{slab} \ , \qquad 2.2.2\text{-}76$$

$$h_{ff} = h_{fff} + h_{ffg} \ , \qquad 2.2.2\text{-}77$$

$$q_{fff} = h_{fff}(T_w - T_\ell) \ , \qquad 2.2.2\text{-}78$$

$$q_{ffg} = h_{ffg}(T_w - T_g) \ , \text{ and} \qquad 2.2.2\text{-}79$$

$$q_{ff} = q_{fff} + q_{ffg} \ . \qquad 2.2.2\text{-}80$$

temperature difference and the burst strain as described in the following paragraphs for ruptured or unruptured channels.

Mode 1: Unruptured Elastic and Thermal Deformation

Within an unruptured channel, the clad is considered purely elastic if it has never gone plastic, ruptured, or the temperature difference between rupture and clad average temperatures is less than 166.7 K (300 F). The inside clad radius for this pure elastic mode is determined by

$$r_{ic} = r_{ic_{cold}} + u_{TC} + u_{CC} + u_e \ , \qquad 2.3.2\text{-}19$$

where

u_{TC} = clad radial displacement due to thermal expansion (m),

u_{CC} = clad radius over-specification factor (m), determined during pin transient initiation, and

u_e = clad radial displacement due to elastic deformation (m).

The clad thermal expansion is determined similarly to that for the fuel.

$$u_{TC} = (r_{N_{HS}+1} - r_{N_f+2}) \ \epsilon_{TC} / 2 \ , \qquad 2.3.2\text{-}20$$

with

N_{HS} = total number of mesh intervals in the heat structure,

r_n = heat structure radius at the inside of mesh interval n or outside of n-1 (m), and

ϵ_{TC} = radial strain function defining fuel thermal expansion as a function of clad average temperature.

where

β^2 = fraction of the channel flow area blocked,

= $(1.0 - A_{blocked}/A_{channel})$.

The flow blockage is obtained via a double table interpolation relative to the normalized heating ramp rate and rupture temperature similarly to the clad burst strain. The table is either user supplied or default NUREG-0630 values listed in Tables 2.3.2-3 and 2.3.2-4. The additive value of the loss coefficient is edited at the time of rupture. The flow blockage loss coefficient is added automatically to the problem unless the user overrides via a new optional input. If added, the form loss is applied to the forward flow direction for the inlet (bottom) junction and the reverse flow direction for the exit (top) junction attached to the volume in which the clad ruptured. The user option to exclude this form loss addition from the junctions has been included for certain non-licensing specialized applications (such as in models that use a single fluid channel in the core with multiple radial heat structure channels).

Another option has been added to the EM Pin model help to minimize user burden when running EM reflooding heat transfer analyses with BEACH (BAW-10166 Section 2.1.3.8.4). This user-controlled option automatically includes code-calculated pin rupture, droplet break-up and convective enhancement adjustments. The input grid parameters are modified with the ruptured values and will be retained for use in the reflooding heat transfer calculations. This model is optional and requires input to activate the calculations. If no input is specified the default is that no rupture enhancements will be calculated.

When this option is selected several sets of calculations will be performed following cladding rupture. The first calculation

$x_1 = \exp [P / (1000*Cl_P)]$,
$x_2 = G / (10^6 * Cl_{MF})$, and
$x_3 = X_{eth}$.

where P is the system pressure in lb/in^2, G is mass flux in $lbm/hr/ft^2$, X_{eth} is the quality at CHF, and Cl_P and Cl_{MF} are the English-to-metric conversion factors for pressure and mass flux, respectively.

The empirical coefficients are:

[b,c,d,e]

Barnett[109].

The Barnett correlation is a widely accepted and applied within the industry for high flow medium pressure CHF. The correlation is given by

$$q_{crit} = 10^6 \, Cl_{BR} \, Cl_{EF} \, \frac{A + B(h_f - h_{in})/Cl_{SE}}{C + L/Cl_{in}} \quad , \qquad 2.3.3\text{-}42$$

where

Cl_{BR} = user input constant (default = 1),

Table H.2. ORNL Thermohydraulics Test Facility (THTF) Benchmark Cases.

Case	Experiment	Pressure (psia)	Power Density (kw/ft)	Mass Flux ($lbm/hr/ft^2$)
13	3.09.10i	0.68	650	21943.9
14	3.09.10j	0.33	610	9333.4
15	3.09.10k	0.10	580	2306.5
16	3.09.10l	0.66	1090	21461.4
17	3.09.10m	0.31	1010	9313.0
18	3.09.10n	0.14	1030	3395.2
19	3.09.10aa	0.39	590	14938.7
20	3.09.10bb	0.20	560	6961.9
21	3.09.10cc	0.10	520	3706.1
22	3.09.10dd	0.39	1170	14615.7
23	3.09.10ee	0.19	1120	8111.9
24	3.09.10ff	0.08	1090	3561.1

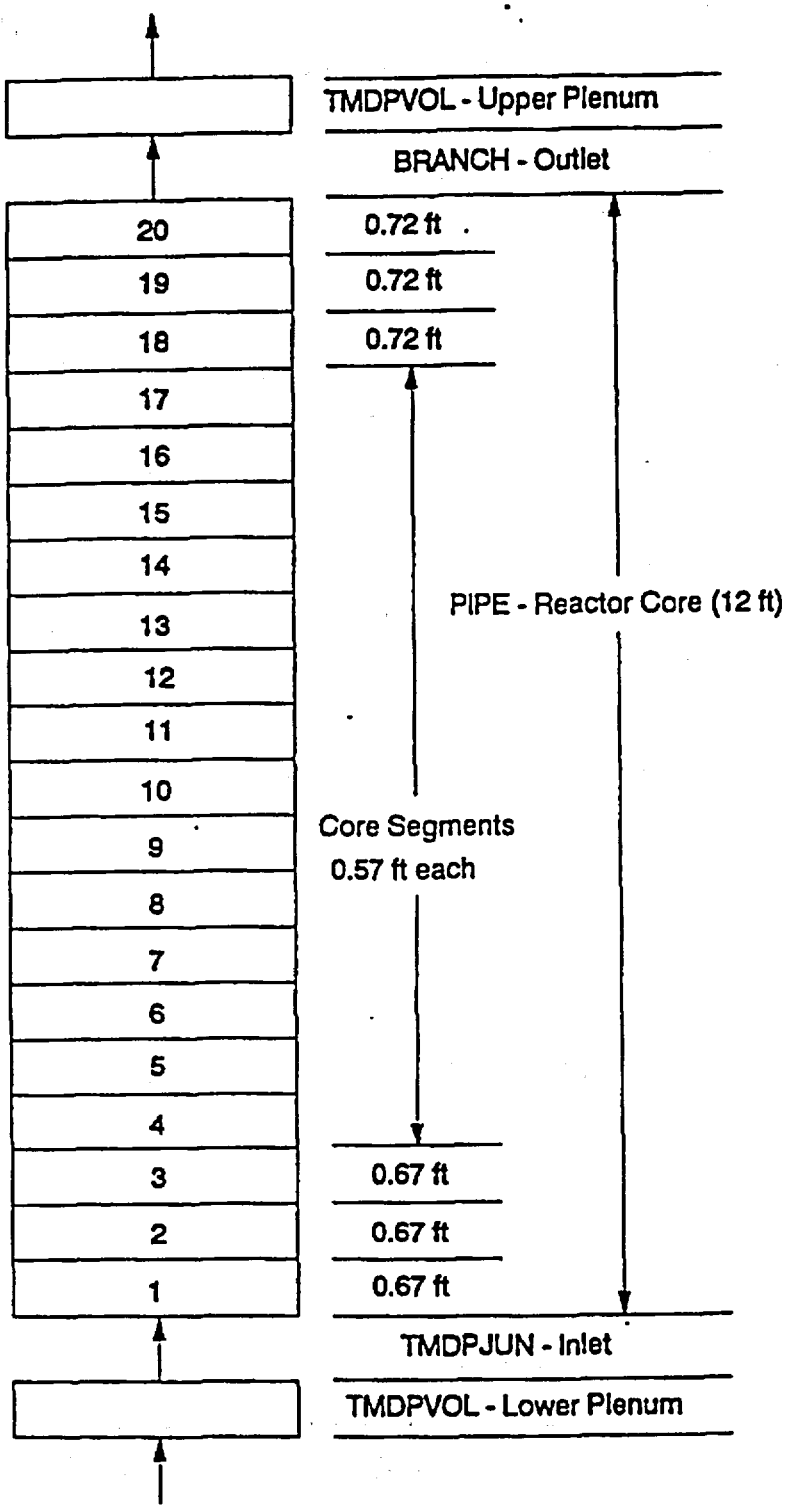

Figure H.1. RELAP5 Model of Hypothetical Reactor Core.

I.2.1. Correlation Form

The critical heat flux was assumed to depend on three parameters:

$$x_1 = \exp[P / (1000 * Cl_P)],$$
$$x_2 = G / (10^6 * Cl_{MF}), \text{ and}$$
$$x_3 = X_{eth}.$$

where P is the system pressure in psia, G is the mass flux in lbm/hr/ft^2, X_{eth} is the quality at CHF, and Cl_P and Cl_{MF} are the English-to-metric conversion factors for pressure and mass flux, respectively.

Based on the work of Farnsworth[142], a general polynomial form was assumed:

$$CHF = FLS\ (a_0 + a_1x_1 + a_2x_2 + a_3x_3^2 + a_4x_1^2 + a_5x_2 + a_6x_3|x_3| + a_7x_1x_2 + a_8x_1x_3 + a_9x_2x_3 + a_{10}x_1^3 + a_{11}x_2^3 + a_{12}x_3^3 + a_{13}x_1x_2x_3) / F, \qquad \text{I-1}$$

where FLS is the bundle specific multiplier used in BWCMV and is defined by

$$FLS = C_1 + C_2L + C_3S + C_4L^2 + C_5LS + C_6S^2, \qquad \text{I-2}$$

in which L = heated length,
S = spacer grid spacing, and
C_i = empirically determined coefficients.

Table I.3. Calculated Local Condition Values.

	Point	Pressure psia	Mass Flux lbm/hr/ft^2	Heat Flux btu/hr/ft^2	Quality
Test 121					
	430	2015	405308	370043	0.2556
	431	2015	721925	461763	0.0969
	432	2015	704141	521065	0.0664
	433	2015	916371	521065	0.0664
Test 160					
	786	2115	527956	287300	0.3641
	787	2385	531861	282880	0.3157
	788	1805	541406	311610	0.3265
	789	1515	519832	373490	0.5620
	789	1515	513721	373490	0.6653
	790	2115	532879	335920	0.3127
	791	2405	519639	329290	0.2604
	792	1800	531920	370175	0.4239
	793	1815	516979	397800	0.4586
	794	2075	508498	349180	0.3110
Test 164					
	2055	1000	2554047	601121	0.2000
	2056	1000	3018628	682772	0.1931
	2057	1000	1588414	363385	0.3162
	2058	1000	2035850	647578	0.2044
	2059	1005	2518548	709520	0.1634
	2060	1005	3030165	751754	0.1683
	2060	1005	3050214	611714	0.1980
	2061	1005	1103392	348591	0.4161
	2062	1010	1575738	404069	0.3199
	2063	760	1879028	372631	0.3371
	2064	760	2634649	444754	0.2812
	2065	765	3096974	713744	0.2090

Table I.3 (continued). Calculated Local Condition Values.

	Point	Pressure psia	Mass Flux lbm/hr/ft^2	Heat Flux btu/hr/ft^2	Quality
Test 164 (continued)					
	2065	765	3147021	468794	0.2528
	2066	755	1617322	374481	0.3567
	2067	750	2115662	392049	0.3122
	2068	750	1627688	338420	0.3935
	2069	745	1026514	327324	0.4569
	2070	750	1049376	347666	0.4291
	2071	1005	2120543	578597	0.2326
	2072	995	1044837	307906	0.4731
	2073	1005	558151	281092	0.6404
	2074	1000	547973	239483	0.5657
	2075	760	538561	378692	0.4393
	2076	755	545706	232086	0.6060

Counter current flow limiting (CCFL) is applied to the junctions at the steam generator plenum and tube inlets. The Wallis correlation from Reference 145 is used in the steam generator tube inlet junction, and the CCFL correlation based on the UPTF data from Reference 146 is used in the steam generator plenum inlet junction. The results of the CCFL calculation will be discussed later. The SBLOCA EM heat transfer model is used for the core heat transfer calculation. This model uses the BWUMV CHF correlation to calculate DNB, and permits return to nucleate boiling when rewetting is calculated during the post-DNB period.

A discharge coefficient of 1.1 is used for subcooled flow and two-phase flow up to 70 percent void fraction, and the two-phase coefficient is reduced to 0.77 for void fraction greater than 70 percent. These relative values were used to match a measured flow, and are consistent with the relationship of discharge coefficients with respect to void fraction discussed in Volume 2 Section 4.3.2.3 of BAW-10168, Revision 2.

Results of the Benchmark

The steady-state initial conditions for the benchmark are presented along with the test conditions in Table 2. To demonstrate model stability relative to time advancement, the EM model was run with a time step advancement of 0.05 seconds (base case) and with a reduced time step of 0.005 seconds. Figures 6 through 10 show the results of the time step study, and confirm that the reduced time step advancement does not change the results. A comparison of the results of the base case (RELAP5/MOD2 EM) with the experimental data identified with instrumentation tag names listed in Reference 142 is presented in Table J.3 and Figures J.11 through J.36 below.

The calculated sequence of major events are presented along with the test data in Table J.3. Due to a facility power limitation,

Table L.1. Comparison of MIST Initial Conditions to RELAP5/MOD2-B&W Values.

Parameter, Units	MIST Value	RELAP5/MOD2-B&W Value
Primary Pressure, psia	1730.0	1726.5
Secondary Pressure, psia	1010.0	1010.0
Core Exit Temperature, F	592.0	593.4
SG Exit Temperature, F	551.0	550.3
Core Exit Subcooling, F	22.0	22.0
Core Power, Btu/s	117.0	119.5
Pressurizer Level, ft	5.0	5.0
SG Secondary Level, ft	4.8	5.0
Core Flow Rate, lbm/s	1.86	1.86

Table L.2. Sequence of Events.

Event	MIST Observation Seconds	Ver 5.0 Prediction Seconds	Ver 14.0 Prediction Seconds
Leak opened	0	0	0
Primary saturates	12	31	34
Pzr level reaches one foot (HPI, AFW, and DH ramp started)	30-42	60	57
Hot leg U-bend voiding interrupts natural circ. (Loop A/Loop B)	54/42	85/130	130/90
High elev BCM begins (Loop A/Loop B)	170/175	180/185	180/180
Break saturates	190	130	140
Secondary refilled and AFW shutoff (SG A/SG B)	480/480	490/440	480/480
Primary and secondary pressures equalize	1560	1500	1650
Secondary blowdown	1710	1500	1650
CFT injection begins	1920	1680	1800